A COMPARATIVE ANALYSIS AND TAXONOMY OF COMETS

By

DAVID JAMES OSIP

A DISERTATION PRESENTED TO THE GRADUATE SCHOOL
OF THE UNIVERSITY OF FLORIDA IN PARTIAL FULFILLMENT
OF THE REQUIREMENTS FOR THE DEGREE OF
DOCTOR OF PHILOSOPHY

UNIVERSITY OF FLORIDA

1995

To Family and Friends

ACKNOWLEDGMENTS

First and foremost, I thank my parents for nurturing and encouraging my curiosity in the heavens and for supporting me unfailingly. I thank my brothers, Phil and Damien, for their support and for pushing me to excel. I am also deeply indebted to my friends, for everything. In particular I would like to thank Wil Martinez and Tony Hatt, two of the best friends anyone could ever have, and Joanna Thomas, my soul mate.

My sincerest thanks go to Drs. Michael A'Hearn, Robert Millis and David Schleicher for introducing me to the wonders of cometary science. Their insights, probing questions, and meticulous methodology have had a profound influence on the way I think and pursue avenues of scientific inquiry. I am extremely grateful for the role that I have been able to play in the far-sighted observational program initiated by Drs. A'Hearn and Millis in 1976. I am fortunate to have collaborated with Drs. A'Hearn, Millis, Schleicher, and Dr. Peter Birch on the massive database accumulated in this program. I thank them for not only making this dissertation project possible, but for making it enjoyable.

I would like to thank my advisor, Dr. Humberto Campins, for guiding me in producing a focused dissertation, while at

the same time helping me expand my horizons in planetary science, infrared studies, and astronomy in general. Humberto has been very unselfish with his time and has always been available to discuss problems and solutions, questions and answers. His contagious enthusiasm is also much appreciated.

I thank the other members of my committee, Drs. Stanley Dermott, Bo Gustafson, Alex Smith, and Martin Vala for their time and effort in overseeing this work.

I also thank Dr. Erzsebet Merenyi for her assistance in exploring neural networks and Steve Larson for his aid in providing an additional data set of cometary spectra.

Special thanks are due to the staff and students of the astronomy department for keeping things running smoothly and for an intellectually stimulating active environment.

Finally, I thank God for the wonderfully odd universe in which we live and the spark of curiosity in our human nature that compels us to understand it.

Thanks all!

Financial support for this research was primarily provided by a NASA Graduate Student Research Program Fellowship, NGT-50959.

TABLE OF CONTENTS

ACKNOWLEDEGEMENTS iii

ABSTRACT vii

CHAPTER 1 INTRODUCTION 1

Historical Background 1
Aristotle-16th Century 2
16th-20th Century 2
A Giant Step, Halley Encounter 10
The Present Work 10

CHAPTER 2 THE DATABASE 14

Observational Method 14
Instrument and Filter Changes 15
Reduction Procedures 16
Reduction to Fluxes 16
Fluxes-Column Abundances of Emission Species 20
Column Abundances - Molecular Production Rates 21
Continuum Fluxes - Dust Production 23
Error Propagation 26
The Comets 27
Other Data Sets 30

CHAPTER 3 COMETARY PROPERTIES 38

Introduction 38
Evaluating Variations with Heliocentric Distance 39
Parameterizing Cometary Chemical Composition 46
Parameterizing Cometary Absolute Productivity 47
Dynamical Properties 55

CHAPTER 4 COMPARATIVE ANALYSIS AND TAXONOMY 72

Parameter Ranges 72
Trends and Correlations 73
Activity Level 74
Gas-to-Dust Ratio 75
Molecular Abundance Ratios 78
Cometary Taxonomy 81
Analysis Tools 83

Restricted Data Set 84
Principal Component Analysis 85
Hierarchical Clustering Algorithms 87
Compositional Classes 88
Classifying the Full Database 90
Interpretation of the Classes 91

CHAPTER 5 SUMMARY 117

New Results 117
Comparison of Results with Previous Studies 119
Directions for Future Work 122

APPENDIX 22 BIN DATA SET 123

LIST OF REFERENCES 129

BIOGRAPHICAL SKETCH 135

Abstract of Dissertation Presented to the Graduate School of the University of Florida in Partial Fulfillment of the Requirements for the Degree of Doctor of Philosophy

A COMPARATIVE ANALYSIS AND TAXONOMY OF COMETS

By

David James Osip

August 1995

Chairman: Humberto Campins
Major Department: Astronomy

A comparative analysis of narrowband photometry observations of 85 comets yields a wealth of information about the nature of comets. The data set consists of 2020 observations obtained over 429 nights between 1976 and 1992 that are fully reduced in a consistent manner to molecular production rates of 5 emission species (OH, NH, CN, C_3, and C_2) as well as a comparative measure of the dust production rate. Ratios of these production rates serve as a means of exploring compositional variation between comets. Vaporization models are used to estimate the active surface area for each comet, which is indicative of intrinsic differences in activity level among comets. Orbital parameters distinguish comets by dynamical age and separate the database into several dynamical classes.

The current investigation confirms a number of results from earlier studies. There are no significant or systematic variations of the various abundance ratios with heliocentric distance. Neither the cometary dust-to-gas ratio nor the activity level vary systematically with dynamical age or with heliocentric distance. There is no conclusive evidence suggesting changes in composition based on dynamical evolution of the comet. Also, this investigation finds for many comets the strong degree of homogeneity in abundance ratios suggested by other studies, particularly among the carbon bearing species.

Results unique to the present database include a significant correlation between the cometary dust-to-gas ratio and perihelion distance of a comet, suggesting mantling effects on the nucleus. Additional evidence for mantling is provided by the large number of comets with very low levels of activity as measured by the surface active area and the low fractional active areas calculated for those comets with nucleus size estimates available.

The most important result from this study, however, is a taxonomic classification of comets separating chemically distinct compositional groupings most likely due to the original formation region. Gradients in temperature or cosmic ray exposure as a function of heliocentric distance in the proto-solar nebula can be invoked to qualitatively explain the observed compositional differences. Future observations measuring other emission species may serve to

further delineate chemically distinct groups among the comet population.

CHAPTER 1
INTRODUCTION

Historical Background

Comets, from the Greek "κομετεξ" meaning long-haired ones, have frightened, confused, intrigued, entertained, and enlightened mankind since time immemorial. Records dating to the first millennium BC from China and the Middle East provide the earliest known observations of these little understood objects. In the 3000 years since then, the notion of comets as harbingers of doom or celestial messengers has only relatively recently given way to a forming understanding of their true nature. As probes of space (which provided the first evidence for the existence of a Solar Wind) and time (near-pristine remnants of the epoch of Solar System formation), these enigmatic objects are just beginning to reveal the many secrets they hold.

One can readily imagine -- or perhaps remember the 1965 apparition of Ikeya-Seki -- the awesome aspect of a luminous heavenly body with a long trailing mane that gradually brightens until visible even in daylight then fades away over the course of several months: What effect such a sight must have had on our ancient forebears! It is easy to understand why the earliest interpretations of these celestial events

equated them with a supernatural source. However, even as comets—themselves appeared to change with time, so has mankind's insight changed over time.

Aristotle-16th Century

In the 4th century BC., Aristotle, in *Meteorology*, suggested that comets occupy the lowest sphere, corresponding to the upper atmosphere, in his system of progressive spherical shells in an Earth centered universe. This insight into the nature of comets was generally accepted for almost two thousand years with the majority of discussion reserved for potential supernatural, often doomsday, meaning associated with these phenomena. It wasn't until the 15th-16th century renaissance of observational astronomy in Europe, and in particular the work of Tycho Brahe and Michael Mastlin measuring the parallax of the bright comet of 1577, that the Aristotelian view of comets as phenomena within the Earth's atmosphere was abandoned and the celestial nature of comets was recognized and accepted. As to their role as omens of doom, the popular press as recently as the 1910 apparition of comet P/Halley still fostered this notion of comets.

16th-20th Century

With their celestial nature demonstrated, the motion of comets became the next natural topic to grapple. Kepler, thinking that comets followed straight lines, concluded that

they must originate outside the Solar System. Contemporaneously, Hooke and Borelli suggested parabolic orbits while an amateur, Sir William Lower, suggested elliptical orbits for comets. It was a century after the work of Brahe that Isaac Newton (1687), with his new theory of gravity, showed that the bright comet of 1680 indeed moved in an elliptical orbit. Newton's law of gravity was conclusively proven to hold well beyond the extent of the known planets when in 1758 the prediction of Sir Edmund Halley (1705) that the comets of 1531, 1607, and 1682 were one and the same and would return in 1758 was validated by the observations of Johann Palitzsch. In 1822 Johann Encke became the next person to successfully predict the return of a comet; comet P/Encke, whose 3.3 year period is still the shortest of any known comet.

These first two recognized and confirmed periodic comets, Halley and Encke, also provided the impetus for much of the future modeling of cometary nuclei. Comet P/Encke provided a puzzle in that it was observed to continually reach perihelion approximately 0.1 days prior to the time predicted after taking into account all planetary perturbations. A brightness asymmetry in the coma of comet Halley lead Bessel (1836) to suggest asymmetric outflow from an embedded central body. He further postulated a non-gravitational effect associated with directional outflow that could explain perihelion shifts like that found in comet P/Encke.

This work laid the foundation for the icy conglomerate solid nucleus (AKA. "dirty snowball") model that Whipple formulated a century later. Whipple's 1950 model gained favor over Lyttleton's competing sand-bank model (1948, 1952) mainly due to its ability to readily match the observational record. Following the work of Wurm (1943) explaining the short-lived gaseous species observed in the coma as dissociation products of stable parent molecules, Whipple proposed a rotating solid nucleus that produced gas and dust via sublimation of the surface. Regions of varying volatile activity, combined with the nucleus rotation, provided the non-gravitational forces necessary to alter the comet's orbit (Whipple, 1950).

While Whipple was advancing our understanding of the cometary nucleus, Polydor Swings (1941, 1942) was tackling a thorny problem in the interpretation of cometary spectra. Fluorescence, the absorption of solar light followed by re-emission, had been put forward to explain the emission features seen in the spectra of comet P/Halley in 1910. The problem was that the violet CN bands (387.5 nanometers) seen in cometary spectra varied and did not match laboratory CN spectra. Swings explained that due to cometary motion relative to the Sun, the absorption lines in the solar spectrum are Doppler shifted and the change in intensity at the exciting wavelengths determines the strength of the fluorescent emission lines in the comet's spectrum. The majority of spectroscopic studies following Swing's work

through the 1970s dealt with the identification of emission lines and bands and their detailed rotational and vibrational structure. Additionally, preliminary efforts were undertaken to begin comparing cometary spectra, using measures of various line and band widths, in search of classifiable differences among comets (e.g. Arpigny, 1973; Donn, 1977).

Thus, through the late 19th and early 20th centuries, the elusive physical nature of comets was slowly being revealed while spectroscopic observations allowed inferences to be made about their chemical constituents. This left the question of the origins of comets, however, which was approached from studies of orbital dynamics. In 1932, Ernst Opik forwarded the notion of a hypothetical cloud of distant comets as being necessary if many comets were observed to have original semi-major axis (a_{orig}) > 10,000 AU [note: original semi-major axis is the semi-major axis of the orbit when calculated back in time prior to any planetary perturbations] (Opik, 1932). Utilizing the values of a_{orig} compiled for 19 observed comets, Jan Oort, in 1950, deduced the existence of Opik's hypothesized cloud, the now famous Oort cloud (Oort, 1950). The existence of the Oort cloud while not directly observed has been confirmed by subsequent dynamical studies, most recently by Brian Marsden (1989) using a far more extensive database of 200 well observed long period comets.

With evidence for the existence of the Oort cloud, the question switched to its creation. A satisfactory answer has

been found in current theories for the formation of the Solar System—stemming from the Laplace-Kant rotating nebula theory. Comets formed in much the same way as planetesimals and planets themselves formed but in orbits that prevented their accretion into the protoplanets. They were then perturbed by proto-Jupiter and by the other forming giant planets, in particular Uranus and Neptune in the region where these icy bodies are believed to have formed. Gradually their orbits diffused outward until eventually most comets were removed from the Solar System. However, once their orbits had grown to aphelion distances greater than 50,000 AU, they were exposed to the perturbations of nearby stars, molecular clouds, and Galactic tidal forces that prevented some 10% of the original population of comets from being lost to interstellar space. The galactic forces, in particular, forced changes in perihelion distance and inclination, removing the comets from further perturbation by the major planets and populating a reservoir estimated to be $\sim 10^{12}$ comets between about 2.0×10^4 and 10^5 AU, the Oort cloud. For excellent up-to-date reviews on the Oort cloud see Weissman (1991, 1995) and Fernandez (1994).

For the comets observed in the past 3-4 centuries, for which good orbit determinations are available, a traditional distinction exists between long-period (LP) comets with orbital periods in excess of 200 years and short-period (SP) comets with periods less than 200 years. These two dynamical classes of comets have several distinguishing features

amongst their orbital parameters. The LP comets are normally in very eccentric orbits essentially randomly oriented on the celestial sphere (i.e. they have no preferred inclination), while the SP comets generally have modest eccentricities and are found primarily in low inclination, i < 35 , orbits. The dynamical differences in these two classes present unique problems when explaining their source region(s). There is no dynamical evidence suggesting an extra-solar origin for any comet observed to date. Current debate focuses not on the direct observation of an interloper from outside the solar system but rather the potential of extra-solar comets being gravitationally captured into the Oort cloud.

The Oort cloud, discussed above, solves the source problem for long-period comets. While comets in the Oort cloud are relatively weakly bound to the solar system, the same forces that helped create the cloud (i.e. perturbations by passing stars, molecular clouds, and the galactic tide) can cause some comets to scatter into the planetary system where they can be observed. Scattering out of such a spherical cloud adequately explains the high eccentricities and random orientations prevalent in long-period comets.

While the Oort cloud naturally explains the isotropic inclination distribution of dynamically new and long period comets, it was questionable whether it could adequately account for the small inclinations of all short period comets, particularly those of the Jupiter family (those with periods of 5-20 years and aphelia near the orbit of Jupiter).

It has been proposed that the short-period comets were merely long-period comets that had suffered repeated planetary perturbations and diffused to short-period orbits (Newton 1893; Everhart 1972). This proposition encounters two problems: 1) how to explain the very different inclination distributions between short and long-period comets; and 2) whether the diffusion process of planetary perturbations is efficient enough to account for the observed SP comet population.

The proposed mechanism to provide the low inclination distribution of SP comets was capture of LP comets with low inclination orbits and perihelia near Jupiter and the other giant planets. The large perturbations from frequent low velocity close approaches to Jupiter (or the other major planets) allow for a rapid transition to orbits of small semi-major axis that could subsequently have their perihelia distances reduced by additional encounters. Under this hypothesis, the orbits of LP comets with high inclinations or with perihelia distant from any planetary orbits evolve slowly and have observable lifetimes that are shorter than the time necessary to evolve to SP orbits. While early efficiency calculations led to strongly conflicting SP comet population estimates (cf. Joss 1973, Delsemme 1973), by 1980 the capture scenario was generally considered quite plausible.

Cometary dynamics took its next step when Fernandez (1980) proposed a trans-Neptunian 'belt' of remnant icy

planetesimals as a more efficient dynamical source for SP comets. This 'belt' had previously been proposed in a seminal paper on the origin of the solar system by Gerard Kuiper (1951)[1] and currently bears his name. Such a disk as proposed by Kuiper fits in with the nebula formation theory discussed above, but has been waiting for observational confirmation. Very recent advances in observational techniques and equipment, particularly charge-coupled devices (CCD) have brought to fruition the searches for members of this proposed Kuiper Belt and to date, 17 objects have been reported (Jewitt + Luu 1994).

Over the last 15 years, much work has been done particularly in the area of computer orbital integrations to explore in detail the possible dynamical sources of SP comets. Evidence is continually mounting for two distinct reservoirs of comets, the Oort cloud and the Kuiper belt, as the sources of dynamically new and short-period comets respectively (cf., Duncan, Quinn, and Tremaine 1988; Mumma, Weissman, and Stern 1993). It is clear that the now confirmed Kuiper belt can efficiently provide many of the low inclination SP comets, especially those of the Jupiter family; however, Halley family comets of high inclination can

---

[1]As noted by Weissman (1995) in an excellent review of the subject, a trans-Neptunian disk of material had been proposed even earlier in a paper by Edgeworth (1949). Kuiper's paper, which referred to the condensation of volatile ices in the region beyond Neptune as a natural explanation of the formation of the icy conglomerate comets of Whipple (1950), has seemingly taken precedence over Edgeworth's discussion focusing on gravitationally bound 'clusters' of particles similar to Lyttleton's (1948) sandbank model of comets.

still be readily explained by a modified capture scenario with their origin in the Oort cloud. A more thorough exploration into the origins of comets is beyond the scope of this work and the reader is referred to the review by Weissman (1995) and references therein for further details.

A Giant Step, Halley Encounter

Cometary science took a quantum leap forward in 1986 with the apparition of comet P/Halley and the successful deployment of six spacecraft that conducted the first in situ studies of a comet. These spacecraft showed the nucleus of Halley to be larger, darker, and of a more irregular surface than many had previously anticipated, although still in quite acceptable agreement with the physics of Whipple's model. Coma studies conclusively showed water to be, by far, the principal constituent. At the same time, the coma was found to be highly structured at all measured scales with dust analyses indicating much higher than expected numbers of the very smallest grains. Several excellent reviews detailing the scientific results of the Halley encounters can be found in Mumma *et al.*, 1993, Heubner *et al.* in "Physics and Chemistry of Comets" edited by Heubner 1990, and Mendis, 1988.

The Present Work

Following the unprecedented success of the international armada of spacecraft that observed Comet Halley, many new

avenues of investigation were opened in cometary science. Of particular interest is the issue of how representative Comet P/Halley is of comets in general and therefore how we can apply what has been learned from Halley to other comets. One spacecraft, Giotto, was reactivated (although at diminished capacity due to instrument damage from particle impacts at close Halley flyby) in the summer of 1992 for a flyby of Comet P/Grigg-Skjellerup (Dickman, 1990), bringing to two our sample of comets studied in situ (sample of three considering the plasma tail analysis of Comet P/Giacobini-Zinner by the ICE spacecraft in 1985). Answers to many specific questions will require detailed analysis of other cometary nuclei. While direct ground based observations of nuclei have proven successful in a small number of cases (cf. Campins *et al.*, 1987; Millis *et al.* 1988; A'Hearn *et al.*, 1989; Campins *et al.*, 1994), earthbound astronomers are ordinarily limited to observing coma and tail phenomena. As a result, both the National Aeronautical and Space Administration, NASA, and the European Space Agency, ESA, have proposed future comet flyby and/or rendezvous spacecraft missions. Even with the fruition of these proposed missions, however, the sample of well studied cometary nuclei will necessarily be small.

While individual comets have been and will be intensively scrutinized either in situ or in wavelength regimes only accessible above the Earth's atmosphere (i.e. using the Infrared Space Observatory, ISO), a thorough exploration into the chemical composition and behaviour of

comets in general is possible with the accumulation of a statistically meaningful database of ground based cometary observations. In order to allow a meaningful comparison among a large number of comets, however, observations have to be obtained with uniform equipment and techniques. Furthermore, the data must be reduced using consistent models and parameters throughout.

In 1976, Drs. M. A'Hearn and R. Millis began a campaign of narrowband photoelectric photometry of comets with the long term goal of creating just such a database to compare relative molecular abundances and gas-to-dust ratios among comets and to investigate the influence of dynamical properties on these measured quantities. A'Hearn and Millis (1980) presented results for 12 comets observed in the first few years of the campaign. Since then a number of individual comets or select groups have also been analyzed separately (cf. Millis *et al.*, 1980, Schleicher *et al.*, 1987, Osip *et al.*, 1992a). The author has been involved with data acquisition, reduction, and analysis of this database since 1989 in an extensive collaborative effort with Drs. D. Schleicher and R. Millis at Lowell Observatory, Dr. M. A'Hearn at the University of Maryland, and Dr. P. Birch at Perth Observatory. A preliminary comparative analysis of all comets in the database was presented at the 1991 Asteroids, Comets, and Meteors symposium (Osip *et al.*, 1992b, A'Hearn *et al.*, 1992). Very recently, we have completed a thorough investigation of the ensemble properties of comets as derived

from over 2000 observations of 85 comets observed from 1976-1992 (A'Hearn *et al.*, 1995).

A detailed description of this full database and the reduction and analysis procedures is presented in Chapter 2. Chapter 3 includes our methodology in determining the ensemble properties of comets, along with appropriate background. Much of the reduction procedure and the data set described in Chapters 2 and 3 are shared with our current paper (A'Hearn *et al.*, 1995). Chapter 4 provides an in depth comparative analysis and taxonomy of comets. Trends between various emission species and dust are explored in addition to trends with dynamical properties. The taxonomic analysis provides the first complete classification of comets based on chemical composition. Finally, Chapter 5 summarizes the conclusions of this analysis and provides direction to future work in the field.

CHAPTER 2
THE DATABASE

Observational Method

The database presented here is comprised entirely of observations made utilizing conventional photoelectric photometers and narrowband filters isolating 5 emission species (OH, NH, CN, C_3 and C_2) and continua. This work was initiated by A'Hearn and Millis in 1976 and includes 2020 observations of 85 comets obtained over 429 nights through the end of 1992. The total number of observations, however, is not evenly distributed over the 85 comets. The median number of observations for a comet is 6, with only a single observation obtained for 14 comets while there were 820 observations of P/Halley. The majority of observations were obtained at either Lowell Observatory or Perth Observatory; however, four other observatories were used including an extensive campaign on comet P/Halley from the Cerro Tololo International Observatory (CTIO).

One 'observation' as defined here represents a set of measurements usually through at least 5 narrowband filters. A typical measurement sequence consisted of sets of 3 ten second integrations in each of two or three filters on the comet followed by a similar integration set on a sky position

about 30 arcminutes from the comet. This would alternate from comet to sky and sky to comet until data were collected for all appropriate filters. While this description illustrates the observational method, it is important to keep in mind that deviations were common. For example, filter integration times of 90 seconds or longer were often employed for faint comets while times as short as 10 seconds were used for bright comets at high airmasses. A night of observing would normally include comet observation(s) along with standard star measurements in all filters extending over a sufficient range of airmass (most often bracketing the comet observations) to accurately determine extinction coefficients. A complete discussion of standard stars and the zero point for the magnitude system can be found in Osborn *et al.* (1990).

Instrument and Filter Changes

Changes in instrumentation occurred over time, including the use of a number of different photomultiplier tubes and both pulse-counting and DC electronic systems. Of greatest importance, however, were changes in filters. The program began with a set of narrowband filters isolating the emission species CN, C_2, and C_3 as well as three continuum regions at 393, 412, and 524 nanometers (A'Hearn *et al.*, 1979). In 1979, filters isolating the emission species OH and NH were added along with an additional continuum filter at 367 nanometers (A'Hearn *et al.*, 1981). By 1984, the standardized

filters of the International Halley Watch (IHW) replaced the earlier filters at wavelengths greater than 365 nanometers (cf. IHW Archive for a detailed description of all filters). The NH filter was retained and the earlier OH filter continued to be used along with the new IHW OH filter for a period of about one year to confirm consistency. As the characteristics of the bandpasses of given interference filters can change over time, evidence for deterioration in any of the filters was closely monitored. Most of the filters have remained remarkably stable; however, several filters from the set at Perth showed systematic shifts of the bandpasses in 1989 and 1990. Data from Perth over this period have therefore been adjusted by factors estimated by convolving synthetic band profiles with the shifted transmission curves.

Reduction Procedures

Reduction to Fluxes

The initial data product consists of Universal Times and object and sky measurements. For pulse-counting systems, count rates were measured and corrected to first order for the dead-time of the detector using

$$n = n_{obs}/[1.0 - n_{obs}{}^{*}\tau]$$

where n and n_{obs} are the actual and observed counting rates and τ is the detector dead-time. For direct-current systems, readings from the DC amplifier were calibrated using standard

voltages. Actual counts were then converted to instrumental magnitudes using

$$m = 20.00 - 2.5 * \log[n_{obj} - n_{sky}].$$

The standard stars defined for the IHW (Osborn *et al.*, 1990) were used for extinction and absolute calibration to reduce the instrumental magnitudes to the standard magnitude system outside the atmosphere. Extinction coefficients were evaluated for each night by least squares fitting of magnitude vs. airmass for individual standards. A global least squares solution using all standards and simultaneously solving for the extinction coefficients and the zero point correction was also often employed. When individual standards indicated hemispheric (East-West) asymmetries, separate solutions were used for each hemisphere. In rare cases, when clear skies were available for only a short period of time, several nights were averaged together to define average extinction coefficients that were then applied. For all but the OH filter, the atmospheric attenuation is linear with airmass and in these cases airmass was calculated via the standard cubic polynomial

$$X = \sec Z - 0.0018167 * [\sec Z - 1] - 0.002875 * [\sec Z - 1]^2 - 0.0008083 * [\sec Z - 1]^3$$

where Z is the refracted zenith distance. In the case of the OH filter, the monochromatic attenuation changes appreciably across the bandpass. Therefore, a pseudo-airmass was modeled such that the attenuation would be linear in this variable.

A detailed description of the modeling procedure can be found in A'Hearn and Vanysek (1992) and references therein.

It is straightforward to convert from the standard system magnitudes to fluxes per unit wavelength in the continuum by simply applying a scale factor depending on the specific wavelength [cf. A'Hearn 1991, A'Hearn and Vanysek 1992]. However, a complication arises when dealing with the IHW 484.5 nanometer continuum filter. This filter includes a weak tail of emission from the $\Delta V = 0$ sequence of the Swan system of C_2. Fortunately, our C_2 filter measurements at 514 nanometers allow us to correct for this contamination in the continuum. Prior to 1992, this correction was done in magnitude units with the correction coefficient derived by A'Hearn (1978) based on theoretical spectra of the Swan bands of C_2. While this method is adequate for a small range of cometary gas-to-dust ratios, it oversimplifies the true situation (where comets with higher gas-to-dust ratios suffer increasingly more contamination) and thus fails to properly deal with contamination in the gassier comets. A'Hearn *et al.* (1995) show that the correction can be solved iteratively for any pair of observed magnitude values at 484.5 and 514 nanometers, and that the correction can be applied linearly to the fluxes such that

$$F_{cor}(4845) = F_{obs}(4845) - 0.034^* (F_{obs}(5140) - F_{obs}(4845)).$$

This correction has been adopted in the present work.

Recent spectral observations indicate that the C_3 band system in gassy comets can contribute flux over a much wider

than previously anticipated spectral range including significant contamination of the continuum bandpasses at 365 and 367.5 nanometers. An acceptable means of correcting for this contamination has not yet been reached, thus the continuum fluxes at these wavelengths are systematically high.

In order to derive the fluxes in the emission bands, the underlying continuum must first be subtracted. Assuming there is no gross structure in the continuum reflectivity of the cometary grains (i.e. they vary linearly with wavelength with respect to solar colors), it is possible to use observations of the comet in a pair of continuum bandpasses along with solar analog colors to evaluate the continuum contribution to an emission band. In this study we have used two pairs of continuum filters; 365-484.5 nanometers for the IHW filter set and 367.5-524 nanometers for the earlier data. For a small number of cases, no measurements were made in the shorter wavelength. In these cases we have either assumed the same continuum color as previously measured for the comet or, barring other observations, we have assumed solar colors. For gassy comets, the C_3 contamination in the 365 and 367.5 nanometer filters results in a systematic underestimation of the fluxes in the NH and C_3 bands that is anti-correlated with the cometary gas-to-dust ratio (i.e. the gassier the comet, the larger the underestimate of the true emission flux in NH and C_3). In the cases of OH and CN, the emission bands are so strong relative to the continuum that even in the

gassiest comets the effect of this flux underestimation is negligible. After removal of the underlying continuum, the emission band fluxes were converted to real units (ergs cm^{-2} s^{-1}) by multiplying by appropriate scale factors for each filter.

Fluxes -- Column Abundances of Emission Species

The emission band fluxes were converted to molecular abundances in the observed column by means of the fluorescence efficiency (L/N), commonly referred to as the g-factor. The g-factor values used in the present reduction are tabulated for a heliocentric distance of 1 ÀU in Table 2.1 along with other reduction factors and their sources.

The fluorescence efficiencies for OH (Schleicher and A'Hearn, 1988) and NH (Kim *et al.*, 1989) were interpolated from tables as a function of heliocentric radial velocity at 1 AU in order to account for the Swings effect -- the change in strength of the rotational lines of molecular spectra due to the Doppler shifting of the solar spectrum associated with the heliocentric radial motion of the comet. They were then scaled by the standard heliocentric distance (r_H) dependence of r_H^{-2}. For CN, a double interpolation in heliocentric radial velocity and heliocentric distance was used to account for the Swings effect as well as known deviations from the standard r_H^{-2} dependence (Schleicher 1983). Again the interpolated values were then scaled by r_H^{-2}. Fluorescence efficiencies for C_2 and C_3 are taken as single values scaled

by r_H^{-2}. The Swings effect is not prevalent in these bands due to the much larger number of lines involved as even a significant effect for an individual line will have basically no effect on the band intensities.

For no species did we take into account the effects of collisions even though they can potentially have a significant effect in the case of OH and NH in the near nucleus coma of an active comet. The reason for not considering collisional quenching was simply that all our observations were made with fields of view far exceeding the expected quenching zones. Variations with solar activity were also not incorporated due to the fact that the solar flux pumping the fluorescence is not in the far UV wavelength regime that changes appreciably over a solar cycle but rather is restricted to a limited wavelength range that is essentially insensitive to the solar activity cycle.

Column Abundances -- Molecular Production Rates

The column abundances for each species were converted to production rates by means of the classic Haser (1957) model. Essentially, cometary activity is taken to be a steady state, spherically symmetric outflow of parent molecules that photodissociates into observed daughter species which continue to expand radially and eventually either further dissociate or decay by ionization. This model is clearly not a rigorous representation, but more physically realistic

models contain more free parameters that in most cases are not known a priori.

Haser modeling consists of two steps. For a detailed description of the original model, the reader is referred to Haser (1957); the following is a brief explanation. First, two scale-lengths are required to infer the spatial distribution in the coma and allow extrapolation from the molecular abundance in a given field of view to the entire coma abundance. Second, the lifetime of the observed species is needed in order to calculate a production rate. If the parent species is known (not the case for most of our species) and a branching ratio for production of the daughter from the parent is also known, the production rate of the parent can likewise be determined. This study is limited to the production rates of the observed species, so the branching ratio is set to one.

The scale-lengths used for this reduction are all recently determined independently from wide-field CCD images and long-slit spectra (Randall *et al.*, 1992, Cochran and Schleicher 1993) and are presented in Table 2.1. The data used for the scale-length calculations did not cover a large enough range of heliocentric distance to determine a unique r_H-dependence. Since the coma itself is basically optically thin, a valid assumption is that all molecules in the coma are irradiated by sunlight. In this case, each molecule should have a mean lifetime before dissociation that varies as r_H^2. This variation is assumed to hold for the scale-

lengths. While it appears consistent with the data over a limited range in r_H, it is not a well determined quantity and could contribute to significant errors in the reduction of observations made at large heliocentric distances. Lifetimes, as indicated above, follow an r_H^2 dependence and in this study are assumed equal to the Haser model scale-lengths divided by a constant expansion velocity of 1 km/s. Expected photochemical lifetimes for OH and NH have been calculated (Schleicher and A'Hearn 1988, Feldman 1993) and the scale-lengths used in this study are consistent with those lifetimes. Photochemical lifetimes have not been independently determined for CN, C_2 or C_3.

As was the case for the g-factors, variations in solar activity have not been incorporated. Variations between quiet and active Sun should contribute to significant changes in the lifetime of H_2O and minor changes in the branching ratio and the lifetime of OH (Crovisier, 1989, Budzien, 1994). However, there is no correlation in any of our data for comets observed at both extremes of the solar cycle, indicating that the effect is not pronounced.

Continuum Fluxes - Dust Production

As a factor to compare intrinsic dust production from comet to comet, we have adopted the parameter $A(\theta)f\rho$, as described by A'Hearn *et al.*, (1984). The formula is

$$A(\theta)f\rho = q*r_H^2*\Delta*F\lambda/\alpha$$

where $A(\theta)$ is the Bond albedo at the observed scattering angle, θ; f is the filling factor of grains in the field of view; ρ is the radius of the circular field of view; r_H and Δ are heliocentric and geocentric distances [measured in AU]; $F\lambda$ is the mean continuum flux averaged over the filter bandpass [in erg cm^{-2} s^{-1} A^{-1}]; α is the angular diameter of the field of view [in arcsec]; and q is a filter dependent numerical coefficient that incorporates the solar flux within the filter bandpass (values of q for each continuum filter are also given in Table 2.1).

Provided the dust flows away from the nucleus without changing its velocity or breaking up and without brightening or darkening, $Af\rho$ will be proportional to the dust production rate. This provision is the equivalent of requiring the continuum brightness to follow a 1/r dependence where r is the distance from the nucleus. Note, however, that the continuum brightness profile should actually fall off faster than 1/r at large values of r due to the effects of solar radiation pressure. This is exactly the explanation used by Jewitt and Meech (1987) to explain departures from a 1/r profile that they observed in 7 comets. However, they observed an additional 3 comets with profiles that could not readily be explained by radiation pressure alone. Baum *et al.* (1992) reporting CCD observations of 14 comets found 10 to have steeper than 1/r brightness profiles in the continuum which they explain as evidence of grain fading (i.e. grains decreasing in albedo or size). Grain fading also adequately

accounts for the other 3 cases of Jewitt and Meech. Fortunately, significant deviations from a 1/r continuum brightness profile were limited to large r values, usually in excess of 10^4 km, greater than the projected aperture size for the majority of our data. Therefore, the assumption of a radial profile brightness of 1/r is appropriate for the aperture sizes used in our present study.

While the Afρ measure of the dust production is rather ad hoc, it serves as an adequate means, essentially independent of the aperture size, of comparing dust production between comets or for the same comet at different times. Again, this comparison does assume that neither the size distribution nor the physical properties of the scattering particles change with time or field of view. But with no available means of independently determining particle properties and size distributions for the observed comets, and with model dependent estimates of actual dust mass loss rates varying by orders of magnitude for P/Halley (where these quantities are constrained by in situ measurements), the Afρ parameter seems as accurate a predictor of dust production as currently possible. This measure of dust production is currently adopted for the IHW archive as well as in other spectrophotometric studies of comets (e.g. Cochran *et al.*, 1992, Storrs *et al.*, 1992) and will be used throughout the present analysis.

Error Propagation

Photometric uncertainties in the raw data were initially determined assuming the most common filter integration time of 30 seconds and using the rms scatter of the individual 1 second integrations. All uncertainties were expressed as percent errors. The best determined emission species was CN. By examining many observations of both faint and bright comets, an expression was derived to correct the uncertainties in the other species based on the well determined CN uncertainty (cf. A'Hearn *et al.*, 1995). Still, for the fainter comets, the filter integration times were usually longer than the assumed 30 seconds and therefore the raw uncertainties are overestimated.

The percentage uncertainties estimated for each filter were then propagated through the reduction procedure described in the previous sections. Additional uncertainties in the extinction coefficients, the zero point of the photometric system, and the flux transformation coefficients were added in quadratically. An additional source of uncertainty, the dominant source for the bright comets, was centering error due to the comet's motion and diffuse nature. In this study, we have quadratically added a centering error of 3% for measurements of the continuum and C_3 and an error of 2% for all other species. These values are higher for the continua and C_3 since these species have the most sharply

peaked spatial distributions. The errors were derived based on estimates of the standard centering precision of the observers and the results of test observations purposely made off center.

The final photometric flux errors provide an adequate representation of statistical uncertainties in the data. These percentage errors in the fluxes are representive of the uncertainties in most other derived parameters (e.g. column densities and production rates). In the case of gassy comets, these final errors underestimate the uncertainty in the C_3 and NH filters since they fail to include the additional error from contamination of the underlying continuum as previously discussed. There may be additional uncertainties, introduced from the choice of model parameters (e.g., scale-lengths, lifetimes), that are not well understood at this time. However, since they affect the results for all comets the same way (i.e. they will not affect a comparative analysis), they are not incorporated.

The Comets

We have rereduced 16 years of raw data adopting the procedures described above in order to create a database that was reduced in a uniform manner removing the effects of changes in instrumentation and model parameters. The resultant database contains 85 comets, 12 of which were observed on multiple apparitions and one, P/Encke, observed on 4 apparitions. The 85 comets are listed in Table 2.2, by

apparition in the case of short period comets, along with the ranges of heliocentric distance over which they were observed both pre- and post-perihelion.

This study includes 47 short period comets, defined as having periods less than 200 years, which is approximately 1/3 of the known short period comets. Further classification based on the Tisserand invariant with respect to Jupiter, T_J, places 39 of these objects as members of the Jupiter family and 8 as Halley family members (cf. Chapter 3 and Levison and Duncan 1994). The remaining comets are classified based on a measure of the dynamical age, $(1/a)_o$ - the reciprocal semi-major axis after integration of the orbit backwards prior to any planetary perturbations. This quantity is basically a measure of orbital energy and their is a very narrow peak in the distribution at a small positive value of approximately 3×10^{-5} AU^{-1}, indicating nearly parabolic orbits (cf. Oort, 1950; 1992). A single passage through the inner solar system will produce an average dispersion in 1/a almost a factor of twenty greater than the width of the observed peak (Oort, 1992). Therefore, the comets occupying this peak are referred to as "new" comets while progression to larger values of 1/a is used as a statistical measure of the number of passages a comet has made through the inner solar system. It is a measure of age in the sense that comets with more passages through the inner solar system have been evolved more by solar heating. Comets Cernis-Petrauskas 1980 IV, Machholz 1985 VIII, Levy 1990 XX, and Okazaki-Levy-Rudenko

1989 XIX are not classifiable, the first two due to parabolic (with $1/a_o = 0$) orbits being determined, and the latter two due to hyperbolic (with $1/a_o < 0$) orbits being determined. Such orbital determinations usually indicate that non-gravitational forces have not been adequately accounted for. In this study we treat these four comets as dynamically new but note that Marsden has suggested that the two hyperbolic comets may be long period in the Oort sense. Six comets are clearly dynamically new ($(1/a)_o < 50 * 10^{-6}$ AU^{-1}) and two others with $(1/a)_o = 53$ and $67 * 10^{-6}$ AU^{-1} could be dynamically new depending on where one places the somewhat arbitrary cutoff. The 27 remaining comets are classified as long period.

There is a general tendency for the comets, observed here over a wide range of heliocentric distance, to be intrinsically the most active due solely to the limiting magnitudes attainable with the available telescopes. The bias towards active comets was further exaggerated in the last few years of the survey when investigations of short term variability required frequent observation of bright comets. Other selection effects are not well defined, although periodic comets were often followed when relatively faint, while the same is not true for new comets. The other known bias is in the number of observations for comets, again with the brightest comets usually being observed over the widest range of heliocentric distance and having the greatest overall number of observations. This becomes important in

subsequent chapters when we must reduce the database to a set of meaningful parameters for each comet, or else the best observed comets like P/Halley will define 'typical' behaviour.

Other Data Sets

In addition to our database, there have been three other long-term observational programs to systematically obtain compositional information for a meaningful number of comets. Since 1978, spectra of approximately 50 comets have been observed at ultraviolet wavelengths by the International Ultraviolet Explorer (IUE) satellite. The only features present in all the IUE cometary spectra are the OH emission bands, while a number of other emission features are usually observed in brighter comets. To date, no uniform data analysis has been undertaken for the entire IUE data set. However, analysis of the first few years of data (cf. Weaver *et al.*, 1981) led the investigators to note the remarkable similarity among cometary spectra which they found suggestive of a similar composition and origin for those comets. The other two moderately extensive compositional surveys are ground based observational campaigns based on Image Dissector Scanner (IDS) visible spectrophotometry.

From 1979 to the present, A. Cochran and her collaborators have collected spectral observations for approximately 100 comets in the continuing McDonald Observatory Faint Comet Survey (Cochran, 1987). Summary

results comparing the abundances of CN, C_2, and C_3 among 48 comets—were published by Cochran (1989) while a subset of 29 "low activity" comets were treated in more detail in a paper by Cochran, Green, and Barker (1989). More recently, further analysis including the abundances of CH and NH_2 and studies of the dust continua and gas-to-dust ratio were performed for smaller subsets of 17 and 18 comets (cf. Cochran *et al.*, 1992 and Storrs *et al.*, 1992 respectively). The general result of the McDonald survey is that the composition of all comets is nearly the same; only one comet, P/Giacobinni-Zinner, clearly stood out as having significantly different molecular abundance ratios from other comets[1] with depletions of the species C_2 and C_3. However, analysis for many comets in their data set provided only upper limits for the C_2 and C_3 molecular abundances. Furthermore, they conclude that, with the exception of $Q(NH_2)/Q(CN)$, the ratios of production rates for a comet remain constant over the observed range of both activity level and heliocentric distance.

The other IDS program consists of observations of a total of 25 comets collected by Newburn and Spinrad (1984, 1985, 1989). They began in 1980 and measured the abundances of CN, C_2, C_3, CH, $O[^1D]$ and dust. Their general results include a clear correlation noted between CN and dust, this

---

[1]Comet P/Giacobini-Zinner has long been known to have anomalous abundances among comets (Brobovnikoff, 1927) and a number of recent studies quantify factor of 5 depletions of C2 and C3 with respect to water and slightly lesser depletions of NH and NH2 (e.g. Cochran and Barker 1987; Schleicher, Millis, and Birch 1987; Beaver *et al.*, 1990).

is in agreement with other observations indicating that CN appears to have at least two parent sources, dust and one or more parent gasses (e.g. A'Hearn *et al.*, 1995). In addition, they note several comets exhibiting depletions in the carbon bearing species relative to water. Comets Grigg-Skjellerup, Brooks 2, and Sugano-Saigusa-Fujikawa were noted as having the smallest amounts of CN, C_2, and C_3 with respect to water (based on $O[^1D]$ measurements), while comet P/Borrelly was found to be depleted in C_2 and to a lesser degree C_3 but not depleted in CN. Finally, in contrast to the results of the McDonald survey, Newburn and Spinrad noted that the $Q(C_2)/Q(CN)$ production ratio changes with heliocentric distance for all comets in their data set. It has been suggested that this apparent heliocentric distance trend may actually be an artifact due to the use of different scale-lengths in the reduction procedures (A'Hearn *et al.*, 1995).

Results from these other compositional surveys will be returned to in subsequent chapters, along with similar analysis of our database. However, it is important to note the fundamental differences between the spectroscopic approach adopted by the other two groups and our own photometric approach. The principal trade off is field of view for spectral resolution. The IDS surveys, with higher spectral resolution for a given field of view, can measure additional spectral features that are weaker relative to the continuum as they can more accurately determine and subtract the underlying continuum. Our use of larger fields of view

can compensate somewhat for this effect as it results in a higher-ratio of the spectral features relative to continuum owing to the steeper radial profile of the continuum. Furthermore, small field of view observations, like those used in the IDS surveys, are inadequate to characterize the spatial distribution of the coma. Thus, in order to avoid the production rate calculations becoming overly sensitive to the spatial distribution model parameters, the IDS surveys require additional measurements offset from the coma's brightest central condensation to be able to independently determine the spatial distribution. Simply, the use of large apertures that sample a much greater fraction of the cometary coma minimizes the effects of any potential inaccuracies in the scale-lengths adopted for the calculation of production rates. Therefore, the comparative analysis that is undertaken here is effectively less model dependent.

In addition to these methodological differences, the use of different model parameters necessarily results in some inconsistencies between data sets. For example, when extrapolating results to water production, our calculations are based on measured OH emission (where OH is the primary, 86%, dissociation product of H_2O) while the other surveys either assume a constant CN/OH ratio or base their calculations on $O[^1D]$ measurements (where $O[^1D]$ is a dissociation product of water at only a few percent level). When inconsistent results are found between our database and these other large data sets, it is important to be aware that

the differences may spawn from the choice of model parameters. This point will be returned to in subsequent chapters.

Table 2.1 Reduction Parameters

Emission Species Parameters

Species	Central Wavelength nanometers	Fluorescence Efficiency erg s-1 mol-1	Ref. #	Haser Scale Length Parent km	Daughter km	Daughter Lifetime sec.	Ref. #
OH	308.5	1.4-4.8E-15	1	2.4E+04	1.60E+05	1.60E+05	6
NH	336.5	4.9-7.6E-14	2	5.0E+04	1.50E+05	1.50E+05	7
CN	387.1	2.4-5.0E-13	3	1.3E+04	2.10E+05	2.10E+05	7
C3	405.0	1.0E-12	4	2.8E+03	2.70E+04	2.70E+04	7
C2	514.0	4.5E-13	5	2.2E+04	6.60E+04	6.60E+04	7

Continuum: Model Parameters

Wavelength nanometers	q-value
365.0	2.244E+17
367.5	2.150E+17
484.5	1.301E+17
524.0	1.330E+17
684.0	1.701E+17

Ref.1 Schleicher and A'Hearn (1988)
Ref.2 Kim et al. (1989)
Ref.3 Schleicher (1983)
Ref.4 A'Hearn et al. (1985)
Ref.5 A'Hearn (1982)
Ref.6 Cochran and Schleicher (1993)
Ref.7 Randall et al. (1993)

Table 2.2 Comets Observed

Comet ID	Comet Name	pre #	range pre-perihelion AU	post #	range post-perihelion AU
AJ	P/Ashbrook-Jackson (1978 XIV)	1	2.347	3	2.288
AR	P/Arend-Rigaux (1984 XXI)	1	1.499	60	1.571-1.664
AUSTI89C1	Austin (1990 V)	23	0.745-1.216	52	0.573-1.722
AUSTIN82G	Austin (1982 VI)	5	0.782-1.216	1	2.08
AUSTIN84I	Austin (1984 XIII)	4	0.548-0.660	3	1.214-2.119
BM	P/Brorsen-Metcalf (1989 X)	12	0.830-1.452	0	-
BOETHIN	P/Boethin (1986 I)	5	1.118-1.272	0	-
BORRELLY	P/Borrelly (1981 IV)	0	-	6	1.320-1.422
BORRELLY	P/Borrelly (1987 XXXIII)	18	1.390-1.398	28	1.359-1.853
BOWELL80B	Bowell (1982 I)	10	3.364-5.554	20	3.366-5.989
BRADFI79C	Bradfield (1979 VII)	0	-	2	0.960-0.978
BRADFI79L	Bradfield (1979 X)	0	-	24	0.570-1.648
BRADFI80T	Bradfield (1980 XV)	0	-	2	0.708
BRADFI87S	Bradfield (1987 XXIX)	6	0.930-1.119	31	0.896-2.289
BROOKS2	P/Brooks 2 (1980 IX)	5	1.984-1.990	0	-
BROOKS2	P/Brooks 2 (1987 XXIV)	5	1.849-1.851	0	-
BUS	P/Bus (1981 XI)	2	2.234	0	-
BUS81D	Bus (1981 XIV)	0	-	1	3.148
CERNIS83L	Cernis (1983 XII)	0	-	8	3.355-3.540
CG	P/Churyumov-Gerasimenko (1982 VIII)	3	1.341-1.356	10	1.354-1.862
CHERNYKH	P/Chernykh (1978 IV)	7	2.628-2.873	0	-
CIFFREO	P/Ciffreo (1985 XVI)	0	-	1	1.715
CP80K	Cernis-Petrauskas (1980 IV)	0	-	3	1.560-1.576
CROMMELIN	P/Crommelin (1984 IV)	2	0.789-0.796	9	0.735-1.092
DARREST	P/d'Arrest (1976 XI)	2	1.164	6	1.164-1.447
DARREST	P/d'Arrest (1982 VII)	0	-	4	1.334-1.654
ELIAS81C	Elias (1981 XV)	0	-	2	4.919-6.187
ENCKE	P/Encke (1977 XI)	1	0.85	6	0.632-0.705
ENCKE	P/Encke (1980 XI)	4	0.753-1.230	0	-
ENCKE	P/Encke (1984 VI)	4	0.634-1.162	12	0.554-0.913
ENCKE	P/Encke (1990 XXI)	18	0.532-0.791	0	-
FAYE	P/Faye (1984 XI)	0	-	1	1.792
FAYE	P/Faye (1991 XXI)	10	1.636-1.726	0	-
FURUY87F1	Furuyama (1988 IV)	1	1.799	0	-
GEHRELS2	P/Gehrels 2 (1981 XVII)	0	-	1	2.362
GS	P/Grigg-Skjellerup (1977 VI)	0	-	7	0.996-1.014
GS	P/Grigg-Skjellerup (1982 IV)	0	-	4	1.076-1.131
GS	P/Grigg-Skjellerup (1987 X)	0	-	1	0.994
GUNN	P/Gunn (1982 X)	3	2.633-2.638	2	4.054
GUNN	P/Gunn (1989 XI)	3	2.520-2.526	0	-
GZ	P/Giacobini-Zinner (1985 XIII)	13	1.053-1.507	14	1.030-1.457
HALLEY	P/Halley (1986 III)	147	0.870-2.630	673	0.670-5.130
HARTLEY2	P/Hartley 2 (1991 XV)	0	-	3	1.033-1.050
HC	P/Haneda-Campos (1978 XX)	1	1.177	0	-
HG85L	Hartley-Good (1985 XVII)	14	0.700-1.671	2	0.924
HI	P/Hartley-IRAS (1984 III)	0	-	1	1.721
HMP	P/Honda-Mrkos-Pajdsakova (1990 XIV)	1	1.154	0	-
HOWELL	P/Howell (1981 X)	0	-	8	2.090-2.101
IAA83D	IRAS-Araki-Alcock (1983 VII)	4	1.009-1.024	2	1.051
IRAS	P/IRAS (1983 XIV)	0	-	3	1.709-1.998
IRAS83O	IRAS (1983 XVI)	0	-	4	2.381-2.678
KK	P/Kearns-Kwee (1981 XX)	7	2.224-2.284	1	2.276

Table 2.2 Continued

Comet ID	Comet Name	pre #	range pre-perihelion AU	post #	range post-perihelion AU
KK	P/Kearns-Kwee (1990 XXV)	0	-	1	2.221
KLEMOLA	P/Klemola (1987 XIV)	0	-	6	1.907-1.919
KOHLER77M	Kohler (1977 XIV)	7	0.991-1.446	0	-
KOPFF	P/Kopff (1983 XIII)	19	1.683-2.152	2	1.607
LEVY90C	Levy (1990 XX)	243	1.053-2.420	35	1.426-3.006
LILLER88A	Liller (1988 V)	0	-	5	1.149
LR84T	Levy-Rudenko (1984 XXIII)	2	1.013	2	1.419-1.897
MACHHO85E	Machholz (1985 VIII)	1	0.906	0	-
MB	P/Metcalf-Brewington (1991 I)	0	-	3	1.600-1.645
MEIER78F	Meier (1978 XXI)	2	2.222-2.858	0	-
MEIER79I	Meier (1979 IX)	1	1.479	0	-
MEIER80Q	Meier (1980 XII)	2	1.523-1.583	6	1.522-2.191
NEUJMIN1	P/Neujmin 1 (1984 XIX)	0	-	1	1.568
NTT87C	Nishikawa-Takamizawa-Tago (1987 III)	1	1.2	1	1.83
OLR89R	Okazaki-Levy-Rudenko (1989 XIX)	3	1.183	86	0.683-1.138
PANTHE80U	Panther (1981 II)	2	1.682-1.689	5	1.854-4.561
RUSSELL4	P/Russell 4 (1984 I)	0	-	2	2.225
SC	P/Smirnova-Chernykh (1984 V)	1	3.558	1	3.56
SG89E1	Skorichenko-George (1990 VI)	2	1.614-1.617	0	-
SHOEMA83P	Shoemaker (1983 XV)	2	3.348-3.378	1	3.334
SHOEMA84F	Shoemaker (1985 XII)	4	2.983-4.957	1	5.59
SHOEMA84R	Shoemaker (1984 XV)	0	-	2	5.519
SHOEMA84S	Shoemaker (1985 II)	1	1.39	3	1.266-1.694
SHOEMAKE1	P/Shoemaker 1 (1984 XVI)	0	-	2	2.005-2.049
SL91A1	Shoemaker-Levy (1992 XIX)	8	0.841-0.941	0	-
SL91D	Shoemaker-Levy (1991 XXIV)	0	-	3	3.039-3.045
SO	P/Stephan-Oterma (1980 X)	17	1.575-1.950	12	1.576-2.170
SORREL86N	Sorrells (1987 II)	3	1.890-2.210	1	2.17
SSF83E	Sugano-Saigusa-Fujikawa (1983 V)	0	-	5	0.513-1.059
ST	P/Swift-Tuttle (1992 XXVIII)	3	0.974-0.985	0	-
SW2	P/Schwassmann-Wachmann 2 (1981 VI)	1	2.196	1	2.14
SW2	P/Schwassmann-Wachmann 2 (1987 XIX)	0	-	1	2.524
TAKAMIZAW	P/Takamizawa (1984 VII)	0	-	4	1.750-2.029
TAYLOR	P/Taylor (1984 II)	1	1.962	0	-
TEMPEL1	P/Tempel 1 (1983 XI)	12	1.517-2.054	0	-
TEMPEL2	P/Tempel 2 (1983 X)	2	1.391-1.467	2	1.384
TEMPEL2	P/Tempel 2 (1988 XIV)	63	1.713-1.719	0	-
THIELE85M	Thiele (1985 XIX)	9	1.322-1.456	0	-
TK90I	Tsuchiya-Kiuchi (1990 XVII)	12	1.276-1.564	4	1.769-1.780
TSUCHINS1	P/Tsushinshan 1 (1985 I)	0	-	1	1.727
TUTTLE	P/Tuttle (1980 XIII)	3	1.116-1.384	0	-
WH	P/Wolf-Harrington (1984 XVII)	0	-	1	1.617
WH	P/Wolf-Harrington (1991 V)	6	1.685-1.946	0	-
WILD2	P/Wild 2 (1978 XI)	10	1.493-1.803	0	-
WILD2	P/Wild 2 (1984 XIV)	4	2.254-2.621	0	-
WILD4	P/Wild 4 (1990 X)	2	2.156-2.159	0	-
WILSON86L	Wilson (1987 VII)	3	2.470-3.250	4	3.527-4.393
WIRTANEN	P/Wirtanen (1991 XVI)	0	-	1	1.118

CHAPTER 3
COMETARY PROPERTIES

Introduction

The aim of this chapter is to elucidate the ensemble properties of comets and develop a means of investigating meaningful variations of these properties among comets. In order to begin comparing results from comet to comet, we must first determine for which properties we can define normal points that are indeed representative of the comet. As our data set contains comets observed over a wide range of heliocentric distance (r_H), we must first characterize how their production rates and abundance ratios vary with r_H. To this end, we have binned our data into 11 evenly spaced bins at intervals of 0.1 in $\log(r_H)$ in order to more readily assess the variation in different comets without being overwhelmed by multiple observations of the same comet.

Each bin of the binned data set consists of weighted mean values for the production rates of the emission species OH and CN, as well as Afρ as a measure of the dust. No heliocentric distance dependence correction is included within a bin; under the assumption that even if the only point in the bin is at one edge, a canonical variation of

$1/r_H2$ would introduce a 10% error[1]. In addition to the production rates, weighted mean values for all molecular abundance ratios (compared to both OH and to CN) along with gas-to-dust ratios are calculated for each bin. Again, no heliocentric distance dependence is included: the justification of this assumption will be elaborated on in the following sections.

The weighted mean values were calculated in linear space for all cases and the weighting was based on the uncertainties associated with the individual points. Weighted standard deviations, expressed as percent errors, were also calculated for all cases. In order to allow for any real changes in an individual comet's activity related to perihelion passage, we have also separated the pre-perihelion from the post-perihelion observations, leading to 22 bins of data. Not all comets are represented both pre- and post-perihelion, nor are they represented in all heliocentric distance bins. The full 22 bin data set is tabulated in the Appendix; all production rates are presented as logarithms and all ratios are presented as log differences, with errors expressed as percents.

Evaluating Variations with Heliocentric Distance

To first order, the best means of evaluating the variation of production rates and molecular abundance ratios

---

[1]This error becomes negligible when averaging the points across the bin for the well observed comets used to evaluate trends in subsequent sections.

with heliocentric distance is by examining those comets which occupy the largest number of our r_H bins. This analysis is valid only to first order because of a selection effect naturally introduced against any comets with very steep variations against r_H. Unless such comets were extraordinarily active, they would not exceed our threshold of sensitivity over a substantial heliocentric distance range. This is indeed the case for many of the short-period comets in our database that have production rates varying steeply with r_H. This steep heliocentric distance dependence is almost certainly due to seasonal effects on nuclei that are only active over a small fraction of their surfaces (e.g. Sekanina 1988). Seasonal variations result from changing pole orientation for a comet around its orbit leading to changes in the exposure time of active surface regions to solar radiation; this effect is analagous to seasonal differences on the Earth.

Six comets in our database have data traversing 5 or more r_H bins: comet P/Halley, the only SP comet in this group; comets Austin 1984i, Austin 1989c1, Bradfield 19791, and Bradfield 1987s, all long-period comets; and comet Levy 1990c, a possible dynamically new comet. Figure 3.1 displays the binned production rate data for OH, CN, and dust for all comets in our database with the above six separated by symbol type.

The first thing we notice in these plots is that no one r_H-dependence can be properly applied to all comets. This

means that barring observations being made to independently evaluate the variation with r_H, a comet's production rates cannot be accurately extrapolated to other heliocentric distances and therefore, it is not possible to properly compare our data set using some form of normalized production rates.

The second feature to notice in these plots is that the variation with r_H departs from a simple power law, especially in the case of OH (figure 3.1 top panel). Three of the highlighted comets peak in their OH production at heliocentric distances between 0.75 and 1.5 AU and have similar or lower production rates closer to perihelion. At small heliocentric distances, inside of 1 AU, we must question how much of the decrease in OH production is real and how much can be simply an artifact due to the use of Haser model scale-lengths that do not adequately account for physical changes in the comet at these distances. For example, at small r_H, significant optical depth in the OH emission spectrum or at the UV wavelengths responsible for the dissociation of water would lead to a larger OH parent scale-length, which in our Haser model would lead to production rates that underestimate the true value. Previous studies have shown that, even in active comets, the OH emission cannot be optically thick (Schleicher and A'Hearn 1988). This leaves significant optical depth in the coma at the water dissociation wavelengths as a plausible alternative. If this were the case, however, we would expect

the effect to correlate well with the absolute OH production rate; the top panel of figure 3.1 demonstrates that this is not the case. This issue will not be fully resolved until spatially resolved long slit spectra of the OH spectral emission region are available for a comet observed at small heliocentric distance. Fortunately, as we will see in the next section and Chapter 4, the uncertainties introduced in the Q(OH)/Q(CN) molecular abundance ratio are not significant enough to appreciably change any of our conclusions.

Comparing comets based on the absolute production rates of the emission species and dust is not possible for objects observed over a wide range of r_H and having varying or undetermined r_H-dependencies. The next option is to evaluate the behaviour of ratios in the production rates (i.e. molecular abundance ratios and gas-to-dust ratios) as a function of heliocentric distance. In figure 3.2, the weighted mean ratios of OH, NH, C_2, C_3, and dust production to the production of CN are plotted as a function of heliocentric distance for our 22 bin data set, again with the 6 comets observed over the widest range separated by symbol type. It is evident that in almost all cases the ratios do not significantly vary even over a large range in heliocentric distance. Furthermore, the variations present for an individual comet are negligible compared to the range of variation amongst comets.

For all ratios, the data at large r_H shows a greater scatter from comet to comet, perhaps indicating greater

intrinsic variation among these comets. While part of this effect—is likely real, it is certainly in part due to poorer signal-to-noise measurements at large r_H. Furthermore, it is also in part attributable to the recurrent problem of high sensitivity in the models to assumed scale-lengths at very large or very small heliocentric distances. While some investigators have adjusted their model scale-lengths in order to minimize or eliminate apparent chemical variations, we note that in the present study, all scale-lengths were independently determined and no such adjustments have been made. Rather than arbitrarily alter model parameters, we allow that the scale-lengths that we have adopted are best used over a restricted range of heliocentric distance, namely inside of 3 AU. This restricted range was determined by testing the effect of varying the parent and daughter scale-lengths and evaluating at what locations the model results drastically changed.

If we exclude the data points at large r_H for comet P/Halley in figure 3.2, for an individual comet, the total range of variation in Q(C2)/Q(CN) or Q(C3)/Q(CN) is less than a factor of 2 while for Q(OH)/Q(CN) and Q(NH)/Q(CN) it is less than a factor of 3. The gas-to-dust ratio is also remarkably constant with r_H for an individual comet, with comet Austin 1984i, of our restricted sample, showing the only noticeable variation between observations made pre- and post-perihelion. The conclusion that we can reach is that these molecular abundance ratios and gas-to-dust ratios do

not have a substantial r_H-dependence, and for observations made over a wide range of heliocentric distance, they can serve as an accurate means of comparing the chemical composition of comets. This is the same general conclusion reached by Cochran *et al.* (1992) from the McDonald survey regarding the emission species ratios. Regarding the gas-to-dust ratio, Storrs *et al.* (1992) point to no obvious trend in this ratio with r_H, but, they note a trend with overall gas production which they extrapolate from the CN production rate. They explain that the trends observed in individual comets cannot be used to assess trends in the ensemble of comets nor are the changes in gas-to-dust ratio with activity sufficient to distinguish among comets. This trend of gas-to-dust ratio with gas production, suggested by Storrs *et al.*, is not confirmed in our present analysis and is also in contrast to the earlier analysis of Williams *et al.* (1989).

Since none of the 6 comets representing our database in 5 or more heliocentric distance bins are members of our largest dynamical group, the Jupiter family, we have extended our analysis of r_H-dependencies to a larger data set in order to confirm our findings. As many of the short-period comets were well observed, just not over a wide range in r_H, we have used the initial individual data to calculate power law slopes for the r_H-dependence of all species both pre- and post-perihelion. Least-squares fits to the individual data for all comets with 4 or more observations over 3 or more nights are given in table 3.1. The variation in heliocentric

distance dependence among comets is quite remarkable, however, in general the variation from species to species within a given comet are modest with only dust production consistently having a shallower slope than the emission species.

While Newburn and Spinrad (1989) noted that the $Q(C_2)/Q(CN)$ ratio changed continuously with r_H for all comets they observed, it is important to note that the variation that they refer to is less than a factor of 3 for all but one comet, and all of their comets were observed in only 1-3 of our r_H bins. Indeed, we too see minor variations in the production rate ratios of some of the same comets, in particular Jupiter family comets observed near perihelion when seasonal effects on the nucleus are most pronounced. Differences in the r_H-dependencies of the emission species in table 3.1 indicate a qualitative agreement with Newburn and Spinrad (1989) regarding continual changes in the abundance ratios, however, the magnitude of this effect is quite small[2], especially when comparing ratios of different comets. Thus, the results in table 3.1 confirm the previous conclusions that it is difficult to compare comets based directly on their production rates as the r_H-dependence of production rates varies substantially among comets. On the other hand, the molecular abundance ratios and gas-to-dust

[2]The magnitude of this effect differs between our analysis and that of Newburn and Spinrad due to the different model parameters adopted.

ratio serve as adequate comparison tools since, for a given comet,—they show only weak systematic trends with r_H.

Parameterizing cometary chemical composition

Since the molecular abundance ratios and gas-to-dust ratio are nearly independent of r_H, we can compare comets observed over a wide range of r_H by parameterizing their chemical composition based on these ratios. This allows us to reduce our database to a set of values for each comet with one mean value for each ratio of abundances. In each case, the individual ratio data (no longer the binned data) were weighted by their observational uncertainties and a mean abundance ratio was calculated representing a comparative measure of that comet's chemical composition. Table 3.2 provides logarithms of the mean ratios of all available production rates with respect to both OH and CN for each of the 85 comets in our survey. Weighted standard deviations, expressed as percents are also provided in table 3.2.

The ratios are calculated with respect to CN as this is our best observed species and as indicated above, for an individual comet, the scatter in ratios, Q(X)/Q(CN), is minor compared to the scatter among comets. Therefore, these ratios are used for our investigation of taxonomic classification of comets based on chemical composition in Chapter 4. In addition, ratios are provided with respect to OH. OH, as the primary dissociation product of water, the principal constituent of comets, is a good measure of the

total production of gas. By comparing species ratioed to this measure of the overall gas production, we can search for trends between species without being overwhelmed by inherent trends in our data due to heliocentric distance dependencies. This method of effectively comparing species normalized to total cometary activity has been successfully used by others (e.g. Newburn and Spinrad 1989) and will be investigated in the comparative analysis of Chapter 4.

Parameterizing cometary absolute productivity

With a measure of the chemical composition of comets suitable for comparative analysis between comets, the next property to determine is a valid comparative measure of productivity. Ideally, we would be able to determine the total amount of dust and gas released by each comet in one perihelion passage. Unfortunately, the present database does not contain sufficient information to accurately determine such quantities.

Other investigators have used visual magnitude measurements to evaluate the inherent activity levels of different comets (most recently, Hughes 1987; Kresak and Kresakova 1987, 1989, 1990; Whipple 1992a). Unfortunately, the data sets collected for analyses of this type are extremely inhomogenous and severely biased by instrumental effects. In these studies, the activity level is usually characterized by two parameters, the absolute magnitude for the comet normalized to heliocentric and geocentric distance

of 1 AU and the heliocentric distance dependence of the visual magnitude. The classical absolute magnitude of a comet, H, has been defined (e.g. Whipple 1992a) as

$$H = m + 2.5n - 5\log(\Delta) - 2.5n\log(r_H)$$

where m is the observed magnitude, n is the inverse power of r_H in the luminosity equation and Δ and r_H are geocentric and heliocentric distances expressed in AU. Typically it is found that for active comets near perihelion a value of approximately 4 is appropriate for n. This value should decrease to the theoretical limit of 2 for comets observed at large r_H if indeed the comets become inactive and are merely reflecting sunlight as inert bodies.

In a series of papers, Kresak and Kresakova (1987, 1989, 1990; hereafter KK1987, KK1989, KK1990 respectively) have accumulated observations covering 575 apparitions of 144 periodic comets from 1770 to 1987 and attempted to create an internally consistent list of absolute total magnitudes for all comets over all observed apparitions. In general, they assumed a brightness dependence on the inverse fourth power of the heliocentric distance and made empirical corrections for instrumental differences: for a detailed explanation regarding their methods, the reader is referred to KK1987, KK1989 and references therein. Searching for physical differences in dynamical classes of comets, KK1987 (their figure 2) report significant differences in the logarithmic cumulative absolute magnitude distributions of Halley-family (period of 20-200 years) and Jupiter-family (period of up to

20 years) comets. Such a difference is also reflected in trends—in the discovery rate of these two groups and was independently confirmed by Hughes (1987) albeit using a data set with large systematic differences in the absolute magnitude values from those adopted by KK1987. The explanation forwarded for these differences was different past orbital evolution or different origin. We will return to these differences in the next chapter when discussing taxonomic classification of comets based on their chemical composition.

A quite different activity index was proposed by Whipple (1992) measuring the increase in activity as the difference in visual magnitudes for comets when observed at their brightest, near perihelion, versus the reflective brightness at large heliocentric distances, assumed due to an inactive nucleus. Ideally, this activity index (AI) is simply the magnitude difference observed for a comet from its inactive state to its state of highest activity. In reality, it turns out that comets are rarely, if ever, actually observed in completely inactive states[3]. Still, while the faint and bright magnitude systems adopted by Whipple are admittedly imperfect, they do retain an internal consistency that is most valuable for comparing classes of comets.

In deference to the problem of inhomogenous data sets and biases introduced by different instruments, Whipple

---

[3]A notable exception exists in 4015 Wilson-Harrington, a 'dormant' comet that currently appears inactive throughout its orbit (Osip *et al.*, 1995; Campins *et al.*, 1995).

wisely chose to apply his 'activity index' to a restricted high quality homogenous database. Using the exceptional data set compiled over 4 decades by Max Beyer (cf. Beyer 1969 and references therein) to provide a uniform magnitude system for the high activity observations, Whipple compiled the low activity magnitude estimates from the separate works of Jeffers, Van Biesbrock, and in large part from Roemer and her associates (references in Whipple 1992). The analysis was restricted to the brighter comets observed by Beyer leading to a database of 32 LP and 15 SP comets. The general conclusions from Whipple's tentative application of his new activity index were; 1) there is no evidence to suggest an effect due to aging among LP comets, 2) nor is there evidence to suggest "a drastically different environment for the origin of LP vs. SP comets, or for large subgroups among them". In chapter 4 we will take issue with this second general conclusion, however, our analysis benefits from the ability to classify comets based on chemical composition rather than only the activity level.

A limitation of visual magnitude studies is that they are not diagnostic of composition. The flux measured in any visual magnitude estimate is an unknown combination of fluorescent emission in the visible spectral region by gaseous species (primarily C_2), and scattering from coma dust particles. When comparing activity levels among comets we would prefer to compare the overall production of known constituents, especially the principle constituent, water.

Alternatively, one could compare the absolute or fractional active-area on comets as investigated for a limited sample by Rickman *et al.*, 1987.

A possible approach, analogous to the visual magnitude studies would be to provide normalized production rates for the various emission species along with calculated heliocentric distance dependencies for those species. However, as explained at the beginning of this chapter, the present database cannot support such a calculation. First, the variation with r_H is simply not known for all species for all comets. Second, there is the practical concern that comets with large perihelion distances are simply not observed at heliocentric distances as small as even the most distant observations of other comets with small perihelia.

In the absence of an ideal measure of the total global gas and dust production, and unable to normalize production rates to a common heliocentric distance for all comets, we compare activity levels by modeling the active surface area responsible for the observed production rates. In this way we can assess variations in intrinsic activity level between comets. By then calculating, for each comet, the maximum water production rate resulting from the derived surface area when exposed to sunlight at perihelion, we also develop a means of assessing variations in the peak activity level between comets.

We adopt the model of Cowan and A'Hearn (1979) to calculate the expected rate of vaporization of water per unit

area from the nucleus. All nuclei are assumed to be dark with a geometric albedo of approximately 0.05. The spacecraft encounters with P/Halley verify a low albedo surface (Keller *et al.*, 1987) as do ground based visible and infrared studies of cometary nuclei (cf. Campins *et al.*, 1994; A'Hearn *et al.*, 1989; Millis *et al.*, 1988; Campins *et al.*, 1987). In all cases, we take the extreme model case of a nucleus with the pole of its rotation axis pointed toward the Sun. This case physically represents a non-rotating nucleus or a nucleus with negligible thermal inertia and leads to the maximum average outgassing per unit area. The other model extreme would be for a nucleus with its rotation axis perpendicular to the sunward direction, representing a rapidly rotating or high thermal inertia nucleus. This extreme case leads to the minimum average outgassing per unit area and subsequently to surface active areas approximately 1.75 times larger than we would have obtained for the opposite extreme (cf. Osip *et al.*, 1992).

The model water vaporization rates are combined with our OH production rates in order to evaluate the minimum nucleus surface active area necessary to provide the observed production. Rather than run the vaporization model for every conceivable heliocentric distance observed in our full database, we have instead utilized the 22 pre- and post perihelion, r_H binned data set. In the cases where no OH measurements were available for a given comet, we have used the CN production rate multiplied by the mean ratio of OH to

CN ($\log(Q(OH)/Q(CN)) = 2.5$; cf. chapter 4, table 4.1). In addition, for dynamically new comets with only pre-perihelion observations, we have used modified CN observations rather than the observed OH production rates. This exception is due to the fact that the pre-perihelion OH production in dynamically new comets is recognized to come primarily from icy grains in the coma rather than the nucleus (cf. A'Hearn *et al*, 1984; Hanner *et al.*, 1984; Campins *et al.*, 1982; A'Hearn *et al.*, 1995). When both pre- and post-perihelion observations exist for dynamically new comets, we have used only the post-perihelion OH data. Owing to both uncertainties in the scale-lengths and to the fact that the vaporization model becomes less reliable at large r_H, we have excluded all observations at heliocentric distances beyond 3 AU. For all data points, we have converted the Haser model OH production rate to a water production rate to compare with the model values. This conversion uses the known branching ratio for the dissociation of water and makes an empirical correction to the scale-lengths to mimic an observed variation as $r_H^{-0.5}$ in the parent outflow velocity. By comparing the water production rate calculated from observations for each comet in each bin to the vaporization rate per unit area predicted by the model for that bin, we estimate the minimum active surface area required for the comet observed at that distance. For any comet observed in multiple bins, the minimum active surface area will vary, most likely due to some form of seasonal variation on the

nucleus (i.e. over the orbit, different fractions of the surface active region will be exposed to sunlight). With the exceptions noted above, we have taken the maximum value of the minimum surface active area for each comet and the results, expressed as km^2, are tabulated in table 3.3. Also in table 3.3 are the maximum water production rates calculated from our vaporization model for the given surface active area if at perihelion. For comets that are active only over a small fraction of their surface, the maximum water production rates in table 3.3 can be in excess of observed water production rates at or near perihelion. This is due to seasonal effects that change the aspect of the active areas through the comet's orbit.

As previously explored for a handful of comets by Rickman *et al.* (1987) and for a subset of our database by Osip *et al.* (1992), we have also calculated fractional active areas for those comets for which nuclear radii estimates are available in the literature. In addition to the in situ measurements of P/Halley (Keller *et al.*, 1987) and the radiometric radii calculated for P/Arend-Rigaux, P/Neujmin 1, and P/Tempel 2 (Campins *et al.*, 1987; Millis *et al.*, 1988, A'Hearn *et al.*, 1989 respectively), we have included the radii estimates for 17 comets by Luu and Jewitt (1990, 1992), Meech (1994), and Scotti (1995). Using these nuclear radii estimates along with our determinations of the active surface area we have calculated the percentage active areas for these comets and also tabulated these results in table 3.3. All

but 3 of the comets with percentage active area estimates are SP, and there is a strong selection effect for determining nuclear radii to comets that are relatively inactive.

Our estimates for the active area for P/Halley are consistent with the values obtained from in situ observations providing some level of confidence in our methods. Note, however, that had we not excluded the data at large heliocentric distances, our observations of P/Halley beyond 3 AU would have led to an estimate of the active area 14 times larger, significantly larger than the known physical dimensions of the nucleus. This is an example of the extreme sensitivity of the models using parameters extrapolated to large r_H as well as uncertainty in the assumption that vaporization of grains does not play a significant role at large r_H. It is already known that in the case of dynamically new comets, there is a pronounced contribution from the grains. Comet Shoemaker 1984r, which was observed only at large r_H, also suggests significant vaporization from grains as the active area estimate exceeds the entire nuclear surface. The implications of icy-grain halos around distant comets is explored in greater detail by A'Hearn *et al.* (1995).

Dynamical Properties

The physical properties attributable to the comets in our database have been broken down to include measures of the chemical composition and of the activity level for each

comet. In addition to these physical properties, each comet has a set of well determined dynamical properties associated with its orbital motion. These dynamical properties include the present orbital parameters; a (semi-major axis), e (eccentricity), i (inclination), and q (perihelion distance), in addition to a measure of the dynamical age of the comet, (1/a)o (the pre-encounter or original reciprocal semi-major axis). This latter parameter measures the comet's age in a statistical fashion as first pointed out by Oort (1950). Dynamically new (DN) comets, those that are entering the inner solar system for the first time, are traditionally distinguished as having values of $(1/a)o < 50*10^{-6}$ AU^{-1}. Large differences in (1/a)o from the values associated with DN comets statistically represent more passages through the inner solar system, therefore this parameter gives a measure of the exposure of comets to solar insolation and thus the dynamical age. In order to search for evolutionary effects, we further separate the LP comets into young (YLP) and old (OLP) at $(1/a)o = 2000*10^{-6}$ AU^{-1}. We have placed the 2 comets with hyperbolic orbits indicated and the 2 comets with parabolic orbits indicated into the DN group.

Levison and Duncan (1994) point out that in orbital integrations of SP comets, most comets move between 'Jupiter-family' and 'Halley-family' many times over their dynamical lifetime if the classical distinction of orbital period is used to separate these groups. They find that the Tisserand Invariant with respect to Jupiter, T_J, is the best diagnostic

for determining to which dynamical family each SP comet belongs. T_J is essentially invariant over a comet's lifetime and therefore is considered a more appropriate parameter for distinguishing these SP dynamical classes. We adopt the same class definitions used by Levison and Duncan (1994) and originally proposed by Carusi *et al.*, (1987) with 'Jupiter-family' (JF) comets having $T_J > 2$ and 'Halley-family' (HF) comets having $T_J < 2$. However, this is still a statistical parameter and is not completely valid in all cases. For instance, comet P/Encke would strictly classify dynamically as an asteroid with $T_J > 3$. Dynamical parameters for all comets in our database are given in table 3.5 along with their dynamical classification. The dynamical properties are taken from the Catalog of Cometary Orbits (Marsden 1994) supplemented with additional information provided by B. Marsden (personal communication). In the case of comets with indeterminate semi-major axis due to estimated eccentricities equal to or exceeding one, no estimation is made for the value of T_J. Following the discussion of Chapter 1, we expect that the DN and LP comets come from the Oort cloud along with the HF comets while the JF comets, at least statistically, come from the Kuiper belt.

The tabulated results from this chapter provide the restricted data set of individual cometary properties to be compared and analyzed in Chapter 4. The molecular abundance and gas-to-dust ratios serve as measures of the chemical composition while the estimated active areas provide the best

means of comparing intrinsic activity levels. These cometary properties along with the dynamical properties of their orbits allow the investigation into evolutionary trends among and within comets. Furthermore, the present data set allows the establishment of the first cometary taxonomy based on differences in chemical composition.

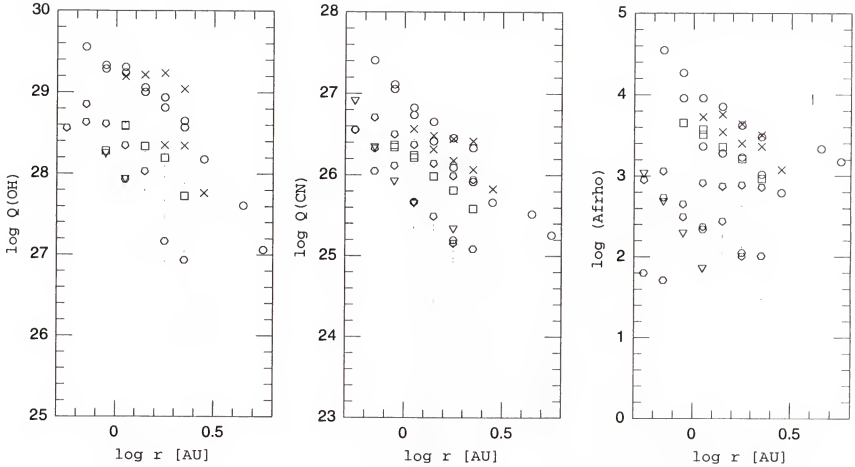

Figure 3.1 Production Rates vs. Heliocentric distance for the 22 bin data set. Different symbols are used to distinguish the 6 comets that are observed over 5 or more r_H bins.

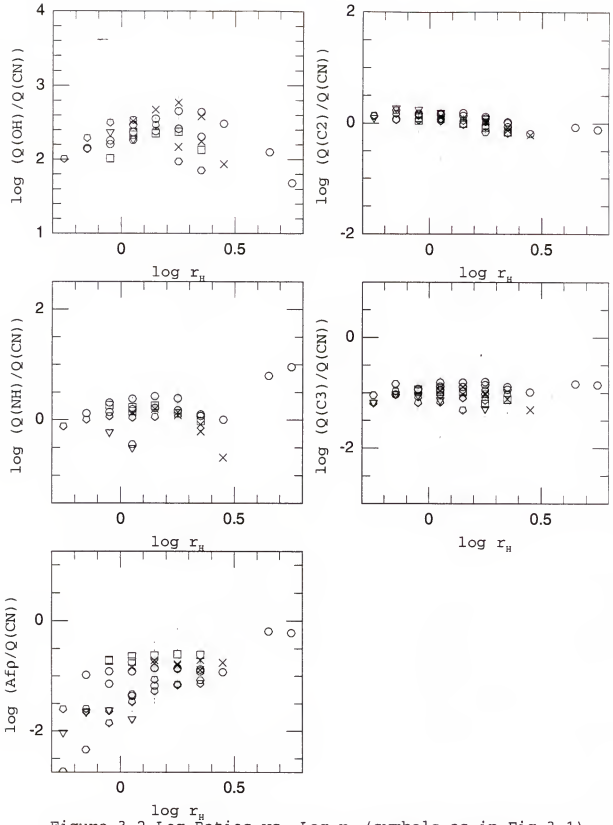

Figure 3.2 Log Ratios vs. Log r_H (symbols as in Fig 3.1)

Table 3.1 Production Rate Slopes

Comet ID	pre/post		log	prod.	rate	vs.	log	rH	power	law	slope	value	
	perihelion	OH	sigma	NH	sigma	CN	sigma	C3	sigma	C2	sigma	Afrho	sigma
AJ	post					4.71	0.92			12.17	2.6	8.89	1.38
AUSTI89C1	pre					1.39	0.13	0.75	0.43	1.82	0.12	-0.08	0.14
	post	1.61	0.19	2.48	0.27	2.91	0.1	3.06	0.2	3.47	0.08	2.38	0.07
AUSTIN82G	pre					2.96	0.42	1.43	1.12	2.97	0.73	0.64	1.93
AUSTIN84I	pre					5.69	0.25	3.15	0.26	4.33	0.26	2.04	3.12
	post	3.54	0.5			1.82	0.34			2.2	1.24	0.74	0.25
BM	pre	3.91	0.13	4.8	0.27	3.4	0.11	3.21	0.11	3.66	0.05	3.75	0.49
BORRELLY	post	12.78	0.43	8.62	0.43	7.65	0.18	6.05	0.75	9.74	0.87	4.59	0.32
BRADFI79L	post	3.14	0.36	2.47	2	3.54	0.27	3.87	0.22	3.7	0.18	3.3	0.21
BRADFI87S	post	1.49	0.21	2.49	0.2	1.93	0.07	2.4	0.15	2.52	0.06	1.68	0.04
CG	post	5.36	0.9	3.23	1.55	3.23	0.88	6.53	1.84	2.64	1.28	1.34	0.81
CROMMELIN	post	4.34	0.28			5.48	0.37	3.48	0.68	3.84	0.51	2.86	0.51
ENCKE	pre	1.78	0.25	1.9	0.42	4.02	0.2	3.47	0.29	3.78	0.2	0.81	0.5
	post	2.86	2.08			3.94	0.39	1.57	0.4	3.11	0.45	2.99	0.49
GZ	pre	3.63	0.2	3.05	0.26	0.75	0.08	1.77	0.12	1.92	0.18	2.08	0.15
	post	2.77	0.33	2.88	0.6	1.31	0.22	0.75	0.73	1.23	0.26	-0.38	0.16
HALLEY	pre	1.94	0.12	3.17	0.12	3.08	0.08	2.88	0.08	3.56	0.08	2.2	0.12
	post	2.04	0.06	1.8	0.06	2.29	0.05	2.2	0.06	2.55	0.05	1.68	0.04
HG85L	pre	0.62	0.15	1.35	0.13	2.06	0.05	1.99	0.05	2.15	0.08	0.29	0.17
IRAS	post					5.78	0.76					6.24	1.09
KOHLER77M	pre					2.55	0.56			2.11	0.43	1.87	0.25
KOPFF	pre	7.91	1.14	9.98	2.66	4.08	0.54	13.36	1.29	4.8	0.88	2.32	0.68
LEVY90C	pre	0.63	0.07	2.2	0.11	0.47	0.06	0.83	0.06	1.02	0.06	0.63	0.09
	post	4.16	0.45	3.67	0.83	1.59	0.12	2.64	0.21	2.67	0.1	1.51	0.15
MEIER80Q	post					3.11	0.19	2.23	0.35	3.12	0.23	2.27	0.26
OLR89R	post					0.77	0.41			1.36	0.28	2.89	0.8
SHOEMA84F	pre					4.99	2.11			4.87	0.65	1.35	0.35
SL91A1	pre	4.5	0.3			1.74	0.32	2.41	0.64	1.62	0.26	2.44	0.6
SO	pre	5.6	0.7			3.36	0.31	1.95	0.81	3.4	0.65	6.33	0.75
	post	9.7	0.85			10.89	0.45			7.24	0.6	9.26	0.57
SSF83E	post	4.63	0.66			6.15	0.52			5.5	0.64	8.55	0.21
TEMPEL1	pre	3.15	1.34	4.72	1.02	2.94	0.78	4.91	0.9	5.93	1.14	1.05	1.24
TEMPEL2	pre									12.49	0.8	3.09	0.98
THIELE85M	pre	7.22	0.84	7.05	0.62	6.42	0.53	7.79	0.93	7.22	0.67	-0.73	0.78
TK90I	pre	3.22	0.62	11.81	4.21	3.16	0.17			3.59	0.61	12.11	2.03
TUTTLE	pre	3.14	0.73			1.71	0.54			1.84	0.22	3.52	0.57
WILD2	pre					2.49	0.32	2.56	0.61	5.48	0.47	1.68	0.28

Table 3.2 Log Production Rate Ratios

Comet ID	OH/CN	NH/CN	C3/CN	C2/CN	Afr/CN	Afr/OH	C2/OH	C3/OH	CN/OH	NH/OH
	sigma%	sigma%	sigma%	sigma%	sigma%	sigma%	sigma%	sigma%	sigma%	sigma%
AJ	•	•	•	-0.20	-22.38	•	•	•	•	•
	•	•	•	33	6	•	•	•	•	•
AR	2.59	-0.06	-0.90	-0.12	-22.66	-25.16	-2.67	-3.52	-2.61	-2.72
	6	163	7	7	4	8	10	10	6	163
AUSTI89C1	2.34	0.02	-1.08	0.01	-23.54	-26.05	-2.43	-3.56	-2.49	-2.43
	1	1	1	0	1	1	1	1	1	1
AUSTIN82G	2.31	•	-0.87	0.30	-23.49	-25.13	-2.21	•	-2.31	•
	11	•	2	1	2	12	11	•	11	•
AUSTIN84I	2.06	-0.44	-0.98	0.08	-24.63	-25.54	-2.17	-3.18	-2.21	-2.70
	4	12	2	1	2	4	4	4	4	13
BM	2.50	-0.05	-1.02	0.12	-23.91	-26.43	-2.39	-3.54	-2.52	-2.57
	1	2	1	1	1	2	1	2	1	2
BOETHIN	2.58	0.14	-0.87	0.10	-23.46	-26.04	-2.50	-3.47	-2.61	-2.47
	3	4	2	1	2	4	3	4	3	5
BORRELLY	2.49	0.21	-1.36	-0.36	-22.84	-25.46	-2.99	-4.00	-2.63	-2.41
	1	1	1	1	1	1	1	1	1	1
BOWELL80B	3.28	0.58	-1.68	-0.39	-22.26	-25.27	-3.43	-3.94	-3.33	-2.06
	5	35	27	24	2	3	4	4	3	3
BRADFI79C	•	•	-1.28	-0.10	-23.49	•	•	•	•	•
	•	•	3	2	3	•	•	•	•	•
BRADFI79L	2.28	-0.49	-1.14	0.18	-23.84	-26.07	-2.10	-3.44	-2.30	-2.77
	1	1	1	1	1	2	1	2	1	2
BRADFI80T	•	•	•	0.35	-23.37	•	•	•	•	•
	•	•	•	2	3	•	•	•	•	•
BRADFI87S	2.15	0.24	-1.00	0.03	-22.67	-24.98	-2.33	-3.34	-2.33	-2.06
	1	1	1	1	1	1	1	1	1	1
BROOKS2	2.60	0.65	-1.43	-0.47	-22.36	-24.97	-3.30	-4.12	-2.71	-2.05
	12	31	34	22	3	11	45	47	11	34
BUS	2.63	•	-1.90	-1.06	-22.96	-25.84	-3.71	-4.23	-2.84	•
	27	•	36	85	9	26	73	44	24	•
BUS81D	3.92	2.20	•	-0.81	-21.37	-25.29	-4.73	•	-3.92	-1.72
	141	146	•	2581	137	37	2578	•	141	64

Table 3.2 Continued

Comet ID	OH/CN	NH/CN	C3/CN	C2/CN	Afr/CN	Afr/OH	C2/OH	C3/OH	CN/OH	NH/OH
	sigma%	sigma%	sigma%	sigma%	sigma%	sigma%	sigma%	sigma%	sigma%	sigma%
CERNIS83L	2.71	-0.27	-1.22	-0.25	-22.23	-25.04	-3.01	-3.97	-2.83	-2.89
	5	92	9	5	2	5	9	10	5	82
CG	2.74	0.29	-1.25	-0.31	-22.42	-25.23	-3.08	-4.11	-2.87	-2.49
	2	7	3	3	1	2	3	4	2	8
CHERNYKH	•	•	-1.66	-0.32	-22.05	•	•	•	•	•
	•	•	13	10	2	•	•	•	•	•
CIFFREO	2.78	0.64	-0.74	-0.37	-22.12	-24.90	-3.15	-3.52	-2.78	-2.14
	23	75	38	90	12	20	92	41	23	77
CP80K	1.95	•	-1.38	0.04	-23.08	-25.03	-1.90	-3.36	-1.96	•
	9	•	14	3	4	10	9	18	9	•
CROMMELIN	2.01	0.25	-1.00	-0.06	-23.63	-25.81	-2.23	-3.27	-2.17	-1.88
	2	2	1	1	1	2	2	4	2	3
DARREST	2.41	0.30	-1.39	0.21	-23.26	-26.14	-2.37	-4.26	-2.62	-2.27
	9	15	8	1	1	10	9	16	9	17
ELIAS81C	•	•	•	•	•	•	•	•	•	•
	•	•	•	•	•	•	•	•	•	•
ENCKE	1.99	-0.42	-1.35	-0.06	-24.31	-26.37	-2.46	-3.35	-2.49	-2.49
	1	3	1	0	1	1	1	2	1	3
FAYE	2.74	0.07	-1.22	-0.42	-22.49	-25.08	-3.13	-3.99	-2.76	-2.70
	2	12	5	5	2	2	5	5	2	12
FURUY87F1	2.58	0.02	-1.06	-0.12	-23.25	-25.83	-2.70	-3.64	-2.58	-2.56
	9	18	7	4	5	10	9	11	9	20
GEHRELS2	2.58	•	•	-0.59	-22.01	-24.59	-3.17	•	-2.58	•
	50	•	•	180	18	48	186	•	50	•
GS	2.71	0.40	-1.00	-0.39	-23.93	-25.95	-2.57	-3.69	-2.74	-2.33
	4	12	6	1	2	6	4	7	4	12
GUNN	2.36	-0.72	-1.38	-0.42	-22.64	-25.95	-3.69	-3.60	-3.25	-2.99
	21	353	42	11	3	18	27	52	18	381
GZ	2.62	-0.16	-1.82	-0.67	-23.24	-25.94	-3.41	-4.58	-2.74	-2.94
	1	2	2	1	1	1	1	2	1	2
HALLEY	2.34	0.20	-0.89	0.13	-22.95	-25.31	-2.29	-3.30	-2.40	-2.17
	0	0	0	0	0	0	0	0	0	0

Table 3.2 Continued

Comet ID	OH/CN	NH/CN	C3/CN	C2/CN	Afr/CN	Afr/OH	C2/OH	C3/OH	CN/OH	NH/OH
	sigma%	sigma%	sigma%	sigma%	sigma%	sigma%	sigma%	sigma%	sigma%	sigma%
HARTLEY2	2.44	0.28	-1.11	0.08	-23.47	-25.92	-2.36	-3.56	-2.45	-2.17
	3	3	2	2	2	3	3	3	3	4
HC	•	•	-0.73	-0.13	-22.24	•	•	•	•	•
	•	•	19	42	16	•	•	•	•	•
HG85L	2.42	0.21	-0.99	0.02	-23.51	-25.96	-2.61	-3.64	-2.63	-2.24
	2	2	1	1	1	2	2	2	2	2
HI	2.36	•	•	-0.09	-23.26	-25.62	-2.45	•	-2.36	•
	6	•	•	4	5	7	6	•	6	•
HMP	2.90	0.67	-0.95	0.23	-23.39	-26.29	-2.67	-3.85	-2.90	-2.23
	20	54	17	7	19	27	20	25	20	57
HOWELL	2.30	•	-1.35	-0.09	-22.77	-25.20	-2.55	-3.73	-2.47	•
	8	•	4	4	0	8	10	10	8	•
IAA83D	2.17	-0.38	-1.74	0.00	-23.68	-25.96	-2.28	-4.06	-2.33	-2.55
	3	6	2	1	2	3	3	3	3	6
IRAS	2.56	0.45	-1.83	-0.93	-22.75	-25.32	-3.48	-4.41	-2.57	-2.03
	9	36	33	22	4	9	24	34	9	41
IRAS83O	2.72	0.98	-0.73	-0.04	-22.17	-24.85	-3.04	-3.59	-2.83	-1.66
	34	49	36	46	10	31	111	58	34	69
KK	2.42	•	-1.73	-0.17	-22.73	-25.36	-2.74	-4.12	-2.69	•
	10	•	12	6	3	9	10	24	10	•
KLEMOLA	2.68	0.73	-1.27	-0.29	-22.14	-24.85	-2.99	-3.98	-2.71	-1.92
	10	32	39	25	4	10	27	43	10	34
KOHLER77M	•	•	-0.88	0.24	-23.64	•	•	•	•	•
	•	•	2	1	2	•	•	•	•	•
KOPFF	2.68	0.14	-1.12	-0.11	-23.09	-25.67	-2.69	-3.92	-2.70	-2.58
	3	4	1	1	1	3	3	3	3	5
LEVY90C	2.57	0.17	-1.03	0.05	-22.76	-25.43	-2.62	-3.73	-2.69	-2.52
	0	0	0	0	0	0	0	0	0	0
LILLER88A	2.18	0.29	-0.98	0.11	-23.01	-25.18	-2.08	-3.16	-2.19	-1.88
	2	2	2	1	2	3	2	3	2	3
LR84T	2.35	0.41	-0.97	0.00	-23.33	-25.74	-2.38	-3.36	-2.39	-1.99
	3	3	2	2	2	3	3	3	3	4

Table 3.2 Continued

Comet ID	OH/CN	NH/CN	C3/CN	C2/CN	Afr/CN	Afr/OH	C2/OH	C3/OH	CN/OH	NH/OH
	sigma%	sigma%	sigma%	sigma%	sigma%	sigma%	sigma%	sigma%	sigma%	sigma%
MACHHO85E	•	•	•	0.04	•	•	•	•	•	•
	•	•	•	3	•	•	•	•	•	•
MB	2.39	0.26	-1.11	-0.09	-23.24	-25.65	-2.51	-3.52	-2.42	-2.17
	3	5	4	2	3	4	3	5	3	5
MEIER78F	•	•	•	-0.12	-22.66	•	•	•	•	•
	•	•	•	3	3	•	•	•	•	•
MEIER79I	•	•	-0.51	0.20	-22.90	•	•	•	•	•
	•	•	4	3	4	•	•	•	•	•
MEIER80Q	2.17	-0.39	-1.12	0.02	-23.44	-25.90	-2.38	-3.45	-2.52	-2.53
	2	15	2	1	2	3	2	3	3	15
NEUJMIN1	2.73	0.40	-0.62	0.05	-22.38	-25.11	-2.68	-3.35	-2.73	-2.33
	32	97	16	20	9	31	36	34	32	102
NTT87C	2.57	•	•	0.10	-23.55	-26.12	-2.47	•	-2.57	•
	8	•	•	3	4	8	8	•	8	•
OLR89R	2.39	0.36	-1.33	-0.17	-23.96	-26.43	-2.25	-3.63	-2.39	-2.03
	3	3	0	0	0	4	3	4	3	4
PANTHE80U	2.21	0.41	-1.20	0.01	-22.92	-25.32	-2.35	-3.40	-2.43	-1.80
	3	3	2	1	2	3	3	3	3	4
RUSSELL4	3.41	1.43	-2.67	0.69	-21.77	-25.15	-3.01	-6.07	-3.47	-2.07
	36	55	28	134	28	23	96	26	37	60
SC	3.15	1.29	-1.24	0.03	-21.87	-25.02	-3.12	-4.39	-3.15	-1.86
	80	100	340	142	50	63	147	342	80	107
SG89E1	2.34	0.30	-1.01	-0.04	-22.87	-25.39	-2.58	-3.55	-2.52	-2.24
	22	10	12	3	3	20	20	25	20	23
SHOEMA83P	•	•	-1.07	-0.03	-22.14	•	•	•	•	•
	•	•	93	29	16	•	•	•	•	•
SHOEMA84F	3.14	•	•	0.62	-22.30	-24.94	-2.54	•	-3.14	•
	31	•	•	8	8	30	30	•	31	•
SHOEMA84R	3.27	•	•	0.60	-21.97	-25.28	•	•	-3.27	•
	60	•	•	100	33	46	•	•	60	•
SHOEMA84S	2.52	-0.29	-1.83	-0.74	-22.64	-25.18	-3.22	-4.35	-2.53	-2.81
	4	41	25	13	2	4	14	24	4	41

Table 3.2 Continued

Comet ID	OH/CN	NH/CN	C3/CN	C2/CN	Afr/CN	Afr/OH	C2/OH	C3/OH	CN/OH	NH/OH
	sigma%	sigma%	sigma%	sigma%	sigma%	sigma%	sigma%	sigma%	sigma%	sigma%
SHOEMAKE1	2.00	-0.18	-1.09	-0.20	-23.33	-25.36	-2.35	-3.12	-2.03	-2.21
	7	23	4	3	3	8	9	8	7	24
SL91A1	2.39	0.37	-1.20	-0.08	-23.18	-25.58	-2.48	-3.60	-2.41	-2.06
	2	2	2	1	1	2	2	2	2	2
SL91D	1.86	0.22	-1.05	-0.30	-22.45	-24.35	-2.15	-2.92	-1.89	-1.74
	7	34	10	8	3	8	10	12	7	36
SO	2.76	0.32	-1.06	0.02	-22.68	-25.47	-2.80	-3.86	-2.81	-2.49
	1	11	1	1	1	1	1	2	1	11
SORREL86N	2.53	0.14	-1.01	-0.28	-22.81	-25.60	-2.98	-3.69	-2.73	-2.68
	4	19	6	5	2	4	6	6	4	20
SSF83E	2.21	-0.04	-1.65	0.22	-23.79	-26.35	-2.16	-4.15	-2.46	-2.51
	3	5	4	1	0	0	2	5	2	5
ST	2.19	-0.32	-0.89	0.01	-23.14	-25.34	-2.19	-3.09	-2.20	-2.52
	3	2	2	2	2	3	3	3	3	3
SW2	2.49	0.20	-1.41	-0.60	-22.72	-25.29	-3.33	-4.27	-2.84	-2.45
	11	39	31	16	5	8	22	31	9	47
TAKAMIZAW	2.90	0.35	-1.40	-1.09	-22.29	-25.21	-4.13	-4.38	-2.94	-2.65
	5	20	15	59	3	5	77	17	5	23
TAYLOR	•	•	•	-0.66	-22.58	•	•	•	•	•
	•	•	•	94	11	•	•	•	•	•
TEMPEL1	2.81	0.29	-1.13	-0.09	-22.88	-25.63	-2.90	-4.06	-2.83	-2.55
	2	5	2	1	1	2	3	3	2	6
TEMPEL2	2.60	•	-0.94	-0.01	-23.46	-25.77	-2.70	•	-2.60	•
	6	•	3	2	3	9	63	•	6	•
THIELE85M	2.70	0.36	-0.88	-0.02	-23.30	-26.02	-2.74	-3.60	-2.72	-2.35
	2	2	1	1	2	2	2	2	2	2
TK90I	2.56	-0.20	-1.00	0.06	-23.78	-26.51	-2.47	-3.56	-2.56	-2.77
	2	6	1	1	1	3	2	3	2	7
TSUCHINS1	2.39	0.48	-0.99	-0.37	-23.18	-25.57	-2.76	-3.38	-2.39	-1.91
	8	16	9	9	5	9	12	11	8	18
TUTTLE	2.53	•	-1.03	0.15	-23.61	-26.15	-2.39	-3.58	-2.54	•
	3	•	3	2	3	4	3	4	3	•

Table 3.2 Continued

Comet ID	OH/CN	NH/CN	C3/CN	C2/CN	Afr/CN	Afr/OH	C2/OH	C3/OH	CN/OH	NH/OH
	sigma%	sigma%	sigma%	sigma%	sigma%	sigma%	sigma%	sigma%	sigma%	sigma%
WH	2.49	-0.30	-2.05	-1.20	-22.93	-25.45	-3.75	-4.55	-2.53	-2.78
	5	33	61	29	3	6	37	60	5	32
WILD2	2.48	0.17	-1.35	-0.21	-22.87	-25.32	-3.12	-3.93	-2.50	-2.27
	14	53	3	2	2	15	35	41	14	56
WILD4	2.71	0.49	-1.77	-0.59	-22.51	-25.51	-3.42	-4.70	-2.86	-2.44
	8	33	168	33	6	10	34	168	8	33
WILSON86L	1.58	0.50	-1.07	-0.26	-22.50	-25.37	-2.86	-3.61	-2.57	-1.26
	6	16	6	7	3	9	12	16	8	20
WIRTANEN	2.52	0.39	-1.05	-0.01	-23.36	-25.88	-2.53	-3.57	-2.52	-2.13
	7	13	9	3	7	9	7	11	7	14

Table 3.3 Activity Parameters

Identities	Maximum Area [km^2]	Log (H2O) @ Perihelion	active area %
AJ	4.33	27.58	3.29
AR	0.55	27.25	0.57
AUSTI89C1	7.46	29.68	•
AUSTIN82G	1.11	28.23	•
AUSTIN84I	1.98	29.31	•
BM	5.65	29.36	•
BOETHIN	5.99	28.52	•
BORRELLY	6.68	28.33	•
BOWELL80B	16.15	27.31	•
BRADFI79C	0.19	27.88	•
BRADFI79L	2.81	28.85	•
BRADFI80T	94.75	30.99	•
BRADFI87S	9.08	28.93	•
BROOKS2	0.54	26.97	•
BUS	1.14	27.01	•
BUS81D	10.22	27.96	46.12
CERNIS83L	279.77	28.55	•
CG	1.28	27.61	•
CHERNYKH	1.33	26.71	4.05
CIFFREO	0.26	26.66	2.40
CP80K	0.65	28.21	•
CROMMELIN	1.22	28.27	•
DARREST	1.69	27.91	•
ELIAS81C	•	•	•
ENCKE	0.72	28.66	1.32
FAYE	2.66	27.67	8.72
FURUY87F1	13.10	28.36	•
GEHRELS2	0.28	26.39	•
GS	0.10	26.96	0.48
GUNN	60.33	28.73	49.40
GZ	7.49	28.62	•
HALLEY	50.50	30.10	38.45
HARTLEY2	4.77	28.65	•
HC	0.04	26.30	•
HG85L	4.39	28.83	•
HI	5.31	28.23	•
HMP	0.16	27.61	2.28
HOWELL	1.37	27.38	6.74
IAA83D	0.97	27.96	•
IRAS	1.85	27.51	•
IRAS83O	2.42	27.33	•
KK	1.59	27.15	7.18
KLEMOLA	0.47	26.92	•

Table 3.3 Continued

Identities	Maximum Area [km^2]	Log (H2O) @ Perihelion	active area %
KOHLER77M	10.03	28.97	•
KOPFF	12.31	28.60	47.04
LEVY90C	112.44	30.02	•
LILLER88A	9.60	28.95	•
LR84T	1.99	28.27	•
MACHHO85E	2.44	30.21	•
MB	7.11	28.10	•
MEIER78F	243.32	30.13	•
MEIER79I	0.81	27.41	•
MEIER80Q	12.54	28.60	•
NEUJMIN1	0.52	27.22	0.12
NTT87C	8.78	28.91	•
OLR89R	15.58	29.38	•
PANTHE80U	45.57	28.90	•
RUSSELL4	1.28	27.05	•
SC	36.14	27.66	•
SG89E1	9.07	28.46	•
SHOEMA83P	18.89	27.38	•
SHOEMA84F	176.12	28.83	3.37
SHOEMA84R	33752.23	28.49	705.31
SHOEMA84S	0.34	27.28	•
SHOEMAKE1	3.01	27.72	28.11
SL91A1	2.39	28.35	•
SL91D	7.18	27.80	•
SO	6.76	28.33	•
SORREL86N	44.48	28.89	•
SSF83E	0.52	28.32	•
ST	40.37	29.58	•
SW2	7.91	27.85	19.65
TAKAMIZAW	11.80	28.32	38.64
TAYLOR	0.81	27.15	•
TEMPEL1	5.29	28.23	•
TEMPEL2	0.70	27.35	0.60
THIELE85M	5.55	28.25	•
TK90I	18.60	29.01	•
TSUCHINS1	0.83	27.42	•
TUTTLE	2.85	28.20	•
WH	2.21	27.59	•
WILD2	4.07	28.12	•
WILD4	2.10	27.57	•
WILSON86L	78.81	29.64	5.44
WIRTANEN	1.95	28.03	•

Table 3.4 Dynamical Parameters

Identities	q [AU]	e	i [deg.]	a [AU]	TJ	(1/a)o
AJ	2.28	0.3999	12.5	3.80	2.8984	0.263000
AR	1.45	0.5987	17.8	3.61	2.7106	0.277000
AUSTI89C1	0.35	1.0002	59.0	•	•	0.000032
AUSTIN82G	0.65	0.9994	84.5	1083.33	0.1006	0.001670
AUSTIN84I	0.29	0.9998	164.2	1450.00	-0.6391	0.000510
BM	0.48	0.9720	19.3	17.14	1.1087	0.058600
BOETHIN	1.11	0.7777	5.8	4.99	2.2671	0.199000
BORRELLY	1.36	0.6250	30.3	3.61	2.5625	0.277231
BOWELL80B	3.36	1.0573	1.7	•	•	0.000027
BRADFI79C	0.41	1.0001	136.2	•	•	0.000033
BRADFI79L	0.55	0.9876	148.6	44.35	-0.6655	0.023300
BRADFI80T	0.26	0.9997	138.6	866.67	-0.4684	0.000964
BRADFI87S	0.87	0.9947	34.1	164.15	0.9884	0.006380
BROOKS2	1.85	0.4902	5.5	3.62	2.8844	0.276000
BUS	2.18	0.3750	2.6	3.49	3.0077	0.286000
BUS81D	2.46	0.9990	160.7	2460.00	-1.8335	0.000703
CERNIS83L	3.32	1.0019	134.7	•	•	0.000045
CG	1.31	0.6292	7.1	3.53	2.7434	0.284000
CHERNYKH	2.57	0.5944	5.7	6.34	2.5873	0.158000
CIFFREO	1.70	0.5441	13.1	3.73	2.7785	0.268000
CP80K	0.52	1.0022	49.1	•	•	0.000000
CROMMELIN	0.73	0.9192	29.1	9.03	1.4826	0.110000
DARREST	1.20	0.6457	17.6	3.40	2.7076	0.293667
ELIAS81C	4.74	1.0007	115.3	•	•	0.000142
ENCKE	0.34	0.8479	11.9	2.21	3.0296	0.451800
FAYE	1.59	0.5782	9.1	3.77	2.7513	0.265000
FURUY87F1	1.68	1.0002	76.7	•	•	0.000177
GEHRELS2	2.36	0.4085	6.7	3.99	2.8914	0.250000
GS	0.99	0.6650	21.1	2.96	2.8100	0.338000
GUNN	2.46	0.3157	10.4	3.60	2.9975	0.277625
GZ	1.03	0.7075	31.9	3.52	2.4642	0.284000
HALLEY	0.59	0.9673	162.2	18.04	-0.6115	0.055700
HARTLEY2	0.95	0.7195	9.3	3.39	2.6416	0.294000
HC	1.10	0.6653	6.0	3.29	2.7628	0.304000
HG85L	0.69	0.9998	79.9	3450.00	0.1822	0.000524
HI	1.28	0.8339	95.7	7.71	0.5413	0.130000
HMP	0.54	0.8219	4.2	3.03	2.5826	0.329000
HOWELL	1.62	0.5075	5.6	3.29	2.9449	0.305000
IAA83D	0.99	0.9901	73.2	100.00	0.4078	0.010500
IRAS	1.70	0.6957	46.2	5.59	1.9615	0.179000
IRAS83O	2.25	1.0002	120.7	•	•	-0.000018
KK	2.22	0.4856	9.0	4.32	2.7780	0.231111
KLEMOLA	1.77	0.6405	11.0	4.92	2.5232	0.203000
KOHLER77M	0.99	0.9995	48.7	1980.00	0.8171	0.000231
KOPFF	1.58	0.5445	4.7	3.47	2.8646	0.289000
LEVY90C	0.94	1.0013	131.6	•	•	0.000000
LILLER88A	0.84	0.9966	73.3	247.06	0.3474	0.004880

Table 3.4 Continued

Identities	q [AU]	e	i [deg.]	a [AU]	TJ	(1/a)o
LR84T	0.92	0.9993	65.7	1314.29	0.4935	0.001300
MACHHO85E	0.11	1.0000	16.3	•	•	0.000000
MB	1.59	0.5934	13.0	3.91	2.6900	0.255000
MEIER78F	1.14	1.0008	43.8	•	•	0.000024
MEIER79I	1.43	0.9732	67.1	53.36	0.6707	0.018600
MEIER80Q	1.52	0.9947	101.0	286.79	-0.2733	0.003970
NEUJMIN1	1.55	0.7756	14.2	6.91	2.1634	0.144000
NTT87C	0.87	0.9957	172.2	202.33	-1.1193	0.005030
OLR89R	0.64	1.0003	90.2	•	•	-0.000218
PANTHE80U	1.66	0.9990	82.6	1660.00	0.2089	0.000581
RUSSELL4	2.13	0.3832	6.2	3.45	3.0024	0.290000
SC	3.56	0.1462	6.6	4.17	3.0071	0.240000
SG89E1	1.57	1.0000	59.4	•	•	0.000053
SHOEMA83P	3.34	1.0000	137.6	•	•	0.000557
SHOEMA84F	2.70	1.0007	116.7	•	•	0.000465
SHOEMA84R	5.49	0.9949	179.2	1076.47	-2.8974	0.001550
SHOEMA84S	1.21	0.9709	13.9	41.58	1.4398	0.024300
SHOEMAKE1	1.98	0.4715	26.3	3.75	2.7301	0.267000
SL91A1	0.84	0.9999	113.5	8400.00	-0.4527	0.000936
SL91D	2.26	0.9935	77.3	347.69	0.4242	0.003060
SO	1.57	0.8600	18.0	11.21	1.8891	0.088900
SORREL86N	1.72	0.9999	160.6	17200.00	-1.5340	0.000371
SSF83E	0.47	1.0000	96.6	•	•	0.000378
ST	0.96	0.9636	113.4	26.37	-0.2811	0.038000
SW2	2.12	0.3906	3.7	3.47	2.9986	0.288000
TAKAMIZAW	1.59	0.5740	9.5	3.73	2.7617	0.267000
TAYLOR	1.96	0.4638	20.5	3.66	2.8141	0.273000
TEMPEL1	1.49	0.5209	10.6	3.11	2.9698	0.321000
TEMPEL2	1.38	0.5444	12.4	3.03	2.9672	0.329000
THIELE85M	1.32	0.9833	139.1	79.04	-1.0068	0.013100
TK90I	1.09	1.0000	143.8	•	•	0.004690
TSUCHINS1	1.51	0.5745	10.5	3.55	2.7950	0.282000
TUTTLE	1.01	0.8226	54.5	5.69	1.6044	0.175000
WH	1.61	0.5388	18.5	3.49	2.7981	0.286857
WILD2	1.49	0.5565	3.3	3.36	2.8811	0.297000
WILD4	1.99	0.4099	3.7	3.37	3.0080	0.298000
WILSON86L	1.20	1.0003	147.1	•	•	0.000067
WIRTANEN	1.08	0.6523	11.7	3.11	2.8214	0.321000

CHAPTER 4
COMPARATIVE ANALYSIS AND TAXONOMY

Parameter Ranges

In order to explore differences among comets and to identify particularly interesting comets in future observations, we now elucidate the full range observed for all parameters in our database. For the dynamical properties, the reader is referred to the Catalog of Cometary Orbits (Marsden 1994, currently 9th edition), which provides a complete listing of orbital parameters for all observed comets. The molecular abundance and gas-to-dust ratios tabulated in the previous chapter are presented as histograms in figure 4.1. Statistics for each ratio are tabulated in table 4.1. The major point of interest in these histograms is that while the ratios are fairly well characterized by a log-normal distribution (i.e. a Gaussian distribution in log space), there are indications of a non-Gaussian component in some of the ratios, most notably that of the minor carbon species, C_3. This provides some of the early evidence of compositional differences among comets suggesting that we are sampling more than one chemically distinct group.

The parameters measuring the comet's activity level are presented as histograms in figure 4.2, with their statistics

also tabulated in table 4.1. The histogram of maximum area in the top left panel of fig. 4.2 is cropped to exclude the active area estimated for comet Shoemaker 1984r. As noted in the previous chapter, the large heliocentric distance of the observations along with potential contribution to the signal from icy grains led to a severe overestimate of the active area for this comet. The lower left panel of fig. 4.2 is just a blown up version of the smaller active area region from the full histogram of the panel above. Our calculated fractional active areas, while only available for a restricted subset of the full database, are plotted as a histogram in the top right panel of fig. 4.2. Again, comet Shoemaker 1984r with greater than 100% active area indicated was excluded from this plot. Finally, the peak H_2O production at perihelion for all our comets is shown in the bottom right panel. The two conclusions to be reached from examination of these plots are that very many comets have similar, low relative activity levels, and that evidence does exist suggesting a fair number of either heavily mantled or volatile depleted comets (at this point, these two cases are observationally equivalent).

Trends and Correlations

Following the purely statistical analysis and inspection of the extent of differences among the individual physical parameters of comets, we now explore correlations among these various physical measures. We also investigate any trends

between the physical and dynamical properties of comets, in particular, any evidence of changes or differences due to evolution or origin. While many plots can be used to show the absence of trends, we will simply state when no apparent correlations were found and reserve plots to illustrate the existence of potentially interesting trends.

Activity Level

No correlation is found between our estimates of the surface active area and any of the molecular abundance ratios, indicating that chemical composition is not directly tied to a comet's intrinsic level of activity. In figure 4.3, we plot a histogram of the logarithm of the comet's active area with the Jupiter-family comets highlighted. This figure illustrates a clear distinction in the data.

There is a clear difference between the average area for JF comets as opposed to any of the other groups, perhaps suggesting evidence for decreasing active area with dynamical age. We find two plausible explanations for such a difference. One option is that comets evolve over time with the deposit of an inert mantle or the exhaustion of volatile material responsible for the decreasing area. A second possibility is that there are primordial differences between the JF and other comets presumably due to origin in the Kuiper belt as opposed to the Oort cloud. Figure 4.4 re-plots the histograms of 4.2, but this time the Jupiter-family comets are highlighted in all panels. Analysis of all of the

histograms is consistent with a scenario having the JF comets heavily mantled but not diagnostic of either evolutionary or primordial differences. The present data do not show a clear evolutionary trend from dynamically new through the LP and HF to Jupiter-family comets. As pointed out in the previous chapter, Whipple (1994) also failed to find any strong evidence in his Activity Index measurements to suggest aging among LP (defined by Whipple as periods > 200 years) comets.

Gas-to-Dust Ratio

Donn (1977), analyzing photographic spectra of 85 comets, pointed out that there were no statistical differences in the ratio of continuum to molecular bands between comets separated by dynamical age classes. This conclusion was based on subjective estimates of the equivalent widths of the emission bands. However, since the radial profiles for the gas and the dust are inherently different and vary differently with heliocentric distance, the measurements made by Donn are sensitive to the field of view used and the heliocentric distance of the observed comet. Our present analysis removes the dependence on field of view and heliocentric distance, quantitatively confirming Donn's conclusion that the gas-to-dust ratio in comets is independent of dynamical age.

Cometary gas-to-dust ratio is not well correlated with any of the molecular abundance ratios measured in the current database as was previously reported by Osip *et al.* (1992).

There is, however, a systematic separation in that the comets with the lowest ratios of the minor carbon species, C_2 and C_3, with respect to either CN or OH are statistically dustier than the majority of other comets. This distinction will be discussed further below when investigating correlations among the emission species. There is no direct correlation of gas-to-dust ratio with either the overall or peak activity level parameters evaluated in the previous chapter.

There is, however, a strong correlation between the dust-to-gas ratio and the perihelion distance of the comet. Figure 4.5 plots this trend as $\log(Af\rho/Q(CN))$ vs. $\log(q)$ for the ensemble of comets in our database showing that comets get dustier with increasing perihelion distance, or inversely comets get gassier with decreasing perihelion distance. In the figure, the comets are separated by symbol type based on their dynamical class and it is clear that the correlation is strong for all dynamical groups. It is important to point out that the data are not suggesting that comets get gassier as they approach the Sun. In the first section of Chapter 3 it is clearly shown that the variation in gas-to-dust ratio for a given comet is negligible compared to the variation among comets and is only weakly dependent on heliocentric distance. Rather, the data suggest systematic differences among comets dependent on how close their perihelion passage is.

Prior to investigating the physical implications of this apparent trend, it is necessary to determine what effects

modeling, observational biases, or additional physical effects could have on the result. One potential factor could be changes, dependent on the heliocentric distance, in the amount or velocity of outgassing. Both the Afρ formalism for the dust production and the Haser model for the emission species production assume constant outflow velocity from the nucleus; therefore, any r_H dependence in the velocity should have no effect on the ratio. In addition, the amount of outgassing per unit area is lower at larger r_H and therefore, the dust lifting should decrease as the flow is insufficient to entrain the larger particles. This would lead to an effect exactly opposite to that which is observed. It is difficult to imagine any effect in the models that would not introduce a trend with r_H for the individual comets yet would result in a correlation with perihelion distance for all comets. Observational biases excluding gassier comets at large r_H due to their diffuse nature[1] are certainly partly responsible for the lower edge of the band of comets in fig. 4.5, but can not be used to explain the upper edge.

Lacking any other explanation, we consider the trend to be a real effect and suggest the following physical explanations. It is possible that effective mantling leading to a greater fraction of the nucleus being covered by an inert crust is a strong function of perihelion distance. A

---

[1]Specifically, the visual magnitudes are dominated by a combination of light scattered from the dust and C_2 emission: at large r_H, the C_2 scale-lengths increase and the gassier comets are very diffuse and therefore, less likely to be observed.

consistent scenario is that the comets with smaller perihelion distances have built up an inert but porous crust and while gaseous emission is diminished, it continues to percolate through the pores, but unable to entrain as much dust proportionally as from a freely vaporizing surface or active vent. The only trouble with this scenario is that while adequate for JF, HF, OLP, and YLP comets, it breaks down for the dynamically new comets. If a comet is entering the inner solar system for the first time, it is unclear how the perihelion distance that it will eventually reach has any effect on its gas-to-dust ratio. The sample of positively determined dynamically new comets in this survey is very small (6 comets) and the data are insufficient to clearly indicate a trend, in this sample, with perihelion distance. It is possible that the additional 4 'unclassified' comets with hyperbolic or parabolic orbit estimates are not actually members of the DN group as we have suggested, but rather they have already made at least one perihelion passage. This could adequately explain the apparent persistence of the trend in the DN family, however, this issue remains unresolved.

Molecular Abundance Ratios

A'Hearn and Millis (1980) in a comparison of 12 comets concluded that there were no correlations between any of the abundance ratios and either gas-to-dust ratio or dynamical age. Similar conclusions have since been reached by other

investigators (e.g. Cochran, 1989; Williams *et al.*, 1989; Cochran *et al.*, 1992). Analysis of the present database also fails to find any strict correlation among any of the molecular abundance ratios and the gas-to-dust ratio or the dynamical age of comets. The general conclusion shared with all the previous studies is that there does not appear to be large scale chemical differentiation inside cometary nuclei[2]. On the other hand, in the present data set some statistical differences are found comparing the molecular abundance ratio ranges observed in JF comets with those of the other dynamical families. In figure 4.6, $\log(Q(C_2)/Q(CN))$ is plotted separated on the abscissa by dynamical family. It is suggested, based on this plot, that the JF includes a compositionally distinct group of comets that apparently is not well represented in other dynamical families. While it may be tempting to also suggest an evolutionary trend in the plot, closer examination precludes such a conclusion. The single datum among YLP comets with a low value of $\log(Q(C_2)/Q(CN))$ is for comet Bus 1981d and has an uncertainty larger than 100%. Comet P/IRAS is the only comet that stands out in this regard among HF comets and with a T_J value of 1.97, numerical integrations of orbits by Levisson and Duncan (1994) indicate that this comet is also likely a Jupiter-family comet. This leaves the OLP comet Shoemaker

---

[2]This conclusion is limited to the species observed in the current studies, all of which are presumably bound in an H_2O lattice, and should not be used to imply anything about the abundances of other species like CO or CO_2.

1984s as the sole standout in the plot outside of the JF. We will return to these important dynamical distinctions when discussing taxonomy in the next section.

Investigating correlations between the various species, we find that OH and NH do not show any consistent trends with any of the other emission species or the dust. The three carbon bearing species - CN, C_2, and C_3 - on the other hand, do exhibit strong correlations. These correlations are shown in Figure 4.7 with three panels plotting $\log(Q(C_2)/Q(OH))$ vs. $\log(Q(CN)/Q(OH))$, $\log(Q(C_3)/Q(OH))$ vs. $\log(Q(CN)/Q(OH))$, and $\log(Q(C_2)/Q(OH))$ vs. $\log(Q(C_3)/Q(OH))$ respectively. While the correlation of C_2 and C_3 is seemingly strong for the majority of comets, we have found it useful to discriminate those comets with $\log(Q(C2)/Q(OH)) > -3.0$ and with $\log(Q(C3)/Q(OH)) > -4.0$ to illustrate that it is this group of comets that is strongly correlated in all carbon bearing species. In all three panels of fig. 4.7, the comets are separated into two point types separating those comets that are correlated in all three species (X) from the others (O); figure 4.8 repeats plots of the same ratios for only the well correlated group, illustrating the strong one-to-one correlation among these three species.

Histograms for each of the molecular abundance ratios along with the gas-to-dust ratio are shown in figure 4.9 with those comets showing correlation in all carbon bearing species highlighted. It is clear from these panels that the highlighted comets represent a population with the remarkable

uniform production rate ratios indicated in other studies. Also evident in these panels, is a statistical difference in the average values of log(Q(OH)/Q(CN)) and log(Afρ/Q(CN)); the group showing correlations among all carbon bearing species also appears to be statistically gassier and richer in carbon with respect to water.

The present database clearly provides strong evidence for differences among comets based on their chemical composition and further possible implications tied to their dynamical properties. In the remainder of this chapter we endeavor to develop a taxonomic classification of comets making use of a variety of statistical tools. This analysis benefits greatly from earlier studies of asteroid taxonomy and the tools developed therein (e.g. Tholen 1984). Our analysis results in the establishment of a consistent framework within which to classify comets.

Cometary Taxonomy

Taxonomic classification of comets based on chemical composition has been waiting on two things. The first requirement has been the uniform analysis of spectrophotometric observations for a statistically significant sample of comets. The second requirement has been evidence within such a study to suggest meaningful compositional groupings among comets.

A'Hearn and Millis (1980), Weaver *et al.* (1981), Cochran (1989), Williams *et al.* (1989), Cochran *et al.* (1992), and

Storrs *et al.* (1992) have all investigated potential compositional differences among comets based on fluorescent emission from various gaseous species as well as reflected continuum from dust and found comets to be reasonably homogenous as a group. Most recently, Cochran *et al.* (1992) observed a 'strong degree of homogeneity in the production rate ratios of many comets' with only comet P/Giacobini-Zinner (GZ) being very different (cf. Cochran and Barker 1987; Beaver *et al.*, 1990). Making use of the largest database studied to date, our analysis generally agrees with this conclusion for the majority of comets (particularly in the three carbon bearing species observed in both studies). But, as indicated in the previous section, we find sufficient evidence suggesting chemically distinct groupings among comets.

Using an earlier version of the current database Osip *et al.* (1992) made a preliminary attempt at quantitatively defining the bounds of "typical" molecular abundance and gas-to-dust ratios in comets and to distinguish several compositional groups. Since then, analysis of the present database has led to the recognition of a class of objects distinguished by their depletions of C_2 and C_3, similar to and in some cases more extreme than the 'proto-typical' depleted comet, G-Z (Schleicher, 1994; A'Hearn *et al.*, 1995). Going even further, in this study we abandon the concept of "typical" abundances and identify and explore at least 5 distinct cometary groups.

Analysis Tools

In order to evaluate compositional variations among comets we have measures of the 4 molecular abundance ratios and the gas-to-dust ratio. To investigate the 5 dimensional space of these ratios we make use of the statistical analysis tools of Principal Component Analysis (PCA) and Hierarchical Clustering Algorithms (HCA). These are the same tools that were adapted and used so successfully to create the most widely adopted asteroid taxonomy (Tholen, 1984). Recently, Howell *et al.* (1994) used a Kohonen type Neural Network to independently classify asteroids utilizing a 65 color database for a subset of objects from Tholen's original 8 color database. Their analysis came to the same general class distinctions as the work of Tholen, with the addition of new sub-groups within the Tholen S class. Unfortunately, after considerable exploration in the hopes of also using this tool, we have found that the relatively sparse data in our current database is not sufficient to make use of Neural Networks in independently classifying comets. Nevertheless, PCA and HCA are very applicable to our data. To make the best possible use of both the PCA and HCA requires a restricted data set that will be described in the following section.

Restricted Data Set

Based on incomplete filter coverage and large observational or modeling uncertainties for some comets, we have limited the data set to be used in determining compositional classes. The principal restriction was that a comet have a minimum of 3 observations over at least 2 nights, with all species represented (i.e. OH, NH, CN, C_3, C_2). Since observations at large r_H suffer from poor signal-to-noise ratios and are most susceptible to uncertainties in the modeling parameters (as discussed in previous chapters), we have limited the restricted data set to observations made at $r_H < 3$ AU. Finally, we have excluded any comets with calculated uncertainties for any of the abundance ratios in excess of 100%.

Ratios with respect to both OH and CN along with standard deviations are given in table 4.2 for the 41 comets in the restricted data set. Dynamical family memberships are also presented in table 4.2 for each of the comets. This restricted database is well representative of the full range of activity level as well as all dynamical classes. These comets serve as the best means of evaluating compositional distinctions and establishing a framework for classifying comets. This will be accomplished using the tools of PCA and HCA along with the additional information provided by dynamical distinctions.

Principal Component Analysis

The interpretation of multivariate data can often be aided by the use of principal components, usually in determining whether a data matrix consisting of many variables can be more concisely described in fewer dimensions. Principal component analysis (PCA) makes no inherent assumptions nor does it actually create or destroy information. This technique simply transforms the data matrix such that the largest amount of total variance in the original variables is accounted for by the first principal component, the next largest amount by the second, and so on. The aim is to put the maximum amount of information into as small a number of variables as possible. This is accomplished in essence by removing redundant information due to correlations between the original data variables.

Mathematically, PCA is easily explained with matrices. Beginning with the original data variables (in our case 5 ratios), a data matrix X is formed by assigning each of the variables as a column in the matrix (in our case we have a 41x5, row=comets x column=ratios, matrix). By means of Singular Value Decomposition (SVD), any matrix can be expressed as the product of 3 special matrices: $X = U D V^T$, where U is the same shape as X (in our case again, a 41x5 matrix), V is a square matrix (in our case 5x5) and D is a diagonal matrix (again 5x5). The columns of the matrix U span the same vector space as do the columns of the original

data matrix X. U is taken as the basis of that vector space since the columns of U are mutually orthonormal (i.e. $U^TU = I$), meaning that the covariance of any two columns is zero and the correlation between any two columns is zero. The columns of U are simply linear combinations of the columns of X with the coefficients determined by the matrices V and D, $U = X V D^{-1}$. For PCA, we are concerned with the cross-product matrix X^TX. Using the SVD equation and knowing that $U^TU = I$ and $D^T = D$, we can evaluate the cross product as: $X^TX = (UDV^T)^T(UDV^T) = VDU^TUDV^T = VD^2V^T$. The principal components are the eigenvectors of X^TX, the columns of V. Consider each principal component or eigenvector as a set of coordinates on the original data variable axes. For a standardized data matrix, each principal component axis is indicated by a line drawn from the origin to a point specified by these coordinates. In this case, the diagonal values of D^2 are the eigenvalues of X^TX and are equal to the variances of the projection of points along each principal component axis. The sum of all eigenvalues is equal to the number of data variables and each eigenvalue ratioed to this sum gives the percent of variance found in that principal component.

The PCA eigenvalues, variance proportion, and eigenvectors for the restricted database are given in table 4.3. Note that approximately 90% of the variance is found in the first three principal components. This means that in searching for compositional classes among comets we can isolate these three principal component axes and seek common

groupings. This is done in figure 4.10, plotting the comets on a series of 3 principal component axes plots. In the first panel of fig. 4.10, we have separated the data into two broad groups by open and filled symbols. These groups illustrate the broad difference between those comets showing strong correlation among all the carbon bearing species (cf. the second section of this chapter) and those that do not show this correlation. Additional symbol types have been used to separate the comets into 7 groups that remain relatively distinct. This separation is based on coherent groupings evident in these plots as well as our results from HCA and statistical analysis of individual abundance ratios that will be treated next.

Hierarchical Clustering Algorithms

The basis of clustering algorithms is some measure of distance between every pair of cases being compared. For this study, we have adopted a complete linkage hierarchical clustering algorithm that uses Euclidean distance as its metric. The Euclidean distance is simply the total distance one would measure between points in the n-dimensional (where in our case n=5) space with a ruler. Hierarchical indicates that the process is sequential. Starting with each case as its own cluster, the two closest clusters are joined then distances from each new cluster are recalculated. Complete linkage specifies when determining distances from newly formed clusters to use the maximum distance from the

individual cluster members. This algorithm has a tendency to favor building smaller clusters in parallel as opposed to single linkage algorithms which are based on the minimum distance between members and tends toward few or single large clusters.

The results of clustering are usually displayed in a dendrogram (tree diagram) with individual cases on the left side (representing leaves) and 'branches' of various length connecting related cases or groups. Branches joining near the left of the diagram indicate comets with more similar compositions. A dendrogram resulting from the cluster analysis of the restricted database is shown in figure 4.11. We have used these results in concert with the results from the PCA to distinguish the 7 compositional groups indicated by various point types in both figures 4.10 and 4.11.

Compositional Classes

The statistical tools of PCA and HCA have separated our restricted data set into 7 groups. Referring back to our individual molecular abundance and gas-to-dust ratios we have evaluated the acceptable range of values suggested for each class of comet. The results of this analysis are given as statistical values in table 4.5 and graphically presented in figure 4.12. While the class borders are not clear for every individual panel of fig. 4.12, the distinction between classes is amply clear when inspecting all the panels. The possible exception is class 7 which could potentially be a

subset of class 6 that contains comets that are extremely similar to each other.

The classes labeled 2,3,4 and 5 all show strong correlations among all the carbon bearing species (CN, C_2 and C_3). Class 2 are distinguished as gassy comets depleted in NH with respect to CN. Classes 3 and 5 differ primarily based on the OH/CN ratio. In class 3, all the carbon species are depleted with respect to OH and thus to water, these comets are also dustier on average than those of class 4. Classes 6 and 7 exhibit significant depletions of the carbon-chain species, C_2 and C_3, and are also relatively depleted of CN with respect to OH. These two classes are also significantly dustier, on average, than any of the other classes. As mentioned above, class 7 could represent a subset of class 6, however, the strong correlations among the species in the comets of this class distinguish them for our purposes. The two comets in class 1 appear gassy and very depleted in C_3. The comets in this group made the closest approaches to the Earth by any comet in the last 200 years and were very diffuse when observed and therefore were more difficult than usual to properly center in our photometer apertures. It is worth noting that the apparent depletions of C_3 and dust could be in part due to extreme centering difficulties that, as mentioned previously, have the greatest effect for these two species. If the depletions are indeed a result of improper centering then these comets should be reclassified as class 2.

Table 4.5 lists all comets in the restricted set along with their dynamical class as well as the new compositional class designation. One point of interest is that class 5 consists of only HF and LP comets all with high eccentricities and inclinations between 30 and 90 degrees. The significance of such distinctions in dynamical properties will become clearer as we improve our statistical sample. The strongest relationship between composition and dynamical class is found for those comets in class 6 (and 7). These are the same comets shown earlier to have significant depletions in the minor carbon species and to all be classified as members of the Jupiter-family with the exception of Shoemaker 1984s. We take this as evidence of primordial differences in comets based on formation region and will return to this in our interpretation of the various classes.

Classifying the full database

We have taken the comets excluded from the restricted database and classified them, when possible, into the 7 classes distinguished among the restricted set comets. For each comet, each compositional parameter was tested to see if, within the uncertainties, it fell within the range of acceptable values for each class. The comets were then assigned to the classes that they matched compositionally. This method actually excludes classes rather than assigns classes but without sufficient observations in all filters we

cannot use a different measure like the principal components to make such an assignment. Classes have been assigned to 70 comets in the full database and are provided in table 4.6. In addition, figure 4.13 repeats the panels of fig. 4.12 including all comets classified in the database showing the same general distinctions.

A number of comets were not classified owing to several different factors. First, comets with observed ratios in only one or two species could not be clearly assigned to one class. Second, those comets with consistently very high ratio uncertainties (i.e. in excess of 100%) were taken as unclassifiable. Finally, those comets observed only beyond 3 AU were also considered unclassifiable under the present scheme owing to the exclusion of all such data from the restricted database.

Interpretation of the classes

In figures 4.12 and 4.13, the class distinctions between comets can clearly be associated with statistical differences in one or more of the compositional parameters. An important question when discussing chemical differences among comets is whether those differences can best be ascribed to either evolution or place of origin. We find no conclusive evidence of classes being correlated with dynamical age, nor do we find evolutionary trends among any of the individual ratios.

Regarding origin, the previously mentioned fact that the comets of class 6 and 7 are almost exclusively JF comets

suggests an intriguing possibility. All of the comets in these groups, including Shoemaker 1984s with its relatively low inclination of 13.9 degrees and a semi-major axis less than 100 AU, could potentially have originated in the Kuiper belt. Therefore, the compositional differences of these groups could be evidence of primordial differences between Kuiper belt comets as opposed to Oort cloud comets. The situation is more complicated than this, however, since roughly half of the JF comets belong to 3 other compositional classes. If we conclude that Kuiper belt and Oort cloud comets have different chemical compositions then we must be willing to explain all JF comets outside of the 6 and 7 classes as originating in the Oort cloud. This explanation, requiring half of JF comets coming from the Oort cloud and half from the Kuiper belt does not agree with most current orbital integration efficiency calculations as discussed in Chapter 1, but it is not ruled out.

A simple distinction between Kuiper belt and Oort cloud is not sufficient to explain the chemical differences of the other compositional classes. Therefore, we propose a different interpretation. The variations are still considered to be primordial but rather than distinguishing only between Kuiper belt and Oort cloud, we suggest that the differences are revealing different formation regions in the early solar system. Under this scenario, temperature gradients in the proto-solar nebula which presumably controlled basic abundances (cf. Yamamoto 1985) could also

inhibit the formation of certain parent molecules. In the case of class 6 and 7 comets that are significantly depleted in C_2 and C_3, the formation of the parent molecules would have been strongly inhibited beyond some boundary distance within the inner Kuiper belt. This allows that the other observed JF comets could have different compositions yet still originate somewhere in the Kuiper belt. It also provides a qualitative explanation to compositional differences among comets originating in the Oort cloud.

Solar nebula accretion disk models suggest temperature ranges at the end of the infall stage to range from 130-180 K at the orbit of Jupiter down to 25-18 K at a distance of 100 AU (Rickman and Huebner 1992 and references therein). Predicting the specific location of regions of comet formation, however, is complicated by an array of additional parameters. Early solar system temperature gradients along with density gradients are smaller in the plane of the rotating disk than are the gradients perpendicular to that plane. Localized variations in conditions due to turbulence, clumping, viscosity, and the possible formation of sub-nebulae can also provide environments of varying degrees of enhancement or depletion for a number of molecular species. Yet another possible ingredient in the complicated recipe of comet formation is the effect of cosmic rays (both solar and extra-solar) in producing or destroying certain parent molecules at different heliocentric distances in the proto-solar nebula. Unfortunately, ignorance of the exact parent

molecules for most of the species observed in our database makes it currently impossible to quantitatively address these problems.

The present database has provided the first evidence for compositional classes among comets and here, we tentatively suggest 7 groupings based on composition and correlations within the measured species. In the final chapter we will summarize our conclusions from the comparative analysis and taxonomy presented here and indicate avenues for future work in the field.

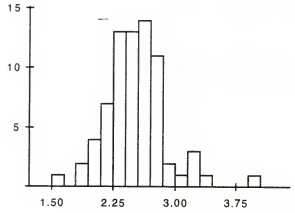

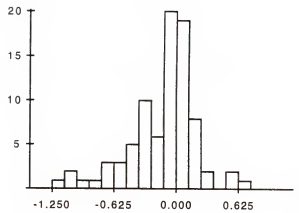

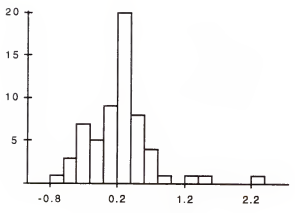

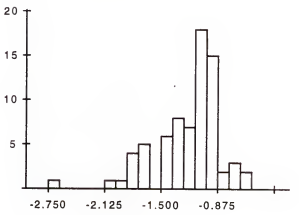

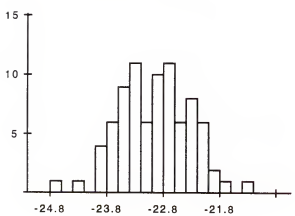

Figure 4.1 # Histograms of Log Ratios

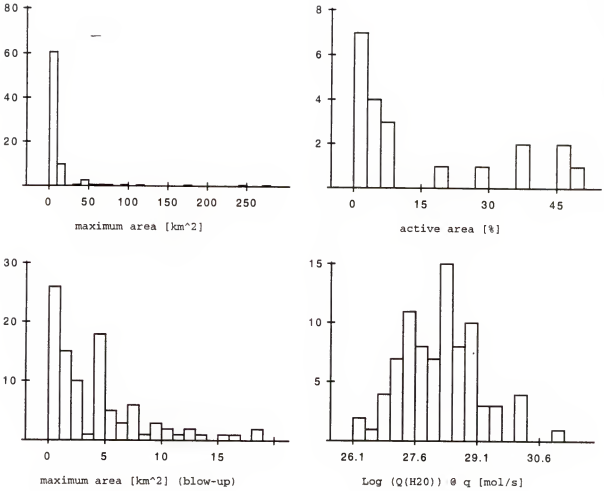

Figure 4.2 # Histograms for Activity Parameters

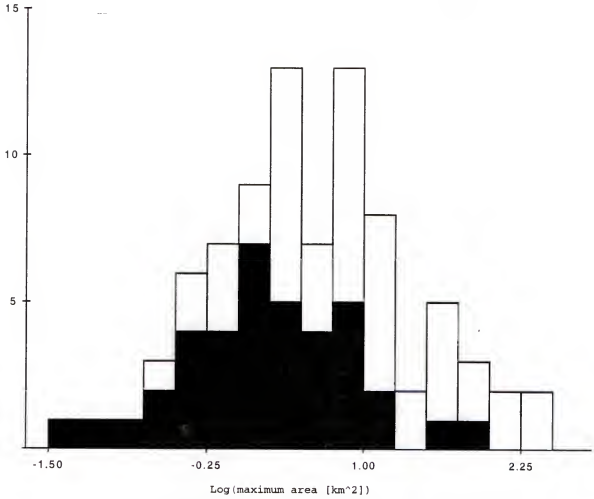

Figure 4.3 # Histogram for Log(Maximum Area)
Jupiter-family comets are highlighted.

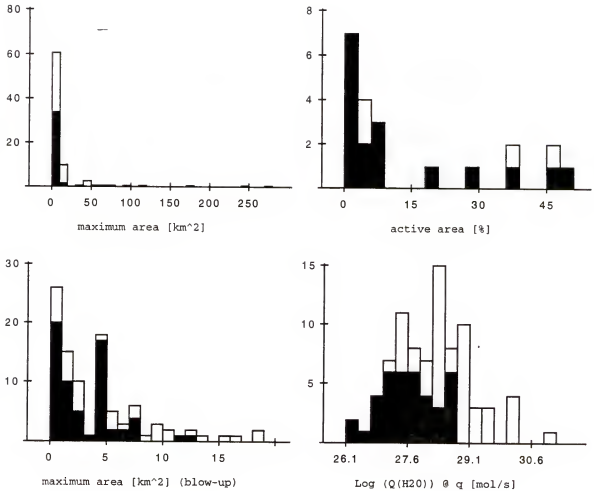

Figure 4.4 # Histograms for Activity Parameters.
Jupiter-family comets are highlighted.

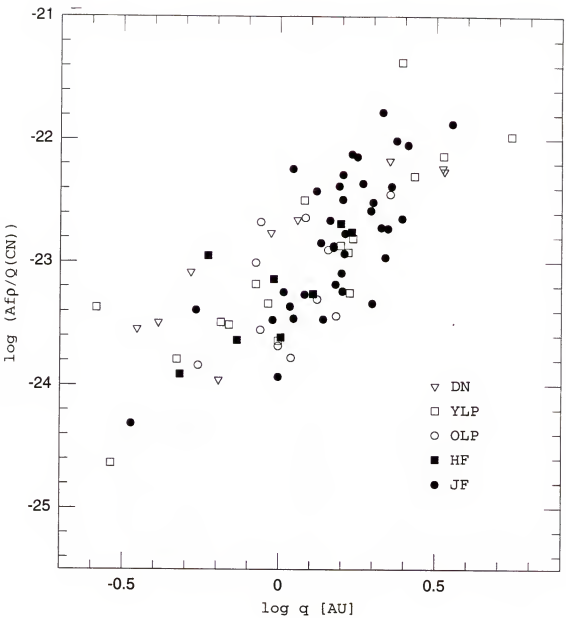

Figure 4.5 Dust-to-Gas Ratio vs. Perihelion distance

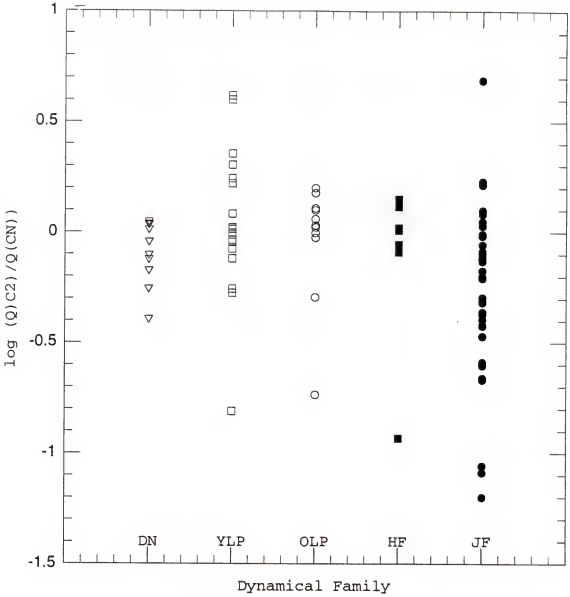

Figure 4.6 Log(Q(C2)/Q(CN)) vs. Dynamical Family

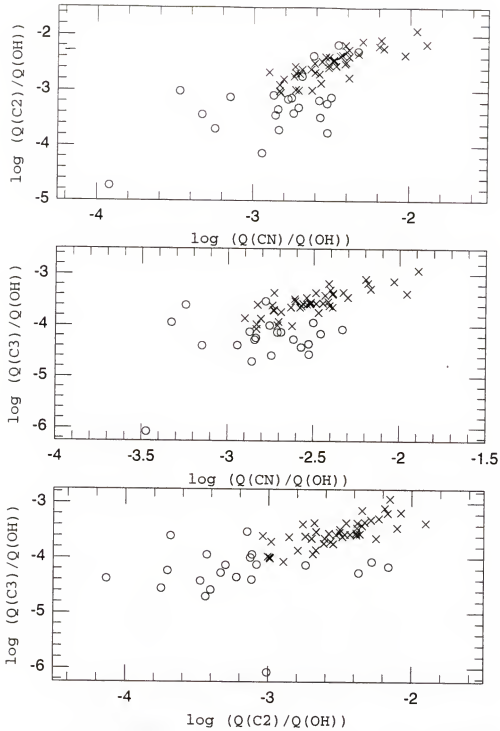

Figure 4.7 Correlations in Carbon Bearing Species.
X's represent comets correlated in all carbon species.
0's represent comets that are not correlated.

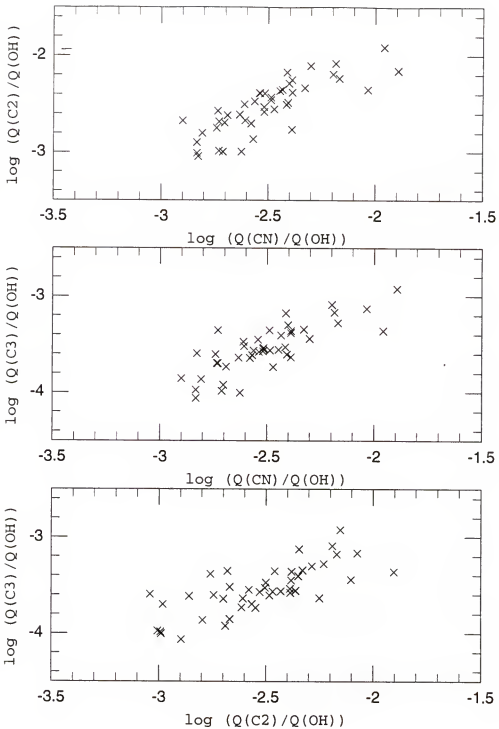

Figure 4.8 Correlations in Carbon Bearing Species. The three plots include only those comets that are well correlated in all 3 carbon bearing species.

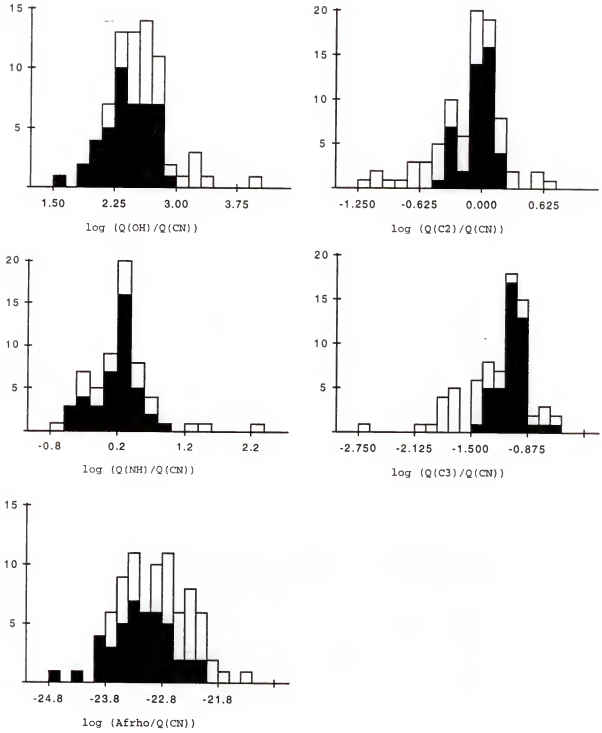

Figure 4.9 # Histograms of Log Ratios.
Comets that are correlated in all 3 carbon bearing species are highlighted.

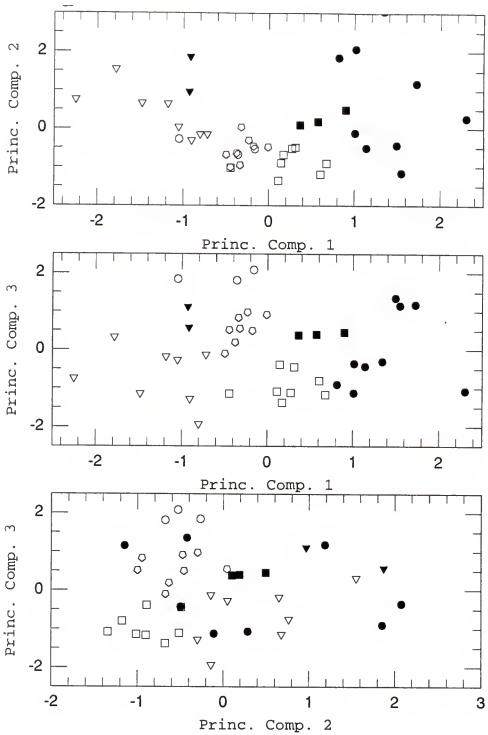

Figure 4.10 Principal Component Plots. Symbols by taxonomic class: 1=filled triangle 2=open triangles, 3=open square, 4=open pentagram, 5=open circle, 6=filled circle, 7=filled square.

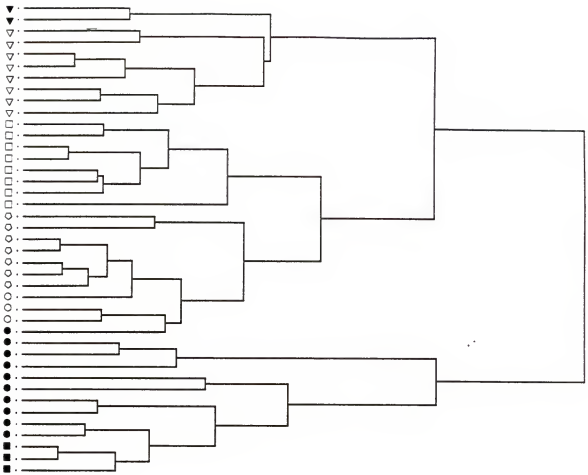

Figure 4.11 Heirarchical Clustering Algorithm Dendrogram

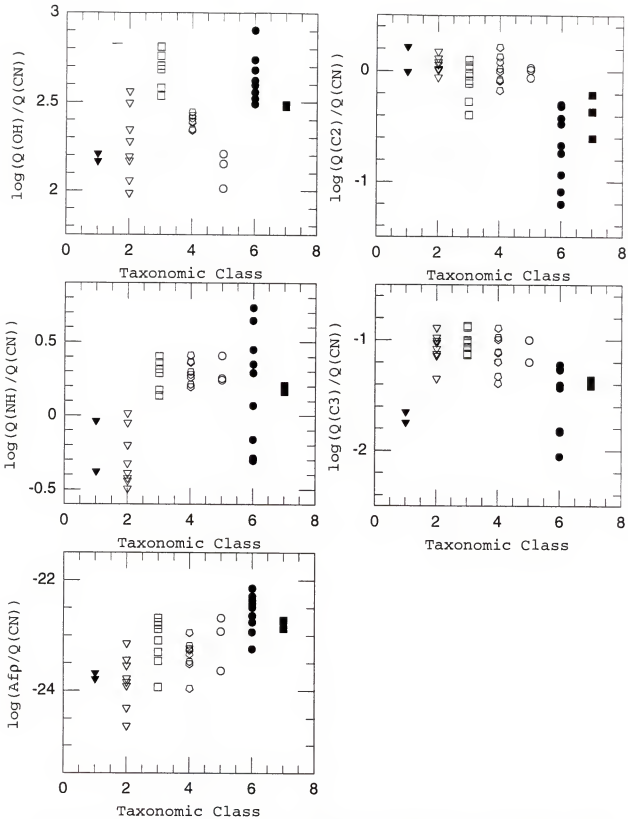

Figure 4.12 Log Ratios vs. Taxonomic Class (Restricted Set)

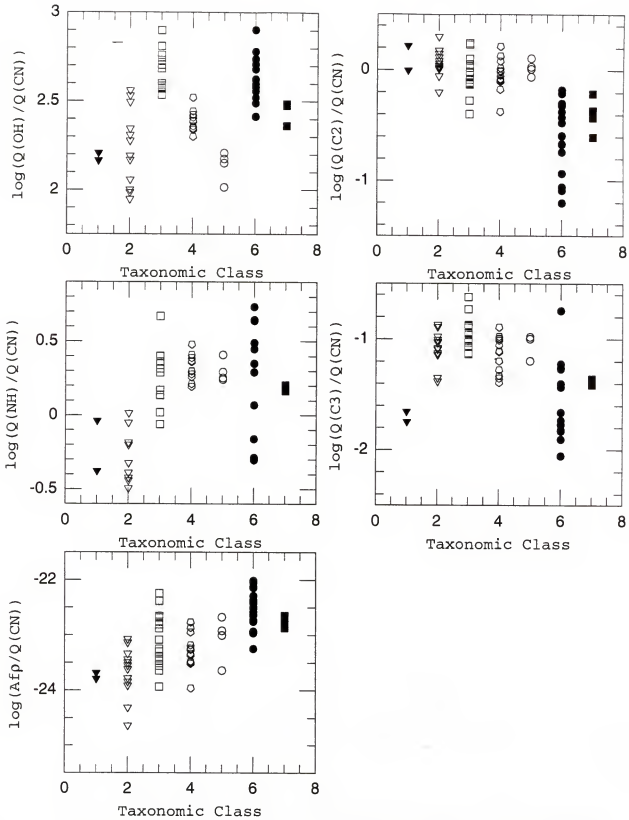

Figure 4.13 Log Ratios vs. Taxonomic Class (ALL COMETS)

Table 4.1 Parameter Ranges

Parameter	Mean	Median	Std. Dev.	Minimum	Maximum
Compositional					
log(OH/CN)	2.520	2.520	0.363	1.583	3.920
log(NH/CN)	0.239	0.254	0.474	-0.723	2.200
log(C3/CN)	-1.206	-1.106	0.363	-2.670	-0.510
log(C2/CN)	-0.135	-0.066	0.351	-1.199	0.690
log(Afr/CN)	-22.949	-22.919	0.621	-24.634	-21.370
Activity					
maximum area [km^2]	19.114	4.075	47.143	0.036	279.770
log (max. area)	0.585	0.610	0.784	-1.439	2.447
log H2O @ q [mol/sec]	28.191	28.229	0.930	26.305	30.993
active area [%]	14.951	5.439	18.011	0.124	49.396

Table 4.2 Restricted Data Set

Comet ID	dyn. family	OH/CN sigma %	NH/CN sigma %	C3/CN sigma %	Log C2/CN sigma %	Prod. Afr/CN sigma %	Rate Afr/OH sigma %	Ratios C2/OH sigma %	C3/OH sigma %	CN/OH sigma %	NH/OH sigma %
AUSTI89C1	DN	2.34	0.02	-1.08	0.01	-23.54	-26.05	-2.43	-3.56	-2.49	-2.43
		0.8	0.9	0.6	0.4	0.5	1.0	0.8	0.9	0.8	1.1
AUSTIN84I	YLP	2.06	-0.44	-0.98	0.08	-24.63	-25.54	-2.17	-3.18	-2.21	-2.70
		3.8	12.4	1.7	1.3	2.1	4.4	3.7	4.4	3.7	12.9
BM	HF	2.50	-0.05	-1.02	0.12	-23.91	-26.43	-2.39	-3.54	-2.52	-2.57
		1.4	1.6	1.2	0.9	1.3	1.7	1.3	1.6	1.4	1.9
BOETHIN	JF	2.58	0.14	-0.87	0.10	-23.46	-26.04	-2.50	-3.47	-2.61	-2.47
		3.1	3.9	2.4	1.3	2.1	3.7	3.1	3.7	3.1	4.7
BORRELLY	JF	2.49	0.21	-1.36	-0.36	-22.84	-25.46	-2.99	-4.00	-2.63	-2.41
		1.0	1.2	1.0	0.7	0.6	1.0	1.0	1.3	0.9	1.5
BRADFI79L	OLP	2.28	-0.49	-1.14	0.18	-23.84	-26.07	-2.10	-3.44	-2.30	-2.77
		1.3	1.2	0.8	0.6	0.9	1.6	1.3	1.5	1.3	1.6
BRADFI87S	OLP	2.15	0.24	-1.00	0.03	-22.67	-24.98	-2.33	-3.34	-2.33	-2.06
		1.0	1.0	0.8	0.6	0.6	1.0	1.0	1.2	0.9	1.4
BROOKS2	JF	2.60	0.65	-1.43	-0.47	-22.36	-24.97	-3.30	-4.12	-2.71	-2.05
		11.6	30.7	33.6	21.7	3.3	10.7	45.1	47.2	11.5	34.2
CG	JF	2.74	0.29	-1.25	-0.31	-22.42	-25.23	-3.08	-4.11	-2.87	-2.49
		2.0	7.4	3.3	2.7	1.4	2.0	3.1	4.2	2.0	7.6
CROMMELIN	HF	2.01	0.25	-1.00	-0.06	-23.63	-25.81	-2.23	-3.27	-2.17	-1.88
		2.2	2.0	1.5	0.9	1.3	2.4	2.1	3.5	2.2	2.8
DARREST	JF	2.41	0.30	-1.39	0.21	-23.26	-26.14	-2.37	-4.26	-2.62	-2.27
		9.2	14.6	8.1	0.9	1.4	10.5	8.7	16.2	8.9	16.7
ENCKE	JF	1.99	-0.42	-1.35	-0.06	-24.31	-26.37	-2.46	-3.35	-2.49	-2.49
		1.3	2.9	1.2	0.5	1.0	1.5	1.3	2.0	1.3	3.3
FAYE	JF	2.74	0.07	-1.22	-0.42	-22.49	-25.08	-3.13	-3.99	-2.76	-2.70
		2.2	11.8	4.8	5.0	1.6	2.3	5.2	5.3	2.2	12.3
GS	JF	2.71	0.40	-1.00	-0.39	-23.93	-25.95	-2.57	-3.69	-2.74	-2.33
		4.3	11.8	5.9	1.3	2.0	5.7	4.4	7.0	4.3	12.2
GZ	JF	2.62	-0.16	-1.82	-0.67	-23.24	-25.94	-3.41	-4.58	-2.74	-2.94
		1.0	1.8	1.7	0.9	0.8	1.1	1.2	1.9	1.0	2.1

Table 4.2 Continued

Comet ID	dyn. family	OH/CN sigma %	NH/CN sigma %	C3/CN sigma %	Log C2/CN sigma %	Prod. Afr/CN sigma %	Rate Afr/OH sigma %	Ratios C2/OH sigma %	C3/OH sigma %	CN/OH sigma %	NH/OH sigma %
HALLEY	HF	2.34	0.20	-0.89	0.13	-22.95	-25.31	-2.29	-3.30	-2.40	-2.17
		0.2	0.2	0.1	0.1	0.1	0.2	0.2	0.2	0.2	0.2
HARTLEY2	JF	2.44	0.28	-1.11	0.08	-23.47	-25.92	-2.36	-3.56	-2.45	-2.17
		2.7	2.9	2.4	1.7	2.3	3.1	2.7	3.2	2.7	3.5
HG85L	YLP	2.42	0.21	-0.99	0.02	-23.51	-25.96	-2.61	-3.64	-2.63	-2.24
		1.6	1.8	1.3	0.8	1.2	1.7	1.6	1.9	1.6	2.3
IAA83D	OLP	2.17	-0.38	-1.74	0.00	-23.68	-25.96	-2.28	-4.06	-2.33	-2.55
		2.5	5.8	2.2	1.2	1.6	2.9	2.6	3.2	2.6	5.6
IRAS	HF	2.56	0.45	-1.83	-0.93	-22.75	-25.32	-3.48	-4.41	-2.57	-2.03
		8.9	36.4	32.6	22.2	3.7	8.9	23.7	33.8	8.9	40.6
KLEMOLA	JF	2.68	0.73	-1.27	-0.29	-22.14	-24.85	-2.99	-3.98	-2.71	-1.92
		10.0	31.7	38.9	25.2	3.9	9.5	27.3	42.6	10.0	33.8
KOPFF	JF	2.68	0.14	-1.12	-0.11	-23.09	-25.67	-2.69	-3.92	-2.70	-2.58
		2.6	4.5	1.1	0.8	0.9	2.7	2.7	3.3	2.6	5.2
LEVY90C	DN	2.58	0.18	-1.03	0.05	-22.76	-25.43	-2.62	-3.73	-2.69	-2.52
		0.4	0.4	0.3	0.2	0.2	0.4	0.3	0.4	0.3	0.5
LR84T	YLP	2.35	0.41	-0.97	0.00	-23.33	-25.74	-2.38	-3.36	-2.39	-1.99
		2.9	3.0	2.4	1.8	2.3	3.2	2.9	3.3	2.8	3.9
MB	JF	2.39	0.26	-1.11	-0.09	-23.24	-25.65	-2.51	-3.52	-2.42	-2.17
		3.4	4.5	3.5	1.9	2.6	3.9	3.4	4.5	3.4	5.4
MEIER80Q	OLP	2.17	-0.39	-1.12	0.02	-23.44	-25.90	-2.38	-3.45	-2.52	-2.53
		2.1	14.7	2.0	1.2	1.8	2.9	2.3	2.8	2.5	14.8
OLR89R	DN	2.39	0.36	-1.33	-0.17	-23.96	-26.43	-2.25	-3.63	-2.39	-2.03
		2.9	3.3	0.5	0.3	0.4	3.8	2.9	3.7	2.9	4.1
PANTHE80U	YLP	2.21	0.41	-1.20	0.01	-22.92	-25.31	-2.34	-3.40	-2.37	-1.80
		2.6	3.4	2.4	1.3	1.6	3.3	2.9	3.2	3.2	4.3
SHOEMA84S	OLP	2.52	-0.29	-1.83	-0.74	-22.64	-25.18	-3.22	-4.35	-2.53	-2.81
		4.1	41.3	24.6	13.2	2.3	4.4	14.2	24.4	4.1	40.8
SL91A1	YLP	2.39	0.37	-1.20	-0.08	-23.18	-25.58	-2.48	-3.60	-2.41	-2.06
		1.7	1.6	1.8	1.0	1.4	2.0	1.8	2.3	1.8	2.1

Table 4.2 Continued

Comet ID	dyn. family	OH/CN sigma %	NH/CN sigma %	C3/CN sigma %	Log C2/CN sigma %	Prod. Afr/CN sigma %	Rate Afr/OH sigma %	Ratios C2/OH sigma %	C3/OH sigma %	CN/OH sigma %	NH/OH sigma %
SO	HF	2.76	0.32	-1.06	0.02	-22.68	-25.47	-2.80	-3.86	-2.81	-2.49
		1.2	10.9	1.3	0.9	0.9	1.3	1.3	1.6	1.2	11.4
SORREL86N	YLP	2.53	0.14	-1.01	-0.28	-22.81	-25.60	-2.98	-3.69	-2.73	-2.68
		3.9	19.4	5.5	5.1	2.5	4.4	6.5	6.4	3.9	19.9
SSF83E	YLP	2.21	-0.04	-1.65	0.22	-23.79	-26.35	-2.16	-4.15	-2.46	-2.51
		3.1	5.1	4.4	1.4	0.3	0.4	1.8	5.0	1.9	5.3
ST	HF	2.19	-0.32	-0.89	0.01	-23.14	-25.34	-2.19	-3.09	-2.20	-2.52
		2.6	2.3	2.2	1.6	2.1	3.0	2.6	3.0	2.6	3.1
SW2	JF	2.49	0.20	-1.41	-0.60	-22.72	-25.29	-3.33	-4.27	-2.84	-2.45
		11.0	38.6	31.3	16.5	4.6	8.3	22.3	30.8	8.6	47.3
TAKAMIZAW	JF	2.90	0.35	-1.40	-1.09	-22.29	-25.21	-4.13	-4.38	-2.94	-2.65
		5.0	19.5	15.4	58.8	2.6	5.0	76.5	17.1	4.9	22.7
TEMPEL1	JF	2.81	0.29	-1.13	-0.09	-22.88	-25.63	-2.90	-4.06	-2.83	-2.55
		2.3	4.7	1.9	1.3	1.3	2.4	2.6	3.4	2.3	5.6
THIELE85M	OLP	2.70	0.36	-0.88	-0.02	-23.30	-26.02	-2.74	-3.60	-2.72	-2.35
		1.6	2.0	1.5	1.1	1.5	2.0	1.6	1.9	1.6	2.4
TK90I	OLP	2.56	-0.20	-1.00	0.06	-23.78	-26.51	-2.47	-3.56	-2.56	-2.77
		2.2	6.3	1.3	0.8	1.4	3.1	2.2	2.7	2.2	6.6
WH	JF	2.49	-0.30	-2.05	-1.20	-22.93	-25.45	-3.75	-4.55	-2.53	-2.78
		5.1	32.6	61.4	29.2	2.6	5.6	36.8	60.3	5.1	32.3
WILD2	JF	2.48	0.17	-1.35	-0.21	-22.87	-25.32	-3.12	-3.93	-2.50	-2.27
		14.3	53.1	2.7	1.5	1.5	14.5	35.1	40.8	14.3	56.2

Table 4.3 Principal Component Analysis

Eigen Values

	Values	Variance Proportion %
e1	2.455	49.1
e2	1.482	29.6
e3	0.484	9.7
e4	0.355	7.1
e5	0.224	4.5

Eigen Vectors

	V1	V2	V3	V4	V5
log (OH.CN)	0.500	-0.238	-0.742	-0.187	-0.329
log (NH/CN)	0.359	-0.546	0.539	-0.530	0.027
log (C3/CN)	-0.288	-0.669	-0.292	0.227	0.577
log (C2/CN)	-0.498	-0.416	0.090	0.145	-0.741
log (Afr/CN)	0.539	-0.156	0.256	0.782	-0.090

Table 4.4 Taxonomic Class Statistics

Log Ratio	class	Mean	Median	Std. Dev.	Mimimum	Maximum
OH/CN						
	1	2.188	2.188	0.030	2.167	2.209
	2	2.261	2.236	0.200	1.987	2.560
	3	2.670	2.694	0.096	2.534	2.810
	4	2.392	2.391	0.035	2.341	2.444
	5	2.125	2.153	0.101	2.014	2.210
	6	2.650	2.622	0.130	2.490	2.904
	7	2.483	2.487	0.006	2.476	2.487
NH/CN						
	1	-0.206	-0.206	0.241	-0.377	-0.036
	2	-0.288	-0.356	0.190	-0.494	0.016
	3	0.245	0.233	0.111	0.136	0.403
	4	0.299	0.289	0.077	0.196	0.411
	5	0.302	0.254	0.093	0.243	0.410
	6	0.199	0.294	0.390	-0.303	0.734
	7	0.192	0.203	0.023	0.166	0.207
C3/CN						
	1	-1.698	-1.698	0.066	-1.745	-1.652
	2	-1.073	-1.051	0.137	-1.347	-0.890
	3	-1.014	-1.019	0.097	-1.133	-0.872
	4	-1.123	-1.109	0.173	-1.389	-0.890
	5	-1.063	-0.996	0.115	-1.196	-0.996
	6	-1.567	-1.429	0.314	-2.051	-1.221
	7	-1.375	-1.360	0.031	-1.410	-1.354
C2/CN						
	1	0.109	0.109	0.158	-0.003	0.221
	2	0.054	0.041	0.072	-0.056	0.177
	3	-0.090	-0.055	0.169	-0.393	0.100
	4	0.014	0.009	0.126	-0.170	0.215
	5	-0.004	0.015	0.047	-0.057	0.031
	6	-0.679	-0.667	0.335	-1.199	-0.294
	7	-0.389	-0.359	0.199	-0.602	-0.206
Afrho/CN						
	1	-23.737	-23.737	0.076	-23.791	-23.683
	2	-23.824	-23.808	0.478	-24.634	-23.139
	3	-23.115	-22.985	0.428	-23.933	-22.685
	4	-23.363	-23.299	0.298	-23.958	-22.948
	5	-23.076	-22.919	0.499	-23.635	-22.674
	6	-22.584	-22.489	0.346	-23.242	-22.141
	7	-22.810	-22.842	0.080	-22.869	-22.718

Table 4.5 Restricted Data Set Classes

Comet ID	Comet Name	Dyn. family	Class
AUSTI89C1	Austin (1989c1)	DN	2
AUSTIN84I	Austin (1984i)	YLP	2
BM	P/Brorsen-Metcalf	HF	2
BOETHIN	P/Boethin	JF	3
BORRELLY	P/Borrelly	JF	7
BRADFI79L	Bradfield (19791)	OLP	2
BRADFI87S	Bradfield (1987s)	OLP	5
BROOKS2	P/Brooks 2	JF	6
CG	P/Churyumov-Gerasimenko	JF	6
CROMMELIN	P/Crommelin	HF	5
DARREST	P/d'Arrest	JF	4
ENCKE	P/Encke	JF	2
FAYE	P/Faye	JF	6
GS	P/Grigg-Skjellerup	JF	3
GZ	P/Giacobini-Zinner	JF	6
HALLEY	P/Halley	HF	4
HARTLEY2	P/Hartley 2	JF	4
HG85L	Hartley-Good (19851)	YLP	4
IAA83D	IRAS-Araki-Alcock (1983d)	OLP	1
IRAS	P/IRAS	HF	6
KLEMOLA	P/Klemola	JF	6
KOPFF	P/Kopff	JF	3
LEVY90C	Levy (1990c)	DN	3
LR84T	Levy-Rudenko (1984t)	YLP	4
MB	P/Metcalf-Brewington	JF	4
MEIER80Q	Meier (1980q)	OLP	2
OLR89R	Okazaki-Levy-Rudenko (1989r)	DN	4
PANTHE80U	Panther (1980u)	YLP	5
SHOEMA84S	Shoemaker (1984s)	OLP	6
SL91A1	Shoemaker-Levy (1991a1)	YLP	4
SO	P/Stephan-Oterma	HF	3
SORREL86N	Sorrells (1986n)	YLP	3
SSF83E	Sugano-Saigusa-Fujikawa (1983e)	YLP	1
ST	P/Swift-Tuttle	HF	2
SW2	P/Schwassmann-Wachmann 2	JF	7
TAKAMIZAW	P/Takamizawa	JF	6
TEMPEL1	P/Tempel 1	JF	3
THIELE85M	Thiele (1985m)	OLP	3
TK90I	Tsuchiya-Kiuchi (1990i)	OLP	2
WH	P/Wolf-Harrington	JF	6
WILD2	P/Wild 2	JF	7

Table 4.6 Taxonomic Classes

Comet I-D	Comet Name	Dyn. family	Class
AJ	P/Ashbrook-Jackson	JF	6
AR	P/Arend-Rigaux	JF	3
AUSTI89C1	Austin (1989c1)	DN	2
AUSTIN82G	Austin (1982g)	YLP	2
AUSTIN84I	Austin (1984i)	YLP	2
BM	P/Brorsen-Metcalf	HF	2
BOETHIN	P/Boethin	JF	3
BORRELLY	P/Borrelly	JF	7
BOWELL80B	Bowell (1980b)	DN	•
BRADFI79C	Bradfield (1979c)	DN	4
BRADFI79L	Bradfield (1979l)	OLP	2
BRADFI80T	Bradfield (1980t)	YLP	•
BRADFI87S	Bradfield (1987s)	OLP	5
BROOKS2	P/Brooks 2	JF	6
BUS	P/Bus	JF	6
BUS81D	Bus (1981d)	YLP	•
CERNIS83L	Cernis (1983l)	DN	•
CG	P/Churyumov-Gerasimenko	JF	6
CHERNYKH	P/Chernykh	JF	6
CIFFREO	P/Ciffreo	JF	6
CP80K	Cernis-Petrauskas (1980k)	DN	2
CROMMELIN	P/Crommelin	HF	5
DARREST	P/d'Arrest	JF	4
ELIAS81C	Elias (1981c)	YLP	•
ENCKE	P/Encke	JF	2
FAYE	P/Faye	JF	6
FURUY87F1	Furuyama (1987f1)	YLP	3
GEHRELS2	P/Gehrels 2	JF	6
GS	P/Grigg-Skjellerup	JF	3
GUNN	P/Gunn	JF	7
GZ	P/Giacobini-Zinner	JF	6
HALLEY	P/Halley	HF	4
HARTLEY2	P/Hartley 2	JF	4
HC	P/Haneda-Campos	JF	3
HG85L	Hartley-Good (1985l)	YLP	4
HI	P/Hartley-IRAS	HF	4
HMP	P/Honda-Mrkos-Pajdsakova	JF	3
HOWELL	P/Howell	JF	4
IAA83D	IRAS-Araki-Alcock (1983d)	OLP	1
IRAS	P/IRAS	HF	6
IRAS83O	IRAS (1983o)	DN	•
KK	P/Kearns-Kwee	JF	6
KLEMOLA	P/Klemola	JF	6
KOHLER77M	Kohler (1977m)	YLP	3
KOPFF	P/Kopff	JF	3
LEVY90C	Levy (1990c)	DN	3

Table 4.6 Continued

Comet ID	Comet Name	Dyn. family	Class
LILLER88A	Liller (1988a)	OLP	5
LR84T	Levy-Rudenko (1984t)	YLP	4
MACHHO85E	Machholz (1985e)	DN	•
MB	P/Metcalf-Brewington	JF	4
MEIER78F	Meier (1978f)	DN	3
MEIER79I	Meier (1979i)	OLP	•
MEIER80Q	Meier (1980q)	OLP	2
NEUJMIN1	P/Neujmin 1	JF	3
NTT87C	Nishikawa-Takamizawa-Tago (1987c)	OLP	3
OLR89R	Okazaki-Levy-Rudenko (1989r)	DN	4
PANTHE80U	Panther (1980u)	YLP	5
RUSSELL4	P/Russell 4	JF	•
SC	P/Smirnova-Chernykh	JF	•
SG89E1	Skorichenko-George (1989e1)	YLP	4
SHOEMA83P	Shoemaker (1983p)	YLP	•
SHOEMA84F	Shoemaker (1984f)	YLP	•
SHOEMA84R	Shoemaker (1984r)	YLP	•
SHOEMA84S	Shoemaker (1984s)	OLP	6
SHOEMAKE1	P/Shoemaker 1	JF	2
SL91A1	Shoemaker-Levy (1991a1)	YLP	4
SL91D	Shoemaker-Levy (1991d)	OLP	•
SO	P/Stephan-Oterma	HF	3
SORREL86N	Sorrells (1986n)	YLP	3
SSF83E	Sugano-Saigusa-Fujikawa (1983e)	YLP	1
ST	P/Swift-Tuttle	HF	2
SW2	P/Schwassmann-Wachmann 2	JF	7
TAKAMIZAW	P/Takamizawa	JF	6
TAYLOR	P/Taylor	JF	6
TEMPEL1	P/Tempel 1	JF	3
TEMPEL2	P/Tempel 2	JF	3
THIELE85M	Thiele (1985m)	OLP	3
TK90I	Tsuchiya-Kiuchi (1990i)	OLP	2
TSUCHINS1	P/Tsushinshan 1	JF	4
TUTTLE	P/Tuttle	HF	2
WH	P/Wolf-Harrington	JF	6
WILD2	P/Wild 2	JF	7
WILD4	P/Wild 4	JF	6
WILSON86L	Wilson (1986l)	YLP	•
WIRTANEN	P/Wirtanen	JF	4

CHAPTER 5
SUMMARY

New Results

The principal conclusion from the present study is that comets can be classified based on observed variations in their molecular abundance and dust-to-gas ratios. Specifically, comets with observational measurements of the dust production and the production of 5 gaseous emission species (OH, NH, CN, C_3 and C_2) are separated into 7 compositional classes. A broad distinction exists between a large fraction of comets exhibiting strong correlations among all the carbon bearing species and a smaller number of comets showing varying degrees of depletion among the carbon chain species. If the present database included only measurements of the three carbon bearing species, this is where the classification would end. The additional observations of OH, NH, and dust, however, lead to a taxonomic classification of comets into 7 distinct groups, the details of which are provided in Chapter 4.

The compositional differences of these groups are taken as indicative of primordial differences associated with different formation regions in the proto-solar nebula. The first strong evidence leading to this interpretation is that

all but one comet separated into classes 6 and 7 are of the Jupiter-family of short period comets, and all comets in these two classes have likely origins in the Kuiper belt. This observation suggests primordial differences in the composition of Kuiper belt versus Oort cloud comets with the distinction shown in classes 6 and 7 to be depletion of the carbon chain species C_2 and C_3. Since roughly half of the Jupiter-family comets (which statistically strongly favor origin in the Kuiper belt) belong to other compositional classes, the interpretation is more complex than just differences between Oort cloud and Kuiper belt. The scenario that is proposed associates differences with actual formation region in the early nebula prior to expulsion to either the Oort cloud or Kuiper belt. Heliocentric distance gradients in either temperature (combined with localized variations in density and pressure) or cosmic ray exposure in the proto-solar nebula would have preferentially destroyed certain parent molecules at certain distances and thus led to the formation of comets of varying molecular abundance ratios. This is one qualitative explanation for the observed classes, but one cannot treat the issue quantitatively until the exact parent molecules are known for each of the measured species.

Another significant result from this study[1] is the strong correlation between dust-to-gas ratio and perihelion distance of comets suggesting an effect due to mantling of

---

[1]This correlation was first pointed out by Osip *et al.*, 1992 and has also been discussed in A'Hearn *et al.*, 1995.

the nuclear surface. Presumably, more effective mantle development occurs for those comets that more closely approach the Sun in their orbits. The large number of comets that have very low levels of activity as measured by the surface active area also suggests either more evidence for the build up of mantles or intrinsically very small comets. With nucleus size estimates available for a growing number of comets, including the in situ measurements of P/Halley, fractional active areas were calculated indicating a strong preference to small percentage active areas and thus providing additional evidence for mantling of comets.

Comparison of Results with Previous Studies

Comparing production rate ratios among several emission species for a reasonable number of comets, previous spectrophotometric studies have concluded there is a remarkable homogeneity in the composition of comets (e.g. A'Hearn and Millis, 1980; Weaver *et al.*, 1981; Williams *et al.*, 1989; Cochran *et al.*, 1992). That is not to say that no comets have been found to have evidence of unusual compositions. Observations from ultraviolet through infrared wavelengths have provided evidence for variations among several molecular species (cf. Budzien and Feldman, 1992; Colom et al., 1992; and Mumma et al., 1993). The number of comets sampled in these studies to date, however, is so small as to preclude the evaluation of meaningful statistical distinctions.

Among the large spectrophotometric investigations, only the present database has provided evidence for a number of compositionally distinct groups among the cometary population. Evaluating the abundance ratios of CN, C_3 and C_2, the McDonald Observatory Faint Comet Survey concluded that only one comet, P/Giacobini-Zinner (G-Z), had significantly different composition (Cochran 1989; Cochran *et al.*, 1992). The depletions of C_2 and C_3 in this comet have been known for half a century and recently quantified in several studies (cf. Beaver *et al.*, 1990 and references therein). Many comets in the McDonald Observatory survey, however, had only upper limits estimated for the C_2 and C_3 production.

In a preliminary analysis of an earlier version of the present database, Osip *et al.* (1992) found a number of comets exhibiting similar or more extreme depletions than those recognized in G-Z. Further evaluation of the present database led to a classification into two groups based on the ratio of CN to C_2, with G-Z as the proto-typical 'carbon chain depleted' comet and the majority of comets labeled as 'typical' (Schleicher, 1994; A'Hearn *et al.*, 1995). While these analyses classified comets based primarily on the CN to C_2 ratio, the current work fully incorporates ratios among 5 emission species and dust to further classify the comets.

The classes labeled 2-5 in Chapter 4 constitute those comets assigned in the previous and concurrent works to 'typical' compositions and the classes 6 and 7 correspond to

the 'depleted' group. Furthermore, inspection of figure 4.12 shows that the classes 2-5 clearly demonstrate the "strong degree of homogeneity in the production rate ratios" observed among the carbon bearing species for nearly all comets sampled in the McDonald Observatory survey. A number of comets from the McDonald Observatory survey, with only upper limit estimates, were observed and classified into the 'depleted' group of A'Hearn *et al.* (1995) and class 6 of this study. Similarly, the comets that were noted as having the more extreme abundance ratios or depletions from the data set of Newburn and Spinrad (1989) exhibit the same relative behaviour in the present study[2]. Thus, for the comets and species studied in earlier surveys, the present analysis is in agreement regarding compositional variations.

The current investigation confirms a number of other results from various earlier studies. First, there are no significant or systematic variations of the various abundance ratios with heliocentric distance for a given comet. Therefore, it is these abundance ratios that are used in comparing compositional differences among comets. Second, neither the cometary gas-to-dust ratio nor the activity level vary systematically with dynamical age or with heliocentric distance. This present analysis confirms quantitatively these same conclusions reached by among others, Donn (1977) and Whipple (1992). Finally, there is no conclusive evidence

---

[2]The one exception is comet P/Stephan-Oterma which Newburn and Spinrad observe to vary over a wide range in the C_2/CN ratio as a function of heliocentric distance.

suggesting compositional changes based on dynamical evolution of comets.

Directions for Future Work

Future work in the field of analyzing compositional differences in comets is proceeding along several complimentary avenues. First, many new species have been and are continuing to be detected in comets at infrared, submillimeter, and radio wavelengths (e.g., Hoban *et al.*, 1991; Krankowsky, 1991; Crovisier 1993). As statistical meaningful samples of comets are observed at these wavelengths and reduced in a uniform manner, further compositional groups may become evident. Second, continued observations of the same species analyzed here for more comets will clarify the full range of chemical variation within and among various groups. Finally, a combination of theoretical, laboratory, and observational work should eventually discriminate among the candidate parent molecules responsible for the observed emission species. With exact parent molecules known, the results of present day analysis of comets can shed light on the conditions found at various points within the forming early solar system.

Astronomers have come a long way since comets were considered irregular atmospheric phenomena and evil omens. Comets, the most primitive members of the solar system, have slowly revealed their true nature and are now beginning to reveal truths about the nature of the solar system itself.

APPENDIX
22 BIN DATA SET

Table A.1 22 Bin Data

Comet ID	log rH [AU]	pre/post perihelion	log Q(OH) [mol/s]	log Q(CN) [mol/s]	log Afrho [1/cm]	OH/CN	NH/CN	C3/CN	Log Production Rate Ratios C2/CN	Afrho/CN	Afrho/OH	C2/OH	C3/OH	CN/OH	NH/OH
AJ	0.35	pre	•	25.13	2.61	•	•	•	•	-0.52	•	•	•	•	•
AJ	0.35	post	•	24.60	2.75	•	•	•	-0.20	0.14	•	•	•	•	•
AR	0.15	pre	27.19	24.62	1.80	2.57	•	-0.89	-0.18	-0.82	-3.39	-2.75	-3.46	-2.57	•
AR	0.15	post	26.75	24.16	2.20	2.59	-0.06	-0.91	0.00	-0.10	-2.70	-2.60	-3.54	-2.62	-2.72
AR	0.25	post	•	23.84	1.79	•	•	•	-0.16	-0.16	•	•	•	•	•
AUSTI89C1	-0.15	pre	28.85	26.71	3.06	2.14	•	-0.97	0.07	-1.65	-3.81	-2.10	-3.11	-2.14	•
AUSTI89C1	-0.05	pre	•	26.50	2.66	•	•	-1.18	0.06	-1.85	•	•	•	•	•
AUSTI89C1	0.05	pre	•	26.37	2.92	•	•	-1.17	0.04	-1.45	•	•	•	•	•
AUSTI89C1	0.15	pre	•	26.14	2.88	•	•	-1.31	0.06	-1.27	•	•	•	•	•
AUSTI89C1	0.25	pre	•	25.99	2.89	•	•	-0.95	0.03	-1.16	•	•	•	•	•
AUSTI89C1	0.35	pre	•	25.94	2.86	•	•	-1.02	-0.17	-1.13	•	•	•	•	•
AUSTI89C1	-0.25	post	28.56	26.55	2.95	2.01	-0.11	-1.18	0.14	-1.60	-3.61	-1.87	-3.20	-2.01	-2.12
AUSTI89C1	-0.15	post	28.63	26.33	2.74	2.29	0.01	-1.03	0.17	-1.59	-3.93	-2.17	-3.36	-2.35	-2.32
AUSTI89C1	-0.05	post	28.62	26.12	2.50	2.50	0.07	-1.08	0.14	-1.63	-4.14	-2.36	-3.58	-2.50	-2.44
AUSTI89C1	0.05	post	28.35	25.66	2.37	2.54	0.05	-1.04	0.08	-1.46	-4.04	-2.49	-3.61	-2.54	-2.49
AUSTI89C1	0.15	post	28.03	25.49	2.44	2.47	0.05	-1.09	-0.02	-1.06	-3.55	-2.53	-3.56	-2.47	-2.43
AUSTI89C1	0.25	post	•	25.16	2.01	•	•	-1.13	-0.05	-1.15	•	•	•	•	•
AUSTIN82G	-0.15	pre	•	26.37	2.80	•	•	-0.95	0.33	-1.57	•	•	•	•	•
AUSTIN82G	-0.05	pre	•	26.04	2.51	•	•	-0.87	0.34	-1.53	•	•	•	•	•
AUSTIN82G	0.05	pre	•	25.75	2.25	•	•	-0.79	0.31	-1.42	•	•	•	•	•
AUSTIN82G	0.35	post	27.03	24.72	1.90	2.31	•	•	0.10	-0.82	-3.13	-2.21	•	-2.31	•
AUSTIN84I	-0.25	pre	•	26.56	1.80	•	•	-1.05	0.12	-2.74	•	•	•	•	•
AUSTIN84I	-0.15	pre	•	26.05	1.71	•	•	-0.84	0.23	-2.34	•	•	•	•	•
AUSTIN84I	0.05	post	27.93	25.67	2.34	2.26	-0.44	-0.95	0.07	-1.33	-3.59	-2.19	-3.21	-2.26	-2.70
AUSTIN84I	0.25	post	27.17	25.20	2.05	1.97	•	-1.02	-0.16	-1.15	-3.12	-2.13	-2.99	-1.97	•
AUSTIN84I	0.35	post	26.94	25.09	2.02	1.85	•	•	0.01	-1.07	-2.92	-1.84	•	-1.85	•
BM	-0.05	pre	28.56	26.04	2.12	2.52	-0.05	-1.04	0.14	-1.92	-4.44	-2.39	-3.55	-2.52	-2.57
BM	0.05	pre	28.32	25.75	1.92	2.57	-0.03	-0.98	0.12	-1.83	-4.40	-2.44	-3.54	-2.57	-2.59
BM	0.15	pre	27.80	25.38	1.40	2.41	-0.26	-1.02	0.08	-1.96	-4.42	-2.33	-3.43	-2.42	-2.67
BOETHIN	0.05	pre	28.41	25.82	2.38	2.61	0.14	-0.87	0.11	-1.45	-4.03	-2.53	-3.50	-2.65	-2.49
BOETHIN	0.15	pre	28.21	25.66	2.18	2.55	0.13	-0.88	0.09	-1.48	-4.06	-2.46	-3.42	-2.56	-2.41
BORRELLY	0.15	pre	28.27	25.68	2.82	2.59	0.16	-1.35	-0.38	-0.86	-3.46	-2.98	-3.95	-2.60	-2.44
BORRELLY	0.15	post	28.06	25.46	2.69	2.61	0.27	-1.37	-0.34	-0.84	-3.46	-3.00	-4.03	-2.64	-2.39
BORRELLY	0.25	post	26.54	24.74	2.28	1.87	0.12	-1.35	-0.32	-0.48	-2.88	-2.68	-3.74	-2.32	-2.24
BOWELL80B	0.55	pre	29.23	25.65	3.59	3.38	•	•	•	-0.08	-3.64	-5.29	•	-3.38	•
BOWELL80B	0.65	pre	28.82	25.41	3.90	2.84	0.92	-0.74	-0.34	0.28	-3.07	-3.91	-4.24	-3.66	-2.30
BOWELL80B	0.75	pre	28.44	24.04	3.64	∞	•	•	1.65	1.57	-2.83	-2.75	•	-4.40	•
BOWELL80B	0.55	post	27.45	25.55	3.43	1.82	0.58	-1.68	-0.39	-0.26	-3.26	-3.32	-3.90	-3.20	-2.05
BOWELL80B	0.75	post	•	•	3.46	•	•	•	∞	•	•	•	•	•	•
BRADFI79C	-0.05	post	•	24.75	1.27	•	•	-1.28	-0.10	-1.49	•	•	•	•	•
BRADFI79L	-0.25	post	•	26.92	3.04	•	•	-1.18	0.10	-2.03	•	•	•	•	•
BRADFI79L	-0.15	post	•	26.35	2.69	•	•	-1.03	0.27	-1.65	•	•	•	•	•
BRADFI79L	-0.05	post	28.26	25.93	2.30	2.37	-0.22	-1.04	0.25	-1.62	-4.09	-2.19	-3.50	-2.37	-2.59
BRADFI79L	0.05	post	27.95	25.66	1.87	2.27	-0.51	-1.13	0.19	-1.78	-4.07	-2.09	-3.43	-2.29	-2.78
BRADFI79L	0.25	post	•	25.34	•	•	•	-1.29	0.09	•	•	•	•	•	•
BRADFI80T	-0.15	post	•	27.45	4.08	•	•	•	0.35	-1.37	•	•	•	•	•
BRADFI87S	-0.05	pre	•	26.37	3.65	•	•	-0.98	0.05	-0.72	•	•	•	•	•
BRADFI87S	0.05	pre	28.59	26.25	3.51	2.33	0.15	-0.98	0.08	-0.74	-3.22	-2.40	-3.45	-2.48	-2.34
BRADFI87S	-0.05	post	28.28	26.34	3.65	2.02	0.26	-0.94	0.10	-0.70	-2.92	-2.12	-3.13	-2.19	1.89

Table A.1 22 Bin Data

Comet ID	log rH [AU]	pre/post perihelion	log Q(OH) [mol/s]	log Q(CN) [mol/s]	log Afrho [1/cm]	OH/CN	NH/CN	C3/CN	Log C2/CN	Production Afrho/CN	Rate Afrho/OH	Ratios C2/OH	C3/OH	CN/OH	NH/OH
BRADFI87S	0.05	post	28.58	26.21	3.57	2.37	0.23	-0.91	0.08	-0.64	-3.01	-2.29	-3.28	-2.37	-2.14
BRADFI87S	0.15	post	28.34	25.98	3.36	2.35	0.26	-0.98	-0.01	-0.63	-2.98	-2.36	-3.33	-2.35	-2.09
BRADFI87S	0.25	post	28.19	25.81	3.21	2.37	0.12	-1.20	-0.08	-0.61	-2.98	-2.45	-3.56	-2.38	-2.25
BRADFI87S	0.35	post	27.73	25.58	2.97	2.13	-0.02	-1.13	-0.16	-0.62	-2.77	-2.29	-3.29	-2.15	-2.19
BROOKS2	0.25	pre	26.97	24.35	2.02	2.60	0.65	-1.43	-0.47	-0.36	-2.97	-3.30	-4.12	-2.71	-2.05
BUS	0.35	pre	27.05	24.43	1.48	2.62	•	-1.90	-1.06	-0.96	-3.84	-3.71	-4.23	-2.84	•
BUSS1D	0.45	post	27.69	23.77	2.40	3.78	2.20	•	-0.81	0.63	-3.29	-4.73	•	-3.92	-1.72
CERNIS83L	0.55	post	28.69	25.96	3.73	2.71	-0.27	-1.22	-0.25	-0.23	-3.04	-3.01	-3.97	-2.83	-2.89
CG	0.15	pre	27.30	24.28	2.12	3.04	0.37	-1.31	0.05	-0.16	-3.20	-2.98	-4.36	-3.04	-2.69
CG	0.15	post	27.55	24.74	2.32	2.77	0.29	-1.25	-0.34	-0.46	-3.24	-3.10	-4.11	-2.85	-2.46
CG	0.25	post	26.99	24.44	2.25	2.55	0.42	-1.80	-0.21	-0.19	-2.76	-2.79	-4.31	-2.57	-2.18
CHERNYKH	0.45	pre	•	24.30	2.50	•	•	-1.66	-0.32	-0.05	•	•	•	•	•
CIFFREO	0.25	post	26.65	23.87	1.75	2.78	0.64	-0.74	-0.37	-0.12	-2.90	-3.15	-3.52	-2.78	-2.14
CP80E	0.15	post	27.26	25.33	2.25	1.95	•	-1.38	0.04	-1.08	-3.03	-1.90	-3.36	-1.96	•
CROMMELIN	-0.15	pre	27.77	25.83	2.15	1.94	0.23	•	-0.19	-1.68	-3.62	-2.13	•	-1.94	-1.71
CROMMELIN	-0.05	pre	27.39	25.45	1.68	1.94	•	•	-0.17	-1.77	-3.71	-2.11	•	-1.94	•
CROMMELIN	-0.15	post	28.06	25.83	2.16	2.19	0.27	-1.07	-0.10	-1.70	-3.89	-2.29	-3.27	-2.21	-1.93
CROMMELIN	-0.05	post	•	25.31	1.85	•	•	-0.95	0.14	-1.46	•	•	•	•	•
CROMMELIN	0.05	post	27.23	24.85	1.64	2.43	•	-0.79	0.15	-1.24	-3.58	-2.30	•	-2.43	•
DARREST	0.05	pre	•	25.28	2.30	•	•	•	0.22	-0.98	•	•	•	•	•
DARREST	0.05	post	•	25.37	2.34	•	•	•	0.19	-1.21	•	•	•	•	•
DARREST	0.15	post	27.47	25.17	1.85	2.41	0.43	-1.50	0.28	-1.43	-4.23	-2.46	-4.35	-2.72	-2.29
DARREST	0.25	post	27.47	25.06	1.64	2.41	0.17	-1.02	0.19	-1.42	-3.83	-2.22	-3.43	-2.41	-2.24
ELIAS81C	0.65	post	•	•	2.67	•	•	•	•	•	•	•	•	•	•
ELIAS81C	0.75	post	•	•	3.57	•	•	•	•	•	•	•	•	•	•
ENCKE	-0.25	pre	27.66	25.92	1.33	1.73	-0.52	-1.24	-0.11	-2.59	-4.35	-1.88	-2.99	-1.76	-2.26
ENCKE	-0.15	pre	27.64	25.58	1.42	2.00	-0.36	-1.14	-0.05	-2.21	-4.24	-2.16	-3.31	-2.15	-2.51
ENCKE	-0.05	pre	27.32	25.35	1.65	2.09	-0.19	-1.01	-0.01	-1.58	-3.67	-2.10	-3.10	-2.09	-2.28
ENCKE	0.05	pre	27.17	24.59	1.03	2.57	•	-1.06	0.00	-1.63	-4.22	-2.62	-3.64	-2.61	•
ENCKE	-0.25	post	•	25.95	1.49	•	•	-1.69	-0.26	-2.46	•	•	•	•	•
ENCKE	-0.15	post	27.83	25.25	1.42	2.71	•	-1.18	-0.04	-1.86	-4.51	-2.74	•	-2.71	•
ENCKE	-0.05	post	27.42	24.95	1.07	2.51	•	-1.08	0.04	-1.89	•	-4.48	-2.54	•	-2.60	•
FAYE	0.25	pre	27.66	24.92	2.63	2.74	0.07	-1.22	-0.38	-0.32	-3.08	-3.13	-3.99	-2.76	-2.70
FAYE	0.25	post	•	25.12	2.20	•	•	•	-0.76	-0.92	•	•	•	•	•
FURUY87P1	0.25	pre	28.35	25.77	2.52	2.58	0.02	-1.06	-0.12	-1.25	-3.83	-2.70	-3.64	-2.58	-2.56
GEHRELS2	0.35	post	26.43	23.85	1.84	2.58	•	•	-0.59	-0.01	-2.59	-3.17	•	-2.58	•
GS	-0.05	post	•	25.11	1.51	•	•	-0.92	-0.44	-1.83	•	•	•	•	•
GS	0.05	post	26.63	23.95	0.84	2.71	0.40	-1.01	-0.30	-2.03	-3.95	-2.57	-3.69	-2.74	-2.33
GUNN	0.45	pre	26.95	24.70	2.26	2.37	-0.78	-1.38	-0.42	-0.65	-3.95	-3.69	-3.60	-3.25	-3.02
GUNN	0.65	post	27.32	24.81	3.32	2.29	0.82	•	•	0.34	-2.11	•	•	-2.82	-1.34
GZ	0.05	pre	28.51	25.72	2.55	2.79	-0.21	-1.80	-0.65	-1.17	-3.97	-3.45	-4.60	-2.80	-3.01
GZ	0.15	pre	28.11	25.73	2.37	2.38	-0.54	-1.95	-0.82	-1.37	-3.76	-3.18	-4.32	-2.38	-2.92
GZ	0.05	post	28.06	25.35	2.15	2.71	0.06	-1.81	-0.64	-1.20	-3.95	-3.37	-4.55	-2.73	-2.67
GZ	0.15	post	27.82	25.29	2.27	2.55	-0.13	-1.82	-0.63	-1.02	-3.57	-3.17	-4.37	-2.55	-2.67
HALLEY	-0.05	pre	29.29	27.05	3.96	2.25	0.31	-0.95	0.18	-1.14	-3.29	-2.11	-3.22	-2.30	-1.96
HALLEY	0.05	pre	29.31	26.74	3.36	2.47	0.38	-0.81	0.17	-1.36	-3.73	-2.27	-3.25	-2.47	-2.09
HALLEY	0.15	pre	29.00	26.41	3.28	2.55	0.43	-0.81	0.19	-1.17	-3.72	-2.37	-3.38	-2.56	-2.13
HALLEY	0.25	pre	28.81	26.09	3.23	2.65	0.39	-0.81	0.12	-0.86	-3.56	-2.64	-3.56	-2.70	-2.30
HALLEY	0.35	pre	28.57	25.92	3.02	2.64	0.10	-0.94	-0.06	-0.91	-3.55	-2.70	-3.60	-2.65	-2.54

Table A.1 22 Bin Data

Comet ID	log rH [AU]	pre/post perihelion	log Q(OH) [mol/s]	log Q(CN) [mol/s]	log Afrho [1/cm]	OH/CN	NH/CN	C3/CN	Log C2/CN	Production Afrho/CN	Rate Afrho/OH	Ratios C2/OH	C3/OH	CN/OH	NH/OH
HALLEY	0.45	pre	28.18	25.67	2.79	2.48	0.01	-0.98	-0.19	-0.92	-3.43	-2.67	-3.47	-2.49	-2.47
HALLEY	-0.15	post	29.55	27.40	4.54	2.15	0.12	-1.03	0.07	-0.98	-3.04	-2.02	-3.09	-2.15	-2.03
HALLEY	-0.05	post	29.33	27.11	4.27	2.20	0.14	-0.93	0.16	-0.90	-3.11	-2.07	-3.15	-2.23	-2.08
HALLEY	0.05	post	29.24	26.83	3.96	2.37	0.19	-0.89	0.15	-0.92	-3.29	-2.23	-3.27	-2.37	-2.18
HALLEY	0.15	post	29.06	26.66	3.85	2.38	0.21	-0.89	0.14	-0.86	-3.24	-2.26	-3.30	-2.40	-2.17
HALLEY	0.25	post	28.94	26.45	3.62	2.41	0.17	-0.86	0.09	-0.85	-3.28	-2.34	-3.31	-2.44	-2.25
HALLEY	0.35	post	28.65	26.33	3.48	2.30	0.07	-0.90	0.02	-0.88	-3.19	-2.30	-3.25	-2.33	-2.24
HALLEY	0.65	post	27.61	25.52	3.33	2.10	0.80	-0.84	-0.07	-0.19	-2.28	-2.25	-3.03	-2.10	•
HALLEY	0.75	post	27.06	25.26	3.17	1.68	0.96	-0.86	-0.12	-0.21	-1.92	-2.23	-2.85	-1.91	-0.78
HARTLEY2	0.05	post	28.31	25.87	2.41	2.44	0.28	-1.11	0.08	-1.47	-3.92	-2.36	-3.56	-2.45	-2.17
HC	0.05	pre	•	23.70	1.46	•	•	-0.73	-0.13	-0.24	•	•	•	•	•
HG85L	-0.15	pre	28.26	26.01	2.36	2.25	0.10	-1.03	-0.01	-1.65	-3.84	-2.19	-3.28	-2.27	-2.05
HG85L	-0.05	pre	28.30	25.78	2.21	2.52	0.26	-0.97	0.12	-1.57	-4.09	-2.40	-3.49	-2.52	-2.26
HG85L	0.15	pre	27.99	25.32	2.00	2.67	0.39	-1.00	0.04	-1.32	-3.99	-2.64	-3.67	-2.68	-2.29
HG85L	0.25	pre	27.88	25.17	2.18	2.71	0.35	-1.01	-0.03	-0.99	-3.72	-2.76	-3.73	-2.73	-2.37
HG85L	-0.05	post	27.87	25.56	2.13	2.31	0.30	-0.93	0.09	-1.43	-3.75	-2.23	-3.25	-2.32	-2.03
HI	0.25	post	27.96	25.60	2.34	2.36	•	•	-0.09	-1.26	-3.62	-2.45	•	-2.36	•
HMF	0.05	pre	26.84	23.94	0.55	2.90	0.67	-0.95	0.23	-1.39	-4.29	-2.67	-3.85	-2.90	-2.23
HOWELL	0.35	post	27.12	23.48	2.01	2.30	1.33	-1.35	-0.09	-0.77	-3.23	-2.55	-3.73	-2.47	•
IAA83D	0.05	pre	27.62	25.34	1.70	2.17	-0.38	-1.80	0.02	-1.70	-3.96	-2.28	-4.06	-2.33	-2.55
IAA83D	0.05	post	•	25.57	1.93	•	•	-0.99	-0.04	-1.64	•	•	•	•	•
IRAS	0.25	post	27.50	24.93	2.20	2.56	0.45	-1.83	-0.93	-0.75	-3.32	-3.48	-4.41	-2.57	-2.03
IRAS	0.35	post	•	24.49	1.71	•	•	•	-0.95	-0.78	•	•	•	•	•
IRAS830	0.35	post	27.37	24.60	2.46	2.65	0.94	-0.68	0.04	-0.21	-2.92	-2.61	-3.33	-2.65	-1.71
IRAS830	0.45	post	26.84	24.15	2.36	2.77	1.20	-0.82	-0.98	0.10	-2.81	-3.87	-3.70	-2.86	-1.40
KK	0.35	pre	26.90	24.54	1.90	2.40	•	-1.73	-0.19	-0.74	-3.37	-2.75	-4.12	-2.68	•
KK	0.35	post	27.19	24.46	2.05	2.73	•	•	0.15	-0.42	-3.15	-2.58	•	-2.73	•
KLEMOLA	0.25	post	26.91	24.22	2.11	2.68	0.73	-1.27	-0.29	-0.14	-2.85	-2.99	-3.98	-2.71	-1.92
KOHLER77M	-0.05	pre	•	26.18	2.66	•	•	-0.83	0.24	-1.53	•	•	•	•	•
KOHLER77M	0.05	pre	•	26.14	2.40	•	•	-0.95	0.22	-1.73	•	•	•	•	•
KOHLER77M	0.15	pre	•	25.72	2.25	•	•	•	0.29	-1.47	•	•	•	•	•
KOPFF	0.25	pre	28.33	25.70	2.64	2.69	0.14	-1.12	-0.11	-1.07	-3.65	-2.69	-3.92	-2.71	-2.58
KOPFF	0.35	pre	•	25.51	2.56	•	•	•	-0.27	-0.95	•	•	•	•	•
KOPFF	0.25	post	28.10	25.47	2.22	2.61	0.08	-1.21	-0.04	-1.26	-3.88	-2.65	-3.82	-2.61	-2.53
LEVY90C	0.05	pre	29.19	26.57	3.73	2.52	0.13	-0.96	0.10	-0.84	-3.36	-2.36	-3.60	-2.52	-2.39
LEVY90C	0.15	pre	29.21	26.48	3.76	2.67	0.19	-1.03	0.09	-0.72	-3.38	-2.59	-3.72	-2.68	-2.48
LEVY90C	0.25	pre	29.24	26.44	3.64	2.77	0.13	-1.03	0.05	-0.80	-3.59	-2.72	-3.79	-2.78	-2.64
LEVY90C	0.35	pre	29.04	26.41	3.50	2.58	-0.21	-1.11	-0.08	-0.89	-3.49	-2.70	-3.69	-2.64	-2.78
LEVY90C	0.15	post	•	26.31	3.54	•	•	-0.89	0.10	-0.77	•	•	•	•	•
LEVY90C	0.25	post	28.35	26.18	3.40	2.17	0.08	-1.01	0.02	-0.78	-2.95	-2.15	-3.18	-2.17	-2.09
LEVY90C	0.35	post	28.34	26.06	3.36	2.24	-0.08	-1.11	-0.13	-0.71	-2.97	-2.40	-3.40	-2.27	-2.34
LEVY90C	0.45	post	27.76	25.83	3.08	1.94	-0.68	-1.30	-0.21	-0.76	-2.70	-2.15	-3.24	-1.95	-2.56
LILLER88A	0.05	post	28.62	26.44	3.43	2.18	0.29	-0.98	0.11	-1.01	-3.18	-2.08	-3.16	-2.19	-1.88
LR84T	0.05	pre	27.93	25.52	2.16	2.42	0.43	-0.96	0.02	-1.36	-3.78	-2.39	-3.37	-2.42	-1.98
LR84T	0.15	post	27.48	25.20	1.93	2.28	0.24	-1.02	-0.06	-1.27	-3.55	-2.34	-3.30	-2.28	-2.04
LR84T	0.25	post	26.93	24.84	1.64	2.09	•	•	-0.18	-1.20	-3.29	-2.27	•	-2.09	•
MACHHO85E	-0.05	pre	•	25.70	•	•	•	•	0.04	•	•	•	•	•	•
MB	0.25	post	28.09	25.73	2.53	2.39	0.26	-1.11	-0.09	-1.24	-3.65	-2.51	-3.52	-2.42	-2.17
METER78F	0.35	pre	•	26.59	4.62	•	•	•	•	0.03	•	•	•	•	•

Table A.1 22 Bin Data

Comet ID	log rH	pre/post	log Q(OH)	log Q(CN)	log Afrho				Log	Production	Rate	Ratios			
	[AU]	perihelion	[mol/s]	[mol/s]	[1/cm]	OH/CN	NH/CN	C3/CN	C2/CN	Afrho/CN	Afrho/OH	C2/OH	C3/OH	CN/OH	NH/OH
MEIER78F	0.45	pre	•	26.57	3.86	•	•	•	-0.12	-0.71	•	•	•	•	•
MEIER79I	0.15	pre	•	24.85	1.95	•	•	-0.51	0.20	-0.90	•	•	•	•	•
MEIER80Q	0.15	pre	28.54	25.79	2.45	2.73	•	-0.96	0.13	-1.42	-4.13	-2.60	-3.67	-2.74	•
MEIER80Q	0.15	post	•	25.96	2.91	•	•	•	0.09	-1.05	•	•	•	•	•
MEIER80Q	0.25	post	28.25	26.04	2.46	2.21	•	-1.11	-0.02	-1.58	-3.79	-2.23	-3.32	-2.21	•
MEIER80Q	0.35	post	27.88	25.73	2.31	2.14	-0.39	-1.15	-0.01	-1.43	-3.57	-2.15	-3.30	-2.14	$\frac{1}{2}$-2.53
NEUJMIN1	0.15	post	27.16	24.43	2.05	2.73	0.40	-0.62	0.05	-0.38	-3.11	-2.68	-3.35	-2.73	-2.33
NTT87C	0.05	pre	28.58	26.01	2.46	2.57	•	•	0.10	-1.55	-4.12	-2.47	•	-2.57	•
NTT87C	0.25	post	•	•	0.64	•	•	•	•	•	•	•	•	•	•
OLR89R	0.05	pre	28.83	26.44	2.40	2.39	0.36	-1.24	0.14	-2.04	-4.43	-2.25	-3.63	-2.39	-2.03
OLR89R	-0.15	post	•	26.42	2.36	•	•	-1.43	-0.20	-2.05	•	•	•	•	•
OLR89R	-0.05	post	•	26.15	2.24	•	•	-1.29	-0.16	-1.93	•	•	•	•	•
OLR89R	0.05	post	•	25.72	1.96	•	•	-1.35	-0.22	-1.79	•	•	•	•	•
PANTHE80U	0.25	pre	28.89	26.07	3.15	2.84	•	•	0.07	-0.92	-3.76	-2.78	•	-2.84	•
PANTHE80U	0.25	post	28.36	26.16	3.24	2.21	0.41	-1.20	0.00	-0.92	-3.13	-2.21	-3.40	-2.21	-1.80
PANTHE80U	0.65	post	28.06	24.42	2.08	3.63	•	•	0.25	-0.34	-3.97	-3.38	•	-3.63	•
RUSSELL4	0.35	post	27.10	23.62	2.07	3.41	1.43	-2.67	0.69	0.23	-3.15	-3.01	-6.07	-3.47	-2.07
SC	0.55	pre	26.46	•	2.68	•	•	•	•	•	-1.78	-1.85	•	•	•
SC	0.55	post	27.80	24.65	2.78	3.15	1.29	-1.24	0.03	0.13	-3.02	-3.12	-4.39	-3.15	-1.86
SG89E1	0.25	pre	28.19	25.86	2.99	2.34	0.30	-1.01	-0.04	-0.87	-3.39	-2.58	-3.55	-2.52	-2.24
SHOEMA83P	0.55	pre	•	25.02	2.87	•	•	-1.07	-0.05	-0.16	•	•	•	•	•
SHOEMA83P	0.55	post	•	24.88	2.97	•	•	•	0.04	0.09	•	•	•	•	•
SHOEMA84F	0.45	pre	•	25.56	3.66	•	•	•	0.82	-0.41	•	•	•	•	•
SHOEMA84F	0.55	pre	28.49	25.35	3.54	3.14	•	•	0.60	0.19	-2.95	-2.54	•	-3.14	•
SHOEMA84F	0.65	pre	27.77	24.65	3.44	3.12	•	•	0.52	0.79	-2.33	-2.60	•	-3.12	•
SHOEMA84F	0.75	post	•	25.39	3.04	•	•	•	0.78	-0.35	•	•	•	•	•
SHOEMA84R	0.75	post	28.73	25.02	3.23	3.27	•	•	0.60	0.03	-3.28	•	•	-3.27	•
SHOEMA84S	0.15	pre	26.94	24.45	1.91	2.49	-0.48	-2.08	-0.78	-0.54	-3.03	-3.27	-4.57	-2.49	-2.97
SHOEMA84S	0.15	post	26.92	24.37	1.71	2.55	-0.22	-1.71	-0.72	-0.67	-3.23	-3.20	-4.26	-2.55	-2.77
SHOEMA84S	0.25	post	26.77	24.17	1.50	2.60	0.70	•	•	-0.67	-3.27	•	•	-2.60	-1.90
SHOEMAKE1	0.35	post	27.47	25.47	2.14	2.00	-0.18	-1.09	-0.20	-1.33	-3.36	-2.35	-3.12	-2.03	-2.21
SL91A1	-0.05	pre	28.19	25.79	2.62	2.39	0.37	-1.20	-0.08	-1.18	-3.58	-2.48	-3.60	-2.41	-2.06
SL91D	0.45	post	27.54	25.67	3.22	1.86	0.22	-1.05	-0.30	-0.45	-2.35	-2.15	-2.92	-1.89	-1.74
SO	0.15	pre	28.28	25.47	2.94	2.81	•	-1.18	-0.03	-0.53	-3.38	-2.85	-3.95	-2.85	•
SO	0.25	pre	27.95	25.18	2.41	2.77	0.31	-0.99	0.05	-0.78	-3.57	-2.75	-3.79	-2.80	-2.49
SO	0.15	post	28.27	25.40	3.02	2.87	•	-1.08	-0.04	-0.39	-3.26	-2.91	-3.95	-2.87	•
SO	0.25	post	27.67	24.97	2.42	2.69	•	-1.05	0.05	-0.54	-3.22	-2.67	-3.76	-2.71	•
SO	0.35	post	26.69	23.72	1.48	2.91	1.35	•	0.41	-0.26	-3.22	-2.60	•	-2.91	-1.56
SORREL86N	0.25	pre	28.88	26.07	3.21	2.82	0.14	-0.92	-0.27	-0.86	-3.69	-3.09	-3.73	-2.82	-2.68
SORREL86N	0.35	pre	28.29	25.76	3.15	2.53	•	-1.07	-0.28	-0.61	-3.14	-2.81	-3.60	-2.53	•
SORREL86N	0.35	post	28.08	25.66	2.93	2.42	•	-1.13	-0.28	-0.73	-3.15	-2.70	-3.55	-2.42	•
SSF83E	-0.25	post	27.85	25.56	1.89	2.10	•	-0.81	0.19	-1.75	-4.02	-2.08	-3.18	-2.35	•
SSF83E	-0.15	post	27.58	25.00	1.07	2.58	0.25	-1.27	0.25	-1.92	-4.50	-2.33	-3.85	-2.58	-2.33
SSF83E	0.05	post	26.46	23.99	-1.28	2.47	-0.11	-1.78	0.34	-3.27	-5.74	-2.13	-4.25	-2.47	-2.58
ST	-0.05	pre	29.42	27.22	4.09	2.19	-0.32	-0.89	0.01	-1.14	-3.34	-2.19	-3.09	-2.20	-2.52
SW2	0.35	pre	27.89	24.99	2.78	2.90	•	-1.37	-0.84	-0.21	-3.11	-3.74	-4.27	-2.90	•
SW2	0.35	post	27.64	25.05	2.23	2.59	0.14	•	-0.58	-0.82	-3.41	-3.17	•	-2.59	-2.45
SW2	0.45	post	25.86	24.51	2.09	1.35	0.74	-2.77	•	-0.42	-1.77	•	-4.12	-1.35	-0.61
TAKAMIZAW	0.25	post	28.31	25.37	3.10	2.94	0.30	-1.44	-1.23	-0.27	-3.22	-4.17	-4.38	-2.95	-2.65

Table A.1 22 Bin Data

Comet ID	log rH	pre/post	log Q(OH)	log Q(CN)	log Afrho				Log	Production	Rate	Ratios			
	[AU]	perihelion	[mol/s]	[mol/s]	[1/cm]	OH/CN	NH/CN	C3/CN	C2/CN	Afrho/CN	Afrho/OH	C2/OH	C3/OH	CN/OH	NH/OH
TAKAMIZAW	0.35	post	26.83	24.37	2.04	2.46	1.08	-0.72	-0.41	-0.34	-2.82	-2.94	-3.08	-2.50	-1.28
TAYLOR	0.25	pre	•	24.65	2.07	•	•	•	-0.66	-0.58	•	•	•	•	•
TEMPEL1	0.15	pre	28.05	25.31	2.34	2.73	0.40	-1.03	-0.11	-0.97	-3.70	-2.46	-3.79	-2.73	-2.33
TEMPEL1	0.25	pre	27.96	25.13	2.39	2.83	0.21	-1.22	-0.06	-0.78	-3.62	-2.92	-4.09	-2.85	-2.64
TEMPEL1	0.35	pre	•	•	1.87	•	•	•	•	•	•	•	•	•	•
TEMPEL2	0.15	pre	•	25.45	2.04	•	•	•	0.15	-1.40	•	•	•	•	•
TEMPEL2	0.25	pre	27.08	24.49	1.66	2.60	•	•	•	-1.18	-3.77	-2.70	•	-2.60	•
TEMPEL2	0.15	post	•	25.70	2.21	•	•	-0.94	-0.05	-1.49	•	•	•	•	•
THIELE8SM	0.15	pre	28.19	25.50	2.24	2.70	0.36	-0.88	-0.02	-1.30	-4.02	-2.74	-3.60	-2.72	-2.35
TK90I	0.15	pre	28.72	26.15	2.27	2.56	-0.20	-1.02	0.09	-1.89	-4.51	-2.47	-3.56	-2.56	-2.77
TK90I	0.15	post	•	26.18	2.52	•	•	-1.06	0.08	-1.66	•	•	•	•	•
TK90I	0.25	post	•	25.76	2.36	•	•	-0.90	0.01	-1.40	•	•	•	•	•
TSUCHINS1	0.25	post	27.16	24.77	1.59	2.39	0.48	-0.99	-0.37	-1.18	-3.57	-2.76	-3.38	-2.39	-1.91
TUTTLE	0.05	pre	28.09	25.55	1.96	2.54	•	-1.03	0.15	-1.60	-4.15	-2.39	-3.58	-2.54	•
TUTTLE	0.15	pre	27.80	25.38	1.62	2.42	•	•	0.14	-1.76	-4.18	-2.28	•	-2.42	•
WH	0.25	pre	27.58	25.06	2.13	2.49	-0.35	-1.76	-1.25	-0.95	-3.48	-3.95	-4.34	-2.54	-2.81
WH	0.25	post	27.47	24.98	2.12	2.49	-0.24	-2.25	-1.15	-0.86	-3.35	-3.64	-4.74	-2.49	-2.73
WILD2	0.15	pre	•	25.59	2.67	•	•	-1.35	-0.13	-0.94	•	•	•	•	•
WILD2	0.25	pre	•	25.11	2.60	•	•	•	-0.37	-0.52	•	•	•	•	•
WILD2	0.35	pre	27.60	25.12	2.31	2.48	0.17	-1.36	-0.61	-0.83	-3.32	-3.12	-3.93	-2.50	-2.27
WILD2	0.45	pre	•	24.77	2.21	•	•	•	-0.90	-0.56	•	•	•	•	•
WILD4	0.35	pre	27.31	24.64	2.27	2.71	0.49	-1.77	-0.59	-0.51	-3.51	-3.42	-4.70	-2.86	-2.44
WILSON86L	0.35	pre	28.89	26.24	3.49	2.65	•	-1.19	-0.25	-0.75	-3.40	-2.90	-3.84	-2.65	•
WILSON86L	0.55	pre	27.68	25.66	3.53	2.00	0.50	-1.17	-0.96	-0.14	-2.15	-2.96	-3.17	-2.00	-1.50
WILSON86L	0.55	post	27.43	25.85	3.61	1.56	0.50	-1.06	-0.23	-0.28	-1.86	-1.76	-2.64	-1.57	-1.10
WILSON86L	0.65	post	27.64	25.09	3.15	2.55	•	•	•	0.06	-2.49	•	•	-2.55	•
WIRTANEN	0.05	post	27.93	25.41	2.05	2.52	0.39	-1.05	-0.01	-1.36	-3.88	-2.53	-3.57	-2.52	-2.13

BIBLIOGRAPHY

A'Hearn, M. F. (1991). In *The Comet Halley Archive Summary Volume*, ed. Z. Sekanina (Pasadena, Jet Propulsion Laboratory), 193.

A'Hearn, M. F., Campins, H., Schleicher, D. G., and Millis, R. L. (1989). Astrophys. J. 347, 1155.

A'Hearn, M. F. and Millis, R. L. (1978). Bull. Amer. Astron. Soc. 10, 588.

A'Hearn, M. F., Millis, R. L., and Birch, P. V. (1979). Astron. J. 84, 570.

A'Hearn, M. F. and Millis, R. L. (1980). Astron. J. 85, 1528.

A'Hearn, M. F., Millis, R. L., and Birch, P. V. (1981). Astron. J. 86, 1559.

A'Hearn, M. F., Millis, R. L., Schleicher, D. G., Osip, D. J., and Birch, P. V. (1992). In *Abstracts for The International Conference on Asteroids, Comets, Meteors 1991*, LPI Contribution No. 765, 1.

A'Hearn, M. F., Millis, R. L., Schleicher, D. G., Osip, D. J., and Birch, P. V. (1995). Icarus, in press.

A'Hearn, M. F., Schleicher, D. G., Feldman, P. D., Millis, R. L., and Thompson, D. T. (1984). Astron. J. 89, 579.

A'Hearn, M. F. and Vanysek, V. (1992). In Comet Halley Archive - Release 1.0 CD-ROM Vol. USA_NASA_IHW_HAL_0019 through 0024 (Arch: E. Grayzeck, D. Klinglesmith, and M. Niedner) International Halley Watch, GSFC, Greenbelt, MD.

Baum, W. A., Kreidl, T. J., and Schleicher, D. G. (1992). Astron. J. 104, 1216.

Bessel, F. W. (1836). AN 13, 345 (#310; June 11, 1836).

Beyer, M. (1969). Astron. Nachr. 291, 257.

Budzien, S. A. and Feldman, P. D. (1992). Icarus 99, 143.

Budzien, S. A., Festou, M. C., and Feldman, P. D. (1994). Icarus 107, 164.

Campins, H. (1985). In *Ices in the Solar System* eds. J. Klinger *et al.* (Dordrecht, Boston, and Lancaster; D. Reidel Publishing), 443.

Campins, H., A'Hearn, M. F., and McFadden, L. A. (1987). Astrophys. J. 316, 847.

Campins, H., Osip, D. J., Rieke, G. H., and Rieke, M. J. (1995). Planet. Space Sci. in press.

Campins, H., Telesco, C. M., Osip, D. J., Rieke, G. H., Rieke, M. J., and Schulz, B. (1994). Astron. J. 108, 2318.

Carusi, A. and Valsecchi, G. (1987). In Interplanetary Matter eds. Z. Ceplecha and P. Pecian (...), 21.

Cochran, A. L. (1987). Astron. J. 92, 231.

Cochran, A. L. (1989). In *Asteroids, Comets and Meteors Vol. III*, eds. G. Lagerkvist, H. Rickman, B. A. Lindlad, and M. Lindgren (Proceedings), 281.

Cochran, A. L., and Barker, E. S. (1987). Astron. J. 92, 239.

Cochran, A. L., Barker, E. S., Ramseyer, T. F., and Storrs, A. D. (1992). Icarus 98, 151.

Cochran, A. L., Green, J. R., and Barker, E. S. (1989). Icarus 79, 125.

Cochran, A. L. and Schleicher, D. G. (1993). Icarus 105, 235.

Colom, P., Crovisier, J., Bockellee-Morvan, D., Despois, D., and Paubert, G. (1992). Astron. Astrophys. 264, 270.

Cowan, J. J. and A'Hearn, M. F. (1979). Moon and Planets 21, 155.

Crovisier, J. (1989). Astron. Astrophys. 213, 459.

Crovisier, J. (1993). In *Asteroids, Comets, Meteors, 1993* eds. A. Milani, M DiMartino, and A. Cellino (Berlin, Kluwer Acad. Pub.), 313.

Delsemme, A. H. (1973). Astron. & Astrophys. 29, 327.

Dickman, S. (1990). Nature 346, 4.

Donn, B. (1977). In *Comets, Asteroids, Meteorites*, ed. A. H. Delsemme (Toledo, U. Toledo), 15.

Duncan, M., Quinn, T., and Tremaine, S. (1988). Astrophys. J.-Lett. 328, L69.

Everhart, E. (1972). Astrophys. Lett. 10, 131.

Feldman, P. D., Fournier, K. B., Grinin, V. P., and Zvereva, A. M. (1993). Astrophys. J. 404, 348.

Fernandez, J. A. (1980). Mon. Not. Roy. Astron. Soc. 192, 481.

Fernandez, J. A. (1994). In *Asteroids, Comets, Meteors 1993*. eds. A. Milan, M. Di Martino, and A. Cellino (Dordrecht, Kluwer), 223.

Halley, E. (1705). *Astronomiae Cometicae Synopsis*, Oxford, (translated as A Synopsis of the Astronomy of Comets, 1705, London).

Hanner, M. S. (1984). Astrophys. J. Lett. 277, L75.

Haser, L. (1957). Bull. Acad. R. Belgique, Classes des Sciences, Ser. 5, 43, 740.

Hoban, S., Mumma, M., Reuter, D. C., DiSanti, M., Joyce, R. R., and Storrs, A. D. (1991). Icarus 93, 122.

Howell, E. S., Merenyi, E., and Lebofsky, L. A. (1994). Journ. Geophys. Res. Vol. 99 No.e5, 10847.

Hughes, D. W. (1987). In *Diversity and Similarity of Comets*, ESA SP-278, 43.

Jewitt, D. and Luu, J. (1994). Astron. J. in press.

Jewitt, D. C. and Meech, K. J. (1987). Astrophys. J. 317, 992.

Joss, P. C. (1973). Astron. & Astrophys. 25, 271.

Keller, H. U. et al. (1987). Astron. Astrophys. 187, 807.

Kim, S. J., A'Hearn, M. F., and Cochran, W. D. (1989). Icarus 77, 98.

Krankowsky, D. (1991). In *Comets in the Post-Halley Era* eds. R. Newburn *et al.*(Tucson, U. Arizona Press) vol. 2, 855.

Kresak, L., and Kresakova, M. (1987). In *Diversity and Similarity of Comets*, ESA SP-278, 37.

Kresak, L., and Kresakova, M. (1989). Bull. Astron. Inst. Czechosl. 40, 269.

Kresak, L., and Kresakova, M. (1990). Bull. Astron. Inst. Czechosl. 41, 1.

Kuiper, G. P. (1951). In *Astrophysics*, ed. J. A. Hynek (McGraw Hill, New York), 357.

Levison, H. F. and Duncan, M. J. (1994). Icarus 108, 18.

Luu, J. and Jewitt, D. C. (1990). Icarus 86, 69.

Luu, J. and Jewitt, D. C. (1992). Astron. J. 104, 2243.

Lyttleton, R. A. (1948). Mon. Not. Roy. Astron. Soc. 108, 465.

Lyttleton, R. A. (1952). Ap.J. 115,333.

Marsden, B. G. (1989). Astron. J. 74, 720.

Marsden, B. G. and Williams, G. V. (1994). Catalog of Cometary Orbits. 9th edition (Cambridge, Minor Planet Center).

Meech, K. J. (1994). Urey Prize Lecture, 1994 Division of Planetary Sciences Meeting, Bul. Amer. Astron. Soc.

Mendis, D. A. (1988). Ann. Rev. Astron. Astrophys. 26, 11.

Millis, R. L., A'Hearn. M. F., and Thompson, D. (1982). Astron. J. 87, 1310.

Millis, R, L., A'Hearn. M. F., and Campins, H. (1988). Astrophys. J. 324, 1194.

Mumma, M. J., Weissman, P. R., and Stern, S. A. (1993). In *Protostars and Planets III*, eds. E. H. Levy and J. I. Lunine (Tucson, U. Arizona Press), 1177.

Newburn, R. L. Jr., and Spinrad, H. (1984). Astron. J. 89, 289.

Newburn, R. L. Jr., and Spinrad, H. (1985). Astron. J. 90, 2591.

Newburn, R. L. Jr., and Spinrad, H. (1989). Astron. J. 97, 552.

Newton, H. A. (1893). Mem. Natl. Acad. Sci. 6, 7.

Newton, I. (1687). *Philosophiae Naturalis Principia Mathematica*, London.

Oort, J. H. (1950). Bull. Astr. Inst. Netherl. 11, 91.

Oort, J. H. (1992). In *Physics and Chemistry of Comets* ed. W. F. Huebner (Berlin, Springer-Verlag), 235.

Opik, E. J. (1932). Proc. Amer. Acad. Astr. Sci. 67, 199.

Osborn, W. H., A'Hearn, M. F., Carsenty, U., Millis, R. L., Schleicher, D. G., Birch, P. V., Moreno, H., and Gutierrez-Moreno, A. (1990). Icarus 88, 228.

Osip, D. J., Campins, H., and Schleicher, D. G. (1995). Icarus 114, 423.

Osip, D. J., Schleicher, D. G., and Millis, R. L. (1992a). Icarus 98, 115.

Osip, D. J., Schleicher, D. G., Millis, R. L., A'Hearn, M. F., and Birch, P. V. (1992b). In *Asteroids, Comets, Meteors 1991* eds. A. W. Harris and E. Bowell (Houston, LPI), 443.

Osip, D. J., Schleicher, D. G., Millis, R. L., A'Hearn, M. F., and Birch, P. V. (1992). Bull. Amer. Astron. Soc. Vol. 24, No. 3, 1001.

Randall, C. E., Schleicher, D. G., Ballou, R. G., and Osip, D. J. (1992) Bull. Amer. Astron. Soc. 24, 1002.

Rickman, H., and Huebner, W. F. (1992). In *Physics and Chemistry of Comets* ed. W. F. Huebner (Berlin, Springer-Verlag), 245.

Rickman, H., Kamel, L., Festou, M. C., and Froeschle, C. (1987). In *Diversity and Similarity of Comets*, ESA SP-278, 471.

Schleicher, D. G. (1983). PhD. Thesis, University of Maryland.

Schleicher, D. G., Millis, R. L., and Birch, P. V. (1987). Astron. & Astrophys. 187, 531.

Schleicher, D. G. (1994). Plan. Space Sci. in press.

Schleicher, D. G. and A'Hearn, M. F. (1988). Astrophys. J. 331, 1058.

Scotti, J. V. (1995). Unpublished manuscript.

Sekanina, Z. (1988). Astron. J. 95, 911.

Storrs, A. D., Cochran, A. L., and Barker, E. S. (1992). Icarus 98, 163.

Swings, P. (1941). Lick Obs. Bull. XIX, 131, 408, 707.

Swings, P. (1942). Ap.J. 95, 270.

Tholen, D. J. (1984). Ph.D. Thesis University of Arizona.

Weaver, H. A., Feldman, P. D., Festou, M. C., A'Hearn, M. F., and Keller, H. U. (1981). Icarus 47, 449.

Weissman, P. R. (1991). In *Comets in the Post-Halley Era*, eds. J. Lewis, M. S. Matthews, and M. Guerrieri (Tucson, U. Arizona Press), 569.

Weissman, P. R. (1995). Ann. Rev. Astron. & Astrophys. 1995, in press.

Whipple, F. L. (1950). Ap.J. 111, 375.

Whipple, F. L. (1992). In *Asteroids, Comets, Meteors 1991* eds. A. W. Harris and E. Bowell (Houston, LPI), 633.

Williams, I. P., Andrews, P. J., Fitzsimmons, A., and Williams, G. P. (1989). In *Asteroids, Comets, and Meteors, Vol III* eds. G. Lagerkvist, H. Rickman, B. A. Lindlad, and M. Lindgren (Proceedings), 471.

Wurm, K. (1943). Mitt. Hamburg. Sternw. 8, No. 51.

Yamamoto, T. (1985). In *Ices in the Solar System* eds. J. Klinger et al. (Dordrecht, Boston, and Lancaster; D. Reidel Publishing), 205.

BIOGRAPHICAL SKETCH

David James Osip was born on the 14th of November, 1967 at the U.S. Naval Base in Rota, Spain. He is the son of Daniel J. Osip and Maureen V. Burgess-Osip and has two brothers, Philip J. Osip (his twin) and Damien M. Osip. He graduated from Bishop Guertin High School in Nashua, NH, in 1985 and enrolled at the Massachusetts Institute of Technology. He received a S.B. degree in earth, atmospheric, and planetary sciences in June of 1989 and took a research assistant position at Lowell Observatory in Flagstaff, AZ. After a wonderful two years at Lowell Observatory, he decided to return to school to pursue graduate studies in astronomy. In the fall of 1991 he enrolled at the University of Florida where he served as a teaching assistant and a research assistant in his first year. For the past three years he has been funded under a NASA Graduate Student Researchers Fellowship studying the chemical composition and evolution of comets. In this time he has also pursued extensive studies in infrared astronomy with his advisor, Dr. Humberto Campins. After four enjoyable years with the students, faculty, and staff of the Astronomy Department, he will receive his doctorate degree in August of 1995. Topping off a great

summer, at the end of August 1995, he will be married to Joanna E. Thomas!